University of Alberta

Cross Flow Filtration of Oil Sands Total Tailings

by

Chenxi Zhang

A thesis submitted to the Faculty of Graduate Studies and Research
in partial fulfillment of the requirements for the degree of

Master of Science
in
Geotechnical Engineering

Department of Civil and Environmental Engineering

Fall 2010
Edmonton, Alberta

Examining Committee

Dr.Dave Sego, Civil and Environmental Engineering

Dr. Ania Ulrich

Dr. Suzanne Kresta

Dr. Nallamuthu Rajaratnam

Dr. Hooman Askari-Nasab

ABSTRACT

This research is a follow up to preliminary studies reported by Beier and Sego (2008) and the objective is to investigate laboratory scale dewatering of oil sands total tailings using cross flow filtration technology. A laboratory experiment was setup in Oil Sands Tailings Research Facility and tests were carried out under different operational conditions using different tailings. The experiments showed clean filtrate water generated under all test conditions. Coarser tailings and higher filter pipe porosity resulted in greater filtrate flux rate. The effect of slurry velocity, residual bitumen, and transmembrane pressure on cross flow filtration performance was also evaluated. A dimensional analysis was developed using the laboratory tests to establish the relationships between measured parameters and to assist and guide future experimental programs.

ACKNOWLEDGEMENTS

I am deeply indebted and appreciate to my supervisor, Dr. Dave Sego, for his excellent guidance and great encouragement during my Master study in the University of Alberta.

I wish to thank the examination committee for their helpful advice and comments on this research.

I would like to thank Nicolas Beier, Dr. Michael Alostaz and Dr. Nallamuthu Rajaratnam for their constructive suggestions on my research and thesis preparation. I also like to thank Christine Hereygers, Steve Gamble and Bret Shandro for their technical support.

Thanks to all my friends in the Geotechnical Engineering group for their kind help and constructive discussions.

I would like to express my gratitude to my parents for their continuous and kind encouragement and support through my study in Edmonton.

Finally, I wish to thank OSTRF (Oil Sands Tailings Research Facility) for the finical support of this research.

TABLE OF CONTENTS

LIST OF TABLES

LIST OF FIGURES

LIST OF ABBREVIATIONS AND SYMBOLS

CT: consolidated/composite tailings

MFT: mature fine tailings

A_f: filtrate area; m^2

A_r: Archimedes number; dimensionless

A_s: surface area of inside of filter pipe; m^2

C: perimeter of cake; m

C_D: the drag coefficient; dimensionless

D_{pipe}: filter pipe inner diameter; m

D_{pore}: pipe pore/slot size; m

d_p: deposited particle size; m

d_{cake}: particle size within cake structure; m

d_n: particle size in tailings slurry; m

d_s: Sauter mean diameter; m

F: Froude number; dimensionless

f_v: fines content of total tailings slurry by volume; %

$f_{v(fines+water)}$: fines content of carried fluid by volume; %

f_w: fines content of total solids by weight (volume); %

g: gravitational acceleration; m/s^2

G_s: specific gravity of solids (both sands and fines); dimensionless

Q: filtrate flow rate; m^3/s

i: hydraulic gradient; dimensionless

J: steady state filtrate flux rate; $m^3/m^2 \cdot s$

J/n_p: normalized filtrate flux rate; $m^3/m^2 \cdot s$;

J_w: filtrate flux rate with pure water; $m^3/m^2 \cdot s$

k: coefficient of hydraulic conductivity; m/s

L: length of dewatering pipe; m

M_s: mass of solids; kg

M_t: total mass of tailings; kg

M_w: mass of water; kg

n_p: porosity; dimensionless

ΔP: transmembrane pressure; Pa (N/m^2)

p_n: mass fraction of different particle size in tailings slurry; %

R_c: filter cake resistance to water, 1/m

R_p: filter pipe resistance to water, 1/m

Re: Reynolds number; dimensionless

S_s: density ratio (solid/fluid); dimensionless

s_w: solid content of total tailings slurry by weight; %

s_v: solid content of total tailings slurry by volume; %

t_{cake}: thickness of cake; m

v_c: deposition velocity; m/s

v_s: slurry velocity; m/s

ρ_{cf}: density of carrier fluid (including fines); kg/m^3

ρ_s: density of total tailings slurry; kg/m^3

ρ_{solid}: density of solid particles; kg/m^3

ρ_{water}: density of water; kg/m^3

μ_{cf}: viscosity of carrier fluid (including fines); $N \cdot s/m^2$

μ_r: relative viscosity; dimensionless

μ_s: viscosity of total tailings slurry; $N \cdot s/m^2$

μ_w: viscosity of filtrate water; $N \cdot s /m^2$

γ_w: unit weight of water; kN/m^3

1 INTRODUCTION

1.1 Background

The research conducted in this study investigated the application of cross flow filtration to dewater oil sands total tailings.

1.1.1 Oil Sands Tailings Slurry Characteristics

The oil sands total tailings slurry from the extraction process is a mixture of sand particles, dispersed fines, water and residual bitumen. The mixture has about 55wt% solids, of which 82wt% are sands and 17wt% are fines (<44μm), and 1wt% of residual bitumen. This tailings stream is characterized as heterogeneous or settling flow. This behavior causes total tailings to form two quasi layers, which flow at different velocities, during pipeline transportation (Sanders et al., 2004).

After deposition into the storage area, particles settle quickly from the slurry forming a beach. The remaining fines form a dilute suspension of about 10wt% solids content that flows into the tailings pond (Morgenstern and Scott, 1995; Sobkowicz and Morgenstern, 2009). After a few years of settling, the fines densify to 30-35wt% solids content with a stable slurry structure and are referred to as Mature Fine Tailings (MFT). Due to the slow consolidation rate, MFT requires decades to complete self weight consolidation and require long term containment of fluid (Chalaturnyk et al., 2002; Sobkowicz and Morgenstern, 2009).

To describe the segregation issue and to understand this behavior, as well as what is needed to alter its behavior, the ternary diagram (Figure 1.1) illustrated by Azam and Scott (2005) is a useful tool. There are several boundaries illustrated. One important boundary for tailings management is the segregating-nonsegregating boundary, which represents the division between two tailings behaviors. Above the boundary, coarse particles settle from the tailings slurry. This leaves the fines suspended within the tailings stream and they eventually form the MFT. Below the boundary, coarse particles are captured in the fines matrix and the total tailings slurry form a nonsegregating mixture when deposited (Morgenstern and Scott, 1995).

One potential solution to prevent segregation is increasing the total tailings stream solids content before depositing into tailings pond, i.e. dewatering technology (Morgenstern and Scott, 1995). As shown in the ternary diagram (Figure 1.1), the total tailings have approximately 40wt% to 60wt% solids content and 10wt% to 20wt% fines content, and are located above the segregation boundary. To achieve a nonsegregating condition using a dewatering method and without reducing the fines content, a solids content about of 70wt% is required. This is easy to illustrate in the ternary diagram (Figure 1.1) by plotting a straight line (dotted line) from total tailings stream region to the nonsegregating region. This line should follow a constant fines content path since fines content will not change during the dewatering process (Morgenstern and Scott, 1995). Based on the calculation (Appendix A), about 50wt% of water needs to be removed from the

total tailings stream to achieve this solids content increase. On a volume bases 33% of the original tailings volume needs to be reduced.

1.1.2 Cross Flow Filtration

Cross flow filtration is a potential technology to achieve the dewatering objective previously documented. The working mechanism of cross flow filtration is shown in Figure 1.2. Compared to traditional dead-end filtration, the slurry flow direction in cross flow filtration is parallel to the filter membrane. The shear stress generated by the flow limits the cake thickness and keeps high filtrate flux rate at a longer time compared to dead-end filtration. In cross flow filtration, a pipeline with small pores or slots is used as the filter membrane. Therefore, since pipeline transportation is used in oil sands industry to deliver total tailings stream from extraction plants to tailings ponds, the dewatering pipelines and cross flow filtration could be utilized as part of the existing pipeline transportation to increase tailings slurry solids content before deposition into a tailings pond or other faculty.

Another potential advantage of applying cross flow filtration in tailings slurry pipeline transportation is water and energy recovery. In the oil sands extraction process, although recycled water from tailings ponds provides approximately 80%-85% of the water usage, it was reported that under current processing conditions, 3.1barrels of freshwater were needed to produce one barrel of oil (Allen, 2008). With the application of cross flow filtration, the filtrate water removed from tailings slurry can be directly reused in the extraction plants. The

heat generated for the extraction process and pipeline transportation can also be recovered with filtrate water. Therefore, with increasing tailings slurry solids content, cross flow filtration can also save water and energy thus reducing green house gases.

Cross flow filtration has been widely used in purification or regeneration of process liquids containing very fine suspensions (Murkes and Carlsson, 1988; Yan et al., 2003). This technology has also been demonstrated as having potential to increase the solids content in coarse tailings by Beier and Sego (2008) and gold mine tailings by Yan et al. (2003). Beier and Sego (2008) conducted experiments on coarse tailings similar to oil sands total tailings, and obtained acceptable filtrate quality and quantity. Yan et al. (2003) performed cross flow filtration on gold mine tailings and achieved an increase of 9wt% in solids content over a 100m filter pipe length. Therefore, based on these achievements, the application of cross flow filtration on actual oil sands total tailings is suitable and good filtration quality and quantity are expected.

1.2 Objectives

This research continues preliminary work done by Beier and Sego (2008). Based on the findings of their study, the primary objective of this research is to investigate the laboratory scale dewatering capacity of oil sands total tailings using cross flow filtration technology under different operation conditions and with different feed tailings. This research program also aims:

1. To investigate the relationship between feed velocity and filtrate quantity (filtrate flux rate) and quality (filtrate water solids content);
2. To evaluate the influence of different oil sands total tailings compositions (particle size distribution) on the cross flow filtration performance;
3. To evaluate the influence of different filter media on the cross flow filtration performance;
4. To investigate the relationship between transmembrane pressure and filtrate quantity (filtrate flux rate) and quality (filtrate water solids content).

1.3 Methodology

A laboratory scale cross flow filtration system was designed and constructed at the Oil Sands Tailings Research Facility (OSTRF). The experimental oil sands total tailings were made by mixing tailings sands, MFT and tap water. The chemistry of tap water is different with tailings water, but for these preliminary tests it was deemed acceptable. The filtrate flow rate was measured and filtrate water samples were taken during test operation to determine filtrate flux rate and filtrate water solids content. The feed tailings samples were collected to determine solids content and fines content at the University of Alberta Geotechnical Center as required.

1.4 Organization of Dissertation

This thesis has been written in paper format. Chapter 1 briefly introduces the oil sands tailings characteristics and cross flow

filtration technology. Chapter 2 details the cross flow filtration theory, laboratory experiment design, execution, observations, test results and discussions. Chapter 3 presents the dimensional analysis based on laboratory results in order to determine the relationship between different parameters in cross flow filtration. Chapter 4 summarizes the achievements of this study and requirements for future research.

1.5 References

Allen, E.W. 2008. Process water treatment in Canada's oil sands industry: I. Target pollutants and treatment objectives. Journal of Environmental Engineering & Science, **7** (2): 123-138.

Azam, S., and Scott, J.D. 2005. Revisiting the ternary diagram for tailings characterization and management. Geotechnical News, December 2005: 43-46.

Beier, N., and Sego, D. 2007. The oil sands tailings research facility. *In* Proceedings of the 60th Canadian Geotechnical Conference, Ottawa ON., 21-25 October 2007. Canadian Geotechnical Society, Ottawa, pp. 1423-1430

Beier, N., and Sego, D. 2008. Dewatering of oil sands tailings using cross flow filtration. *In* Proceedings of the 61st Canadian Geotechnical Conference, Edmonton, AB., 21-24 September 2008. Canadian Geotechnical Society, Edmonton, pp. 761-768

Chalaturnyk, R.J., Scott, J.D., and Őzüm. B. 2002. Management of oil sands tailings. Petroleum Science and Technology, **20**(9&10): 1025-1046.

Morgenstern, N.R., and Scott, J.D. 1995. Geotechnics of fine tailings management. *In* Proceedings of the GeoEnvironment 2000 ASCE Specialty Conference, New Orleans, Louisiana, 24-26 February 1995. American Society of Civil Engineering, New York, pp. 1663-1683

Murkes, J., and Carlsson, C.G. 1998. Crossflow filtration: theory and practice. John Wiley & Sons Ltd., New York.

Ripperger, S., and Altamnn, J. 2002. Crossflow microfiltration – State of the art. Separation and Purification Technology, **26**: 19-31.

Sanders, R.S., Schaan, J., Hughes, R., and Shook, C. 2004. Performance of sand slurry pipelines in the oil sands industry. The Canadian Journal of Chemical Engineering, **82**: 850-857.

Sobkowicz, J.C., and Morgenstern, N.R. 2009. A geotechnical perspective on oil sands tailings. *In* Proceedings of the 13th International Conference on Tailings and Mine Waste, Banff, AB, Canada., 1-4 November 2009. University of Alberta Geotechnical Center, Edmonton, AB, Canada, pp. xvii-xli.

Yan, D., Parker, T., and Ryan, S. 2003. Dewatering of fine slurries by the Kalgoorlie Filter Pipe. Minerals Engineering, **16**: 283-289.

1.6 Figures and Tables

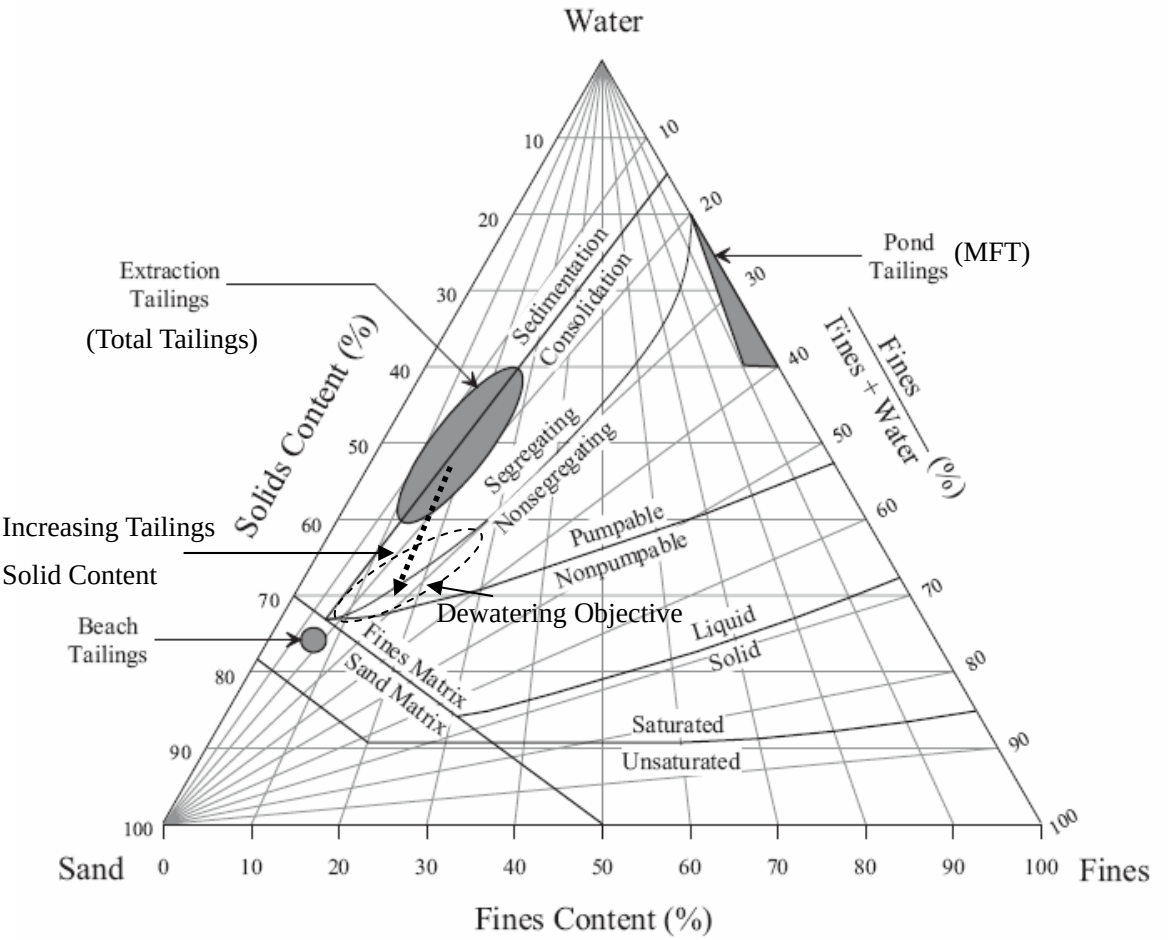

Figure 1.1 Ternary diagram for the dewatering purpose on oil sands total tailings (modified after Azam and Scott, 2005 and Beier and Sego, 2008)

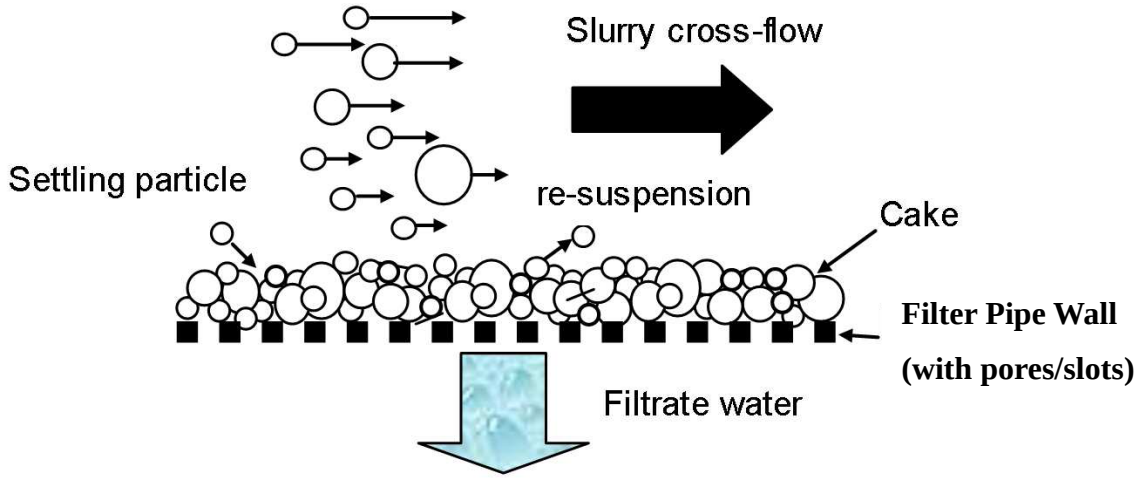

Figure 1.2 Working mechanism of cross flow filtration (Beier and Sego, 2008)

2 CROSS FLOW FILTRATION OF OIL SANDS TOTAL TAILINGS: LABORATORY EXPERIMENTS

2.1 Introduction

Oil sands tailings, which are produced from the bitumen extraction process, are deposited as a slurry with an average of 55wt% solids content (percentage of total solids of tailings slurry) and 17wt% fines content (percentage of particles <44μm of total solids). The whole oil sands total tailings are characterized as heterogeneous or segregating slurry during pipeline transportation (Sanders et al., 2004). After discharge from the pipeline into the disposal area, particles settle and form a beach, leaving a 10wt% fines content suspension in the fluid flowing to the pond (Morgenstern and Scott, 1995; Sobkowicz and Morgenstern, 2009). After a few years of settling, the remaining fines achieve 30-35wt% solids content with a stable structure, which is called Mature Fine Tailings (MFT). Due to its very slow consolidation rate, MFT needs many decades to settle and dewater before it achieves a trafficable surface as required by regulators (ERCB Directive 074) (Chalaturnyk et al., 2002; Sobkowicz and Morgenstern, 2009).

Consolidated/composite tailings (CT) technology has been implemented by industry to reduce the above described segregation by combining together MFT, gypsum ($CaSO_4$) and coarse sands (cyclone under flow). Although CT technology produces non-segregating tailings, it still segregates unless carefully deposited. Another concern of CT is the addition of gypsum, which results in accumulation of Ca^{2+} in the recycle water negatively impacting bitumen extraction efficiency (Chalaturnyk et al., 2002; Sobkowicz and Morgenstern,

2009).

To avoid adding chemicals and to prevent segregation, increasing total tailings solids content to over 70wt% before deposition is a potential solution. With the increase in tailings slurry solids content, the heated water removed from tailings slurry can be reused in extraction to save energy. Cross flow filtration is a potential technology to achieve these dewatering objectives and has been demonstrated by Yan et al. (2003) and Beier and Sego (2008).

2.2 Introduction of Cross Flow Filtration

2.2.1 Working Mechanism

In cross flow filtration, the slurry to be filtered flows parallel to the filter membrane. The working mechanism of cross flow filtration is shown in Figure 2.1. The flow direction is perpendicular to the building-up of filter cake, therefore shear stresses generated by the flow limits the cake thickness to maintain high filtrate flux rate for a longer period compared to dead-end filtration that rapidly builds cake thickness. Filtrate flux rate (J; $m^3/s \cdot m^2$) is a measure of how much filtrate volume flows across a given area of the membrane during a given time interval. It is calculated as (filtrate flow rate)/(filter membrane surface area). Hwang and Hong (2006) compared cross flow filtration and dead-end constant pressure filtration. They found that cross flow filtration always gave a higher filtrate flux rate under a fixed filtration pressure since a thinner filter cake formed in cross flow filtration.

Due to the slurry flow direction in cross flow filtration, woven hose and porous/slotted pipes have been used as filter membrane. Yan et al. (2003) evaluated the first while Beier and Sego (2008) the second. This pipe filter membrane allows the application of cross flow filtration as part of the total tailings slurry pipeline transportation used in the oil sands industry.

Oil sands total tailings are classified as a heterogeneous slurry in pipeline transportation and could be represented using the Saskatchewan Research Council (SRC) Two-Layer model (Sanders et al., 2004). This model considers fully stratified flow with a high velocity, low solids concentration in the upper layer and a slower moving, high solids concentration in the lower layer. Fines are considered as part of the carrier fluid (Sanders et al., 2004). Therefore, when applying cross flow filtration to total tailings, it is expected that coarse particles within the tailings slurry settle onto the filter membrane at the beginning of operation due to their settling characteristic. Some fine particles, which are smaller than the filter membrane pores/slots, also drain with the filtrate water in the initial stage. As operation continues, coarse particles settle to build bridges across the filter openings and form a stable cake on the filter membrane. The filtration seepage force holds the particles on the side and top of the filter pipe forming a thin filter cake (Beier and Sego, 2008).

During a cross flow filtration operation, more fine particles are brought to the filter cake because of seepage forces in the filtrate water.

The accumulation of fine particles increases the filter cake resistance and reduces filtrate flux rate. As this decreases, the seepage force decreases and leads to fewer but finer particles being deposited in the cake, which further decreases the filtrate flux rate (Altmann and Ripperger, 1997). This process continues until the filtrate flux rate attains steady state (Hwang et al., 2006; Lu et al., 1993). A detailed scheme of this process is shown in Figure 2.2.

2.2.2 Application of Cross Flow Filtration

Cross flow filtration technology has been used in many fields for purification or regeneration of process liquids containing fine suspensions (Murkes and Carlsson, 1988; Yan et al., 2003). It is widely used with fine particle slurries but few studies have demonstrated its application with coarse tailings. Yan et al. (2003) applied cross flow filtration to gold mine tailings using a 48mm diameter flexible, woven steel hose. The slurry sample used had a D_{80} of 35μm and a solids density of 2730kg/m^3. From their laboratory test, an increase in solids content, from 44wt% to 53wt%, was obtained over a 96m length under 160kPa transmembrane pressure and 2.17L/s (1.2m/s) feed flow rate.

Beier and Sego (2008) examined use of cross flow filtration to dewater coarse tailings (mixture of sands and kaolinite). Their tailings mixture was similar to the oil sands total tailings (55wt% solids content with 15wt% fines content). They studied cross flow filtration using two different filter pipes. One was a 50mm inner diameter polyethylene porous pipe with 40μm pore size and the other one was a

50mm inner diameter PVC bottom slotted pipe with 250μm wide and 55mm long slots. For both cases studied, suitable filtrate water quality could be achieved but the bottom slotted pipe required time to obtain clean filtrate. The filtrate flux rate generated from the porous pipe was nearly an order of magnitude greater than from slotted pipe in their study. This could be attributed to the larger open surface (porosity) of the porous pipe (34%) compared to the bottom slotted pipe (3%). They operated another cross flow filtration test using porous pipe and high solids content tailings (70wt% with 15wt% fines content). The filtrate water quality was also acceptable and a higher transmembrane pressure (69kPa for 55wt% solids content test; 110kPa for 70wt% solids content test) was required to produce a similar filtrate flux rate as the test using 55wt% solids content tailings. Based on these experimental results, it was concluded that approximately 450m of 50mm diameter porous pipe would be required to dewater the oil sands total tailings stream from 55wt% solids content to 70wt% under 2.26L/s (1.15m/s) feed flow rate. The performance of cross flow filtration carried out by Beier and Sego (2008) successfully produced an acceptable filtrate quality and quantity, and indicated that the technology held promise for dewatering oil sands total tailings. This study is a follow up to Beier and Sego (2008).

2.3 Parameters Related To Cross Flow Filtration

There are a number of parameters that affect the performance of cross flow filtration, including slurry velocity, transmembrane pressure, slurry particle size distribution and solids content, operation temperature, and filter membrane properties (Murkes and Carlsson,

1988; Yan et al., 2003).

2.3.1 Slurry Velocity

Slurry velocity is a fundamentally important factor in cross flow filtration (Murkes and Carlsson, 1988). Higher velocity generally provides higher shear rate which reduces the cake thickness and results in a higher filtrate flux rate (Yan et al., 2003).

Dahlheimer et al. (1970) conducted experiments using a fiber hose to dewater a kaolin slurry with a concentration of 80g/L. They concluded that there was a direct correlation between the filtrate flux rate and flow velocity. Yan et al. (2003) demonstrated a linear relationship between slurry velocity (0.7m/s to 2.4m/s) and filtrate flux rate (1.5×10^{-2}L/ s·m^2 to 8×10^{-2}L/ s·m^2).

How slurry velocity affects the filter cake and its structure can be explained using the "selective cut-diameter" mechanism. The term "selective cut-diameter" for particle deposition during cross flow filtration means there exists a critical particle size (cut-diameter), below which the particles deposit on the filter membrane to form a cake (Lu et al., 1993). This mechanism is explained using Rupperger and Altmann's (2002) description (Figure 2.3) that estimates filtration drag force and slurry lift force as a function of particle size. The slope of the lift force versus particle diameter is steeper than that of drag force. Therefore if a particle is smaller than a certain size (cut-diameter), which is the intersection point of drag force line and lift force line, these particles will settle due to the net filtration drag

force, and a particle larger than the cut-diameter will not settle due to the net lift force.

For a given particle size distribution, increasing slurry velocity not only generates higher shear stress on the cake surface, but it also results in a smaller selective cut-diameter. This results in fewer but finer particles settling to form a finer cake with a higher resistance to the filtrate. Moreover, Lu and Hwang (1995) demonstrated the existence of a cut-diameter using the probability of particle deposition. Based on their modeling, the probability of particle deposition on the cake surface suddenly reduced to low values when the particle size exceeded a certain size, which is the cut-diameter. Hwang and Hong (2006) demonstrated that at high slurry velocity, the reduction of cake mass played a more significant role than the increase of cake resistance to filtration. Therefore increasing slurry velocity could improve filtrate flux rate.

2.3.2 Transmembrane Pressure

Transmembrane pressure is another important factor because cross flow filtration is essentially a pressure-driven process (Yan et al., 2003). Higher transmembrane pressure forces more filtrate liquid to flow through the filter membrane and increase filtrate flux rate. To the contrary, higher transmembrane pressure can also compact the cake structure reducing the filtrate flux rate. It was found that the increase of filtrate flux rate with transmembrane pressure will continue to a point, after which the filtrate flux rate will not increase or may even decrease with increasing transmembrane pressure (Murkes and

Carlsson, 1988). Sethi and Wiesner (1997) concluded that for large particles (1μm), operating at higher pressure caused the steady state to be achieved earlier and the increase of filtrate flux rate over the entire operation.

Ripperger and Altmann (2002) presented cross flow filtration experiments using monodisperse silica particles. They observed that the filter cake thickness increased linearly and irreversibly with transmembrane pressure, which meant with the decrease in transmembrane pressure cake thickness did not change significantly.

Dahlheimer et al. (1970) investigated the effect of a sudden increase in transmembrane pressure using a kaolin slurry during cross flow filtration. The experiment was first operated under 124kPa (18psi) for 1 hour and then changed to 689.5kPa (100psi) rapidly while using similar slurry velocity. The filtrate flux rate increased significantly from 4.9×10^{-2} to 20.1×10^{-2}L/ s·m^2 (95 to 370gpd/ft^2) 1.5 minutes after the pressure increase. But after one hour operation, the ultimate filtrate flux rate decreased to almost the same as was measured under 124kPa (18psi). They used an extrapolation method to find the filtrate flux rate value right after the pressure change. The value was 28.9×10^{-2}L/s·m^2 (530gpd/ft^2) and it demonstrated the direct proportionality between the transmembrane pressure and filtrate flux rate, i.e. (689.5kPa)/(124kPa) = (28.9×10^{-2}L/ s·m^2)/(4.9×10^{-2} L/ s·m^2).

Yan et al. (2003) found that there was an increase in recycled feed slurry total solids content (wt%) with increased transmembrane pressure during their cross flow filtration test. This indicated that more water was removed from the tailings stream under higher transmembrane pressure resulting in higher solids content in recycled slurry. This observation demonstrated that filtrate flux rate increased with transmembrane pressure.

Another concern of increasing transmembrane pressure is the quality of filtrate liquid. Beier and Sego (2008) observed that although increasing pressure led to higher filtrate flux rate, fines within the filtrate liquid also increased. Therefore the optimal transmembrane pressure should produce both good filtrate flux rate and filtrate quality.

2.3.3 Slurry Particle Size Distribution

Particle size distribution appears to have a strong influence on filtrate flux rate. Hwang et al. (2006) observed that for particles larger than 1μm, the deposition probability decreased with increasing of particle size. This means larger particles are more easily swept away from the cake surface as they arrive. This mechanism could also be explained using Rupperger and Altmann's (2002) description (Figure 2.3; section 2.3.1). Under a certain filtrate flux rate, the net lift force increases with particle size and then results in less deposition as the particle size increases. For a slurry with a wide particle size distribution, it is expected that more particles are deposited initially under the higher filtrate flux rate which produces higher seepage drag

forces and a larger cut-diameter. As the particles deposition continues, filtrate flux rate and filtration drag forces decrease, resulting in fewer and finer particles being deposited (smaller cut-diameter). This finer deposition increases cake resistance further decreasing the filtrate flux rate (Altmann and Ripperger, 1997). The whole process repeats until a balance develops between lift force and drag force, then the filtrate flux rate reaches steady state (Hwang et al., 2006; Lu et al., 1993).

Ripperger and Altmann (2002) also described that, for a given slurry, the percentage of particles in the 50 to 500nm range would control the steady state filtrate flux rate. This is because particles within this range have a minimum effective back-transport mechanism, which means if these particles are deposited, they will be difficult to reincorporate into the slurry. Based on the MFT particle size distribution data shown in Figure 2.4, about 20wt% of the particles were smaller than 500nm with dispersed condition. Therefore the total tailings containing 15wt% fines content is expected to have 2wt% of particles smaller than 500nm.

Another concern of applying cross flow filtration to the oil sands tailings is the presence of coarse particles within the tailings slurry. It is expected these coarse tailings will form a cake structure with enhanced coarse sized particles and result in higher filtrate flux rate.

2.3.4 Slurry Solids Concentration

Generally, cross flow filtration is insensitive to the slurry solids concentration (Murkes and Carlsson, 1988). Yan et al. (2003)

observed this phenomenon as well. In conventional dead-end filtration, the increase in feed solids concentration means higher particle deposition rate and thicker cake development that reduces filtrate flux rate, but in cross flow filtration, the slurry velocity generates a higher shear force with a higher slurry solids concentration. This shear limits the cake thickness and maintains an approximately constant filtrate flux rate on the membrane and along the pipe length. Yan et al. (2003) operated a cross flow filtration test using 100m of filter pipe and a feed tailings slurry with approximately 44wt% solids content. The increase of slurry solids content after the first 48m was 2-3wt%, and 5-6wt% after the second 48m. The greater increase of solids content in the second 48m was mainly due to higher slurry density measured in this section and these test results matched the assumption that filtrate flux rate remained nearly constant over the pipe length.

Beier and Sego (2008) performed cross flow filtration using coarse tailings (mixture of sands and kaolinite). Two cross flow filtration tests were performed on tailings with different solids content, one at 55wt% and the other one at 70wt%. Both tailings contained 15wt% fines content. The tailings with the higher solids content required a higher transmembrane pressure (110kPa) to obtain similar filtrate flux rate compared to the lower solids content tailings (69kPa). They expected as solids content increases along the filter pipe length, an increase in transmembrane pressure is needed to maintain constant filtrate flux rate.

2.3.5 Filter Membrane Media Properties

The filter membrane/media properties are important in cross flow filtration (Ripperger and Altmann, 2002). The membrane pore size should be small enough to ensure that particles are retained on the membrane and a clean filtrate liquid passes through the pipe wall. Although the ultimate filtrate flux rate is controlled by the cake, it needs time to develop and generate clean filtrate liquid if the membrane pores are too large.

The membrane porosity is another important characteristic. Greater porosity leads to a higher filtrate flux rate even under low pressure.

The membrane resistance to filtrate water is also important since it controls the initial filtrate flux rate and contributes to the total layer resistance to filtrate water (Ripperger and Altmann, 2002).

Yan et al. (2003) presented that for large particles, if the membrane radius is not sufficiently large compared to the cake thickness, filtrate flux rate will increase with membrane radius even under the same shear rate. The reason is that the formation of the cake restricts the available filtrate area, and with an increase of filter membrane radius, the available filtrate area increases and results in higher filtrate flux rate. Sethi and Wiesner (1997) suggested that the slit or outside-in geometry is more favorable for larger particles (>1μm) than the inside-out filter pipe membrane. Further requirements are membrane strength, chemical and thermal stability.

2.3.6 Temperature

Higher operational temperature leads to higher filtrate flux rate due to lower viscosity (Murkes and Carlsson, 1988). This relationship is the same for all membrane processes because the filtrate flow rate through a filter membrane pore is inversely proportional to the fluid viscosity (Yan et al., 2003). Dahlheimer et al. (1970) observed using fiber hose and a kaolin slurry concentration at 20g/L, the temperature affected the filtrate flux rate significantly, from 16.4×10^{-2}L/ s·m^2 (300gpd/ft^2) at 20^0C to more than 43.6×10^{-2}L/ s·m^2 (800 gdp/ft^2) at 55^0C.

Even though high operating temperature resulted in high filtrate flux rate, the major concern of high operation temperature is the filtrate membrane thermal stability and whether higher temperatures reduces the quality of the filtrate. (Murkes and Carlsson, 1988; Ripperger and Altmann, 2002).

2.4 Experiment

2.4.1 Materials

The oil sands total tailings used in this study consisted of beach sands, MFT and tap water prepared to 55wt% total solids content and 15wt% fines content (<44μm). The MFT was from Albian Sands External tailings pond (ASE Main Pond) and was obtained in June 2007. The beach sands samples were from Syncrude Canada Ltd. and Suncor Canada Ltd. as beach sands from Albian Sands was not available. The particle size distributions of these materials are presented in Figure 2.4. The particle size distribution of beach sands was determined using sieve analysis (ASTM D422-63) and the particle size distribution of

MFT was determined using hydrometer tests (ASTM D422-63 and ASTM D4221-99). In order to maintain the chemistry of MFT, the water used in non-dispersed hydrometer test was tailings pond water. According to Millar et al. (2010), in order to minimize the influence of interparticle interactions, a solids suspension of 2.5wt% (25g dry soil) was used instead of the normal 5wt% (50g dry soil) in non-dispersed hydrometer test.

The water used to make the tailings was tap water. That is because the total water volume required in this study was large and tap water was considered suitable for this preliminary study.

Three different experimental tailings were used in this study. Tailing 1 was made with Syncrude beach sands, Albian Sands MFT and tap water. Tailing 2 was made with Suncor beach sands, Albian Sands MFT and tap water. Tailing 3 was made with 50wt% Syncrude beach sands and 50wt% Suncor beach sands. The particle size distributions of these three synthetic tailings based on dispersed MFT condition are shown in Figure 2.5. Tailing 2 had a coarser particle size distribution while Tailing 1 had a finer distribution

2.4.2 Filter Membranes

Two different filter pipes were used during this study. One was a stainless steel porous pipe with nominal 40μm pore size and 49% porosity. The other one was a stainless steel slotted pipe with 250μm slot width but only 13% porosity. The details and photos of these two filter pipes are provided in Table 2.1 and Figure 2.6. The stainless

steel porous pipe was manufactured by Mott Corporation. The pipe material was metal powder compressed into the desired shape and then the powder was sintered in a controlled atmosphere furnace. The stainless steel slotted pipe was provided by Johnson Screens. The pipe was made by wrapping wires on a frame to form continuous slots in the pipe.

2.4.3 Feed Tanks

Two different feed tanks used in this study. One was a cone shape tank and the other one was a cylinder shape tank. The cylinder tank was equipped with a paddle mixer to mix tailings slurry during test operation. The sketch of these two tanks is shown in Figure 2.7.

2.4.4 Test Setup

A schematic of the cross flow filtration equipments is presented in Figure 2.8. Figure 2.9 shows the photo of experiment setup. The system is a closed circuit pipe loop. Beach sands, MFT and water were mixed in the feed tank. After all materials were fully mixed, the prepared tailings were then delivered into the filter pipe using a progressing cavity slurry pump and connecting pipes.

Two pumps were used in this research program. The first pump was a Monyo® 2L6 progressing cavity pump and is shown in Figure 2.9. This pump has a 50mm (2-inch) diameter inlet connected to the feed tank and a 25mm (1-inch) diameter discharge end connected to the pipeline and flow meter. The second pump used in the cross flow

filtration tests was a twin Monyo® 500 36701 progressing cavity pump and is shown in Figure 2.10. This twin pump has 50mm (2-inch) diameter inlet connected to the feed tank and 50mm (2-inch) diameter discharge end connected to the pipe loop. This pump could provide a flow rate up to 6.5m^3/hour.

The dewatered tailings were returned to the feed tank using flexible rubber hoses. A trough was placed beneath the filter pipe to collect and convey the filtrate to a measuring system or to return it to the feed tank. A Coriolis type mass flow meter was attached to the pipeline to provide simultaneous measurement of slurry density and mass flow, as well as to measure volumetric flow. Two digital pressure gauges, with 0-200kPa (0-30psi) range, were attached at both ends of the filter pipe to measure the transmembrane pressure. A 50mm (2-inch) gate valve was placed at the discharge end of the filter pipe to adjust the transmembrane pressure.

Filtrate water samples were collected at 15 to 60 minutes intervals. At each sample interval, filtrate flow rate was measured using a graduated cylinder, and feed flow rate and transmembrane pressure were recorded using the flow meter and pressure gauges. Samples of feed slurry were also obtained as required. The detailed measurement data of each test (e.g. filtrate flux rate/filtrate solids content versus time) is contained in Appendix B.

2.5 Results

A summary of different test conditions in this study is included in

Table 2.2. This table shows the information on the filter pipe, tailings type, feed slurry velocity, transmembrane pressure and feed tank type used in each test. The slurry velocity and transmembrane pressure numbers given in this table are average values recorded during each test and detailed information for each test is listed in Appendix B.

Also, this table gives a brief description of each test with the different operational condition, e.g. different fines content. As shown in this table, the porous filter pipe was used for Test 1 to Test 6 and Test 12 to Test 16, while the slotted filter pipe were used for Test 7 to Test 11. Tailing 1 is the major tailings used in this research, and it was used in Test 1 to Test 4, Test 7 to Test 10 and Test 12 to Test 14. Tailing 2, a coarser tailings composition, was used in Test 5, Test 11, Test 15 and Test 16. Tailing 3 was only used in Test 6. The cylinder tank with a paddle mixer was used in Test 1 to Test 11, while the cone tank was used in Test 12 to Test 16.

Filtrate data (filtrate flux rate) for all tests are shown in Figure 2.11. As shown in this figure, most tests can achieve quasi-steady state after one hour operation. The quasi-steady state as used in this thesis is when the filtrate flux rate becomes constant. Generally the tests using slotted pipe (dotted line) gave lower filtrate flux rate than the tests performed using porous pipe (solid line). For the tests using porous pipe, those carried out using the cone tank (solid symbols) generated higher filtrate flux rate than those using the cylinder tank (empty symbols). The highest filtrate flux rate shown in this figure was for Test 15, which was the first cross flow filtration test using the porous

pipe. Detail description about the effect of feed tank types, filter pipe types, tailings types and slurry velocities will be documented in the following presentation.

Figure 2.12 illustrates the filtrate quality data (solids content) of all tests except Test 16. As shown in this figure, all cross flow filtration tests achieved high quality filtrate water (<0.5wt% solids content) regardless of the pore/slot size. It is shown that Test 8 and Test 9, which used slotted pipe with the larger pore/slot size, required more time to produce the high quality filtrate water. Most of the tests using porous pipe generated clean filtrate water (<0.5wt% solids content) from the beginning of the test. The photograph of filtrate water drops exiting the pipe is shown in Figure 2.13. In Test 16, although the filtrate flux rate was high, it was observed that clean filtrate water was obtained within 5 minutes of the start.

2.5.1 Filtrate Flux Rate with Pure Water through Filter Pipes

Pure water was pumped through both filter pipes (porous pipe and slotted pipe) to observe the pipe wall resistance to water. Figure 2.14 shows the variation of filtrate flux rate with transmembrane pressure and feed slurry velocity using porous pipe. Though pure water was used in this test, some fines from feed tank and connecting hoses still flowed into pipe pores with filtrate water. Since the amount of fines was small, the effect of fine particles was assumed negligible.

As shown in Figure 2.14, the slurry velocity did not affect the filtrate flux rate as no cake formed. It was observed that if the gate valve at

the filter pipe discharge was completely closed, all water was drained out and the transmembrane pressure increased to 276kPa (40psi). Compared to the filtrate flux rate data shown in Figure 2.11, it is observed that the filtrate flux rate was around 0.16 L/s·m^2 with pure water under 120kPa pressure. This is close to the test operating pressure but well below the filtrate rate of 0.01 L/s·m^2 measured during this test resulting from the filter cake formation. This comparison shows that generally one order magnitude decrease in filtrate flux rate happens with the presence of filter cake.

The pure water test operated with slotted pipe had different behavior. It was observed that under different feed flow rate conditions, all water drained when the discharge gate valve was closed and no transmembrane pressure was generated within the filter pipe.

Based on the observations above, smaller pore/slot size has a higher resistance to filtrate water. With the presence of the filter cake, the filtrate flux rate is dominated by the resistance of the cake structure compared to the resistance offered by the filter pipe.

2.5.2 Effect of Slurry Velocity on Filtrate Flux Rate

Figure 2.15 and Figure 2.16 show the effect of slurry velocity on the filtrate flux rate using stainless steel porous pipe and slotted pipe respectively. Tailing 1 and the cylinder tank were used and filtrate water was recycled in all tests. A larger progressing cavity pump (TARBY 1-206T036CDQ) was used in Test 4 and Test 10 to achieve higher feed flow rate. Therefore the whole experiment setup was

relocated in Oil Sands Tailings Research Facility (OSTRF). Since the flow meter was hard wired in the piping, it could not be moved, a TransPort^{TM} PT868 model transit-time ultrasonic flow meter was used in Test 4 and Test 10 to measure the feed flow rate. The flow rate provided from this flow meter varied from 70L/min to 300L/min (0.84m/s to 3.61m/s). Due to the great variation in feed flow rate measurement an estimated number (>2m/s) was used to indicate the slurry velocity condition in these tests. Although the increase in slurry velocity from Test 1 (0.89m/s) to Test 3 (1.08m/s) was small due to pump capacity limitation, the velocity improvement was 20% and provides an indication of the relationship between velocity and filtrate flux rate.

As shown in Figure 2.15, although the filtrate flux rate increased with slurry velocity, the relationship between slurry velocity and filtrate flux rate was not linear. The increase of filtrate flux rate from Test 1 to Test 3, which was 0.0012L/s·m^2 was greater than that from Test 3 to Test 4, which was 0.0006L/s·m^2.

Another observation in Test 4 is highlighted with a dashed circle in Figure 2.15. After 53min operation, the pump capacity was increased from 60% to 65% to observe how increasing feed velocity during the test influenced the filtrate flux rate. It was observed that an increase in filtrate flux rate (from 0.005 to 0.0055L/s·m^2) occurred as the pump capacity was increased. Although the filtrate flux rate decreased again after increasing slurry velocity, there was still an improvement in the filtrate flux rate with an increase in velocity during this test.

Figure 2.16 shows the effect of slurry velocity on filtrate flux rate using the slotted pipe. This figure shows that the increase of slurry velocity decreased the filtrate flux rate. This was not consistent with the observation shown in Figure 2.15 for the porous pipe. Another observation for Test 10 was that at the beginning of cross flow filtration operation, the filtrate flow was very high and filtrate water was dirty. But after 1~2min operation, the filtrate flux rate dropped significantly and clean filtrate water resulted.

2.5.3 Effect of Particle Size on Filtrate Flux Rate

2.5.3.1 Effect of Sands Particle Size

Figure 2.17 and Figure 2.18 show how coarse particles (different sands composition) in the tailings slurry affect filtrate flux rate with the porous and slotted pipe respectively. The cylinder tank was used and filtrate water was recycled during these tests to maintain the solids content constant. The experimental tailings used in these tests had the same fines content but were made using different tailings sands. As introduced in section 2.4.1, Tailing 2 had a coarser particle size distribution, while Tailing 1 was made from the finer tailings sands. As shown in these two figures, the coarser tailings results in higher filtrate flux rate (0.003-0.005L/s·m^2) than finer tailings (0.0024-0.0035L/s·m^2).

Another observation is that the difference in filtrate flux rate with different tailings slurry using porous pipe (Figure 2.17) was a little greater than the difference when using slotted pipe (Figure 2.18). It

appears that the filtrate membrane with smaller pore size is more sensitive to tailings particle size distribution.

2.5.3.2 Effect of Fines Content

Figure 2.19 shows the effect of different fines content on filtrate flux rate when using slotted pipe as the filter membrane. Figure 2.20 presents the variation of quasi-steady state filtrate flux rate with slurry fines content. As discussed earlier, most tests achieved quasi-steady state after one hour operation. Thus the quasi-steady state filtrate flux rate of Test 8 was the average after one hour. For Test 7 and Test9, the quasi-steady state was achieved after half hour. The average after half hour operation was then used as the quasi-steady state filtrate flux rate for these tests. The observation is that lower fines content (Test 9) generated higher filtrate flux rate ($0.004 L/s \cdot m^2$) compared to the higher fines content tailings ($0.0024 L/s \cdot m^2$).

2.5.4 Effect of Slurry Solids Concentration on Filtrate Flux Rate

Figure 2.21 shows how increasing the slurry solids content during cross flow filtration operation affected filtrate flux rate. Tailing 1, porous pipe and cone tank were used in both tests. The difference between these two tests was that in Test 12, the filtrate water was recycled during the test while in Test 14, the filtrate water was removed at a rate of 4L/hour, which allowed the tailings slurry solids content to increase from 55wt% at the beginning to about 70wt% after 3 hours of operation.

As shown in this figure, the filtrate flux rates for both tests were similar. It appears that increasing tailings solids content during cross flow filtration has little effect on the filtrate flux rate but the internal pressure does increase as the solids content increases.

2.5.5 Effect of Filter Pipe Type on Filtrate Flux Rate

Figure 2.22 and Figure 2.23 show the effect of type of filter pipe on filtrate flux rate. The cylinder tank was used and the filtrate water was recycled in all tests. Tailing 1 was used in tests shown in Figure 2.22 and Tailing 2 was used in tests shown in Figure 2.23. As shown in both figures, the tests using porous pipe, which has higher porosity and smaller pore size, generate higher filtrate flux rate (0.0035-0.005L/s·m^2) than tests using slotted pipe (0.0024-0.003L/s·m^2).

In Figure 2.24, the filtrate flux rate of all tests are normalized to porosity, i.e. (Filtrate Flux Rate)/(Porosity), to show the relationship between filtrate flux rate and filter pipe pore/slot size. The normalized filtrate flux rate physically means the amount of filtrate flow per open surface area per second. As shown in this figure, slotted pipe with larger slot size generated higher filtrate flux rate (0.018-0.023L/s·m^2) compared to porous pipe with smaller pore size (0.007-0.01L/s·m^2).

2.5.6 Effect of Bitumen on Filtrate Flux Rate

Two feed tanks were used in this research. When the cone tank was used, it was observed that a bitumen froth formed on top of the slurry in the tank, while in the cylinder tank it did not form when the paddle

mixer was used. The bitumen froth was observed on the inside of the filter pipe, which reduced the filtrate area when the cylinder tank was used as part of the test apparatus.

Figure 2.25 and Figure 2.26 show the effect of bitumen froth on filtrate flux rate. Porous pipe was used and filtrate water was kept recycling in all tests. Tailing 1 was used in the tests shown in Figure 2.25 and Tailing 2 was used in tests shown in Figure 2.26.

Both figures showed that, as the bitumen froth flowed with the slurry inside the filter pipe, the filtrate flux rate decreased. Another observation from these figures is that the presence of bitumen caused greater reduction in filtrate flux rate ($\Delta J=0.0035 L/s \cdot m^2$), almost 40%, with the coarser tailings (Tailing 2/Figure 2.26), while the reduction in filtrate flux rate was about 20% with Tailing 1 ($\Delta J=0.001 L/s \cdot m^2$).

2.5.7 Effect of Transmembrane Pressure on Filtrate Flux Rate

Figure 2.27 shows the effect of a slight increase in transmembrane pressure on filtrate flux rate. Tailing 1, cylinder tank and porous pipe were used and the filtrate water was recycled in both tests. As shown in this figure, Test 1, which had higher transmembrane pressure ($\Delta P=35 kPa$), generated slightly higher filtrate flux rate than Test 2 ($\Delta J=0.0002 L/s \cdot m^2$).

In order to observe the relationship between filtrate flux rate and transmembrane pressure, a higher pressure test was conducted with the filter cake under nearly dead-end filtration situation.

Before each high pressure test, a cross flow filtration test operated for 2 hours to generate the filter cake. After this 2-hour test, the ball valves on both sides of dewatering pipe were closed and a reservoir with fine tailings was then connected to the dewatering pipe. The fine tailings slurry was used to simulate the fines portion of the experimental tailings and was made by mixing 50wt% MFT and 50wt% tap water. An air compressor with a pressure gauge was connected to the reservoir and the fine tailings were delivered under the deserved pressure into the filter pipe. The air pressure was applied at different levels until steady filtrate flow was achieved. Filtrate water samples were collected at the beginning of each pressure change and the steady filtrate flux rate is measured under each pressure level. Figure 2.28 shows the sketch of high pressure test setup and Figure 2.29 shows a photograph of the test setup.

Two high pressure tests were carried out to investigate how transmembrane pressure affects the filtrate flux rate. Test HP1 was carried out following Test 1, which used Tailing 1, and the transmembrane pressure was applied from high to low value. Test HP2 was done following Test 6 using Tailing 3, and the pressure was increased from low to high pressure value. All the filtrate flux rate data were measured after steady filtrate flow was obtained.

The test results are presented in Table 2.4 and Figure 2.30. In Test HP1, clean filtrate water was obtained after 5min of operation and the filtrate flux rate dropped significantly with time under the high pressure 793kPa (115psi). The highest filtrate flux rate (0.0037L/s·m^2)

in Test HP1 was obtained under 758kPa (110psi). In Test HP2, clean filtrate was observed at each pressure level. The highest filtrate flux rate (0.0083L/s·m^2) in Test HP2 was obtained under 552kPa (80psi).

2.5.8 Filter Media Plugging

One concern of cross flow filtration using small pore size filter pipe is the potential blinding of pores within the pipes. During this study, the filter pipes were cleaned using a hot water flush and pressure wash from outside to minimize any potential internal clogging effect.

Porous pipe, cone tank were used and filtrate water were kept recycling in all tests shown in Figure 2.31. Tailing 1 was used in Test 12 and Test 13 while Tailing 2 was used in Test 15 and Test 16. Test 15 was the first cross flow filtration test using the steel stainless porous pipe, which was operated on Aug. 14th, 2008. Test 12 was operated one month later, on Sep.16th, 2008. Test 16 was carried out on Nov. 28th, 2008, and Test 13 was operated on Sep.02nd, 2009.

Since the operation conditions for both Test 15 and Test 16 were similar, it seems a higher filter pipe resistance was observed in Test 16 and it resulted in lower filtrate flux rate. This observation indicates that the presence of bitumen and fines in the slurry caused clogging inside pores and increased resistance. Test 12 and Test 13 were also operated under similar conditions but the filtrate flux rate data were similar, which indicates that there was little extra clogging during the one year of operation.

The observations above show that the cleaning method did not fully remove bitumen and fines from the porous pipe. Since Test 12 was operated only one month after Test 15 and little extra clogging occurred after Test 12, it is reasonable to postulate that the higher filter pipe resistance was developed mainly following the initial test (Test 15) and the cleaning method maintained similar filter pipe resistance for all cross flow filtration tests operating following Test 15.

2.5.9 Heat Generation

Figure 2.32 shows the temperature variation during each cross flow filtration test. Temperatures were always within 40-50^{0}C during the tests because of the friction between the tailings slurry, filter cake and pipe wall. The comparison between Test 12 and Test 14 shows that with increasing solids content during the cross flow filtration operation, more friction was generated and the temperatures increased more rapidly. The comparison between Test 2 and Test 4 shows that more heat was generated under increasing slurry velocity. Although the input energy was not measured in this research, the higher temperatures generated with higher solids content and velocity indicated significant energy consumption.

2.6 Discussion

2.6.1 Effect of Slurry Velocity on Filtrate Flux Rate

As shown in Figure 2.15 and introduced in section 2.5.2, the increase of filtrate flux rate from Test 1 (0.89m/s; slurry velocity) to Test 3 (1.08m/s) was higher than that from Test 3 to Test 4 (>2m/s). Under lower velocities (Test 1 & Test 3), the coarse particles in the tailings

slurry were deposited on the filter membrane first and formed a coarse cake structure. Based on the deposition velocity prediction shown in Table C.1 (Appendix C), the slurry velocities in both tests were lower than the d_{90} deposition velocity. Therefore the coarsest particles settle at the beginning of both tests to form a coarse filter cake. Since the slurry velocity in Test 3 was 10% higher than in Test 1, it did not affect the cake structure significantly. As the cake structure did not change, a slightly higher slurry velocity during Test 3 reduced the cake thickness resulting in an improved filtrate flux rate. In Test 4, a significant higher slurry velocity was used compared to Test 1 and Test 3. According to the deposition velocity prediction (Table C.1), this higher flow rate caused few coarse particles to be deposited at the beginning of test. Then based on the "selective cut-diameter" phenomenon introduced in section 2.3.1, the high filtrate flux rate at the beginning of Test 4 allowed fine particles to enter the filter cake structure and significantly increase its resistance to filtrate flow. Therefore, the finer cake structure compared to Test 1 and Test 3 counteracted the benefit associated with the higher feed flow rate and resulted in lower increase in filtrate flux rate. The feed flow rate was increased after 53min during Test 4, which is highlighted with a dashed circle in Figure 2.15. An increase in filtrate flux rate was observed after the velocity increased. This observation indicated that increasing slurry velocity assisted with stripping particles from the cake surface layer and reduced the cake thickness, which improved filtrate flux rate.

Therefore, although thinner cake thickness was achieved under high slurry velocities, which improved filtrate flux rate, a finer cake structure that can develop could counteract this improvement. As a result, Test 4 conducted with higher slurry velocity compared to Test 3 only showed a small increase in filtrate flux rate.

As shown in Figure 2.16, the slurry velocity increase can result in a decreased in filtrate flux rate. The reason for the lower filtrate flux rate under higher slurry velocity situation (Test 10) was also due to the "selective cut-diameter" phenomenon and the deposition of finer particles into the thinner cake. At the beginning of Test 10 operation, the filtrate flow was extremely high and a large amount of dirty filtrate water drained from the pipe. Compared to Test 4, Test 10 had much higher filtrate flow at the beginning and few coarse particles were deposited. The high filtrate flow brought an increasing amount of fine particles, probably more than in Test 4, into the cake structure to form a finer matrix. This fine matrix then significantly increased the cake resistance resulting in lower filtrate flux rate. Therefore it appears that the amount of fine particles that was incorporated into the cake structure had an important impact on the filtrate flux rate. It can counteract the benefit of higher slurry velocity.

Based on these observations, for the oil sands tailings slurry, the improvement of filtrate flux rate with slurry velocity is not linear and higher slurry velocity may even reduce filtrate flux rate (Test 10/slotted pipe). Therefore, it is expected that if the cross flow filtration test is first operated under a low velocity to allow a coarse

cake structure to develop, and then a higher slurry velocity is applied after this stable cake has formed, an optimal filtrate flux rate may be achieved.

2.6.2 Effect of Particle Size on Filtrate Flux Rate

Particle size distribution affects filtrate flux rate. As discussed earlier, the percentage of particles in the 50 to 500nm range determines the ultimate filtrate flux rate since these particles increase the cake resistance by forming stable deposits in the cake. For the oil sands total tailings, the particle size distribution of coarse particles (sands) also influences the filtrate flux rate since it impacts the cake structure. In this section, the effect of different coarse particles and fines content will be discussed

2.6.2.1 Effect of Coarse Particles (Sands) Distribution

As shown in Figure 2.17 and Figure 2.18, it is observed that the coarser tailings particle size distribution (Tailing 2) resulted in a higher filtrate flux rate. Based on the heterogeneous characteristic of the total tailings, coarse particles settled from tailings slurry at the beginning of the cross flow filtration test and formed the filter cake. Therefore the cake structure was affected by the size distribution of initially settled coarse particles. If feed velocity and transmembrane pressure are the same, coarser tailings generally deposit to form a cake structure with lower resistance to flow, which allows more filtrate water through and higher filtrate flux rate is achieved.

2.6.2.2 Effect of Fines Content

The observation in Figure 2.19 and 2.20 shows that lower fines content (Test 9) generated higher filtrate flux rate. Since the same MFT was used in all these three tests, lower fines content corresponded to lower percentage of particles within the 50 to 500nm range. As described in section 2.3.3, this percentage is inversely proportional to the filtrate flux rate. Therefore higher fines content tailings slurry has more particles within 50 to 500nm range deposited in cake structure and a lower filtrate flux rate is expected.

2.6.3 Effect of Slurry Solids Concentration on Filtrate Flux Rate

If the cross flow filtration technology could be implemented, the effect of increasing tailings slurry solids content with filter pipe length must be accounted for.

As shown in Figure 2.21, the filtrate flux rates of both tests were similar and the transmembrane pressure increased as solids content increased. It appears that increasing the tailings solids content during cross flow filtration operation does not affect the filtrate flux rate. The reason could be the greater shear force generated when the higher solids concentration slurry is flowing (Yan et al., 2003), and this higher shear force limits the cake thickness and maintains filtrate flux rate.

It was also observed that a higher transmembrane pressure may also be required under high solids contents, which is consistent with Beier and Sego's (2008) observation. According to Beier and Sego (2008), a

higher transmembrane pressure, in their case 69kPa for 55wt% tailings and 110kPa for 70wt% tailings, was required to dewater high solids contents tailings.

Since there was little change in filtrate flux rate with increasing solids content, it is expected that the slurry flow regime did not change from 55wt% to 70wt% solids. The calculation of Reynolds number in Appendix D (Table D.1) shows that the slurry flow remains turbulent as the solids content increased to 70%wt.

2.6.4 Effect of Filter Pipe Type on Filtrate Flux Rate

Filter pipe (filtrate membrane) characteristics are important to the filtrate flux rate. Higher porosity gives higher filtrate flux rate and smaller pore size generates clean filtrate faster when compared to the larger pore size.

Figure 2.22 and Figure 2.23 both show that higher filtrate flux rate was generated from tests using porous pipe, which has higher porosity and smaller pore size. This observation is consistent with Beier and Sego (2008) and demonstrates that higher porosity could produce higher filtrate flow.

Figure 2.24 shows that the filter pipe with larger pore/slot size (slotted pipe) generated higher filtrate flux rate than filter pipe with smaller pore/slot size. Based on the relationship shown in this figure, it is expected that under the same porosity situation, a filter pipe with larger pore/slot size generates greater filtrate flux rate.

2.6.5 Effect of Bitumen Froth on Filtrate Flux Rate

As shown in Figure 2.25 and Figure 2.26, bitumen froth inside the filter pipe reduced the filtrate flux rate, and the decrease was higher with the coarser tailings (Figure 2.26). This difference was due to different feed tanks used in this research. The cylinder tank with a paddle mixer mixed bitumen froth into the tailings slurry and caused a reduction in filtrate area. Therefore, in order to achieve an optimal filtrate flux rate, a preliminary procedure to remove the bitumen froth, such as cycling oil sands total tailings inside a cone shaped tank, is recommended before delivering the slurry into the filter pipe.

2.6.6 Effect of Transmembrane Pressure on Filtrate Flux Rate

In Figure 2.27, the cross flow filtration test under slightly higher transmembrane pressure situation (Test 1) provided slightly higher filtrate flux rate. This observation indicates that higher transmembrane pressure produces higher filtrate flux rate.

A high pressure test was utilized to find the relationship between filtrate flux rate and transmembrane pressure under higher pressure, up to 758kPa (110psi). The detailed description of test setup and operation was outlined in section 2.4.6.

Based on the results in Table 2.4 and Figure 2.30, a higher filtrate flux rate could be obtained as the pressure increased. It appears that an optimal pressure results in the highest filtrate flux rate and the test procedure also affects the filtrate flux rate. The optimal filtrate flux rate was much higher in Test HP2 than Test HP1. Since Tailing 3 (Test

HP2) had a coarser particle size distribution than Tailing 1, it is expected that filter cake with coarser structure underwent less compaction resulting in higher filtrate flux rate under the high pressure. Because both high pressure tests were operated under near dead-end filtration situation, the actual cross flow filtrate flux rate under the same pressure level should be greater since cake thickness would decrease under the shear force of the flowing tailings.

2.7 Conclusion

1. The tests operated with pure water showed different behaviors with two filter pipes. The test operated with porous pipe (smaller pore/slot size) required pressure to force filtrate water through the pores while with slotted pipe (larger pore/slot size) the filtrate water freely drained.
2. Generally, one order magnitude decrease in filtrate flux rate is observed under similar transmembrane pressure with the formation of filter cake (around 0.16L/s·m^2 with pure water; up to 0.01L/s·m^2 with filter cake) using porous pipe. The filtrate flux rate is mainly affected by the resistance within the filter cake structure.
3. Higher slurry velocity results in a thinner cake containing higher amount of fines. The increased fines in the cake reduce the improvement associated with the thinning of cake. Increasing feed velocity from 0.89m/s to 1.08m/s resulted in greater improvement of filtrate flux rate (ΔJ=0.0012L/s·m^2) than from 1.08m/s to over 2m/s (ΔJ =0.0006L/s·m^2).

4. In order to achieve the optimal filtrate flux rate, it is recommended that the cross flow filtration test is first operated under a low velocity to allow a coarse cake structure to develop. After the coarse stable cake has formed, a higher slurry velocity is then applied to reduce cake thickness. This operation procedure is expected to achieve thinner cake thickness without the large accumulation of fines in cake structure and result in better filtrate rate.
5. Tailings with coarse particle size distribution have higher filtrate flux rate (0.003-0.005L/s·m^2 with coarse tailings; 0.0024-0.0035L/s·m^2 with fine tailings). The coarse cake structure results in an increase in hydraulic conductivity. Higher fines content (<44μm) result in lower filtrate flux rate (0.0024L/s·m^2 with 15wt% fines content tailings; 0.004L/s·m^2 with 10wt% fines content tailings). Increased fine particles in 50 to 500nm range within the cake increased the resistance to flow through the cake.
6. The cross flow filtration technology is less sensitive to slurry solids content. Therefore the filtrate flux rate is nearly constant along the filter pipe length. A higher transmembrane pressure may be required as slurry solids content increases to maintain the filtrate flux rate.
7. Higher pipe porosity always gives higher filtrate flux rate. Larger pore/slot size needs time to generate clean filtrate water. Based on the normalized filtrate flux rate data, the larger pore/slot size produces a higher filtrate flux rate regardless of porosity for a particular pipe (0.018-0.023L/s·m^2 for slotted pipe; (0.007-0.01L/s·m^2 for porous pipe).

8. The presence of bitumen froth reduces filtrate area and results in lower filtrate flux rate (ΔJ=0.001-0.0035L/s·m^2). A pre-treatment to remove the bitumen or preventing bitumen froth from flowing with slurry is necessary to achieve the optimal filtrate flux rate.
9. There is an optimal transmembrane pressure to produce the highest filtrate flux rate when the pressure is gradually increased during cross flow filtration. Comparing the high pressure test data, the cake formed from coarser tailings slurry undergoes less compaction under high pressures and results in higher filtrate flux rate.
10. Clean filtrate water (<0.5wt% solids content) is achieved under all test conditions. Filter pipe with larger slot/pore size needs additional time to generate clean filtrate water.
11. Filter pipe cleaning method used in this research did not fully remove bitumen and fines that clogging the pores. The high filter pipe resistance was developed following the first test and following the cleaning, similar resistance was measured for the rest tests.
12. Heat generation due to friction between the slurry, filter cake and pipe wall raises the temperature of each slurry siginificantly. Higher slurry velocity and solids content both generate higher temperature.

2.8 References

Altamnn, J., and Ripperger, S.1997. Particle deposition and layer formation at the crossflow microfiltration. Journal of Membrane Science, **124**: 119-128.

Azam, S., and Scott, J.D. 2005. Revisiting the ternary diagram for tailings characterization and management. Geotechnical News, December 2005: 43-46.

Beier, N., and Sego, D. 2007. The oil sands tailings research facility. *In* Proceedings of the 60th Canadian Geotechnical Conference, Ottawa ON., 21-25 October 2007. Canadian Geotechnical Society, Ottawa, pp. 1423-1430

Beier, N., and Sego, D. 2008. Dewatering of oil sands tailings using cross flow filtration. *In* Proceedings of the 61st Canadian Geotechnical Conference, Edmonton, AB., 21-24 September 2008. Canadian Geotechnical Society, Edmonton, pp. 761-768

Chalaturnyk, R.J., Scott, J.D., and Őzüm. B. 2002. Management of oil sands tailings. Petroleum Science and Technology, **20**(9&10): 1025-1046.

Cumming, I.W., Holdich, R.G., and Ismail, B. 1999. Prediction of deposit depth and transmembrane pressure during crossflow microfiltration. Journal of Membrane Science, **154**: 229-237.

Dahlheimer, J.A., Thomas, D.G., and Kraus, K.A. 1970. Hyperfiltration: Application of woven fiber hoses to hyperfiltration of salts and crossflow filtration of suspended solids. Industrial &

Engineering Chemistry Process Design and Development, **9**(4): 566-569

Hameed, M.S., and Al-Mousilly, D.S. 2001. Hydrodynamic studies in crossflow filtration. Filtration & Separation, **38**(2): 35-39

Hwang, K.J., and Hong, M.T. 2006. Effect of slurry rheology on the performance of cross-flow filtration. Journal of Chemical Engineering of Japan, **39**(7): 693-702

Hwang, K.J., Hsu, Y.L., and Tung, K.L. 2006. Effect of particle size on the performance of cross-flow microfiltration. Advanced Powder Technology, **17**(2): 189-206

Lu, Wei-ming., and Hwang, Kuo-jen. 1995. Cake formation in 2-D cross-flow filtration. American Institute of Chemical Engineers Journal, **41**(6): 1443-1455

Lu, Wei-ming., Hwang, Kuo-jen., and Ju, Shang-Chung. 1993. Studies on the mechanism of cross-flow filtration. Chemical Engineering Science, **48**(5): 863-872

Miller W.G., Scott, J.D., and Sego, D.C., 2010. Influence of the extraction process on the characteristics of oil sands fine tailings. CIM Bulletin Paper 4613

Morgenstern, N.R., and Scott, J.D. 1995. Geotechnics of fine tailings management. *In* Proceedings of the GeoEnvironment 2000 ASCE Specialty Conference, New Orleans, Louisiana, 24-26 February 1995. American Society of Civil Engineering, New York, pp. 1663-1683

Murkes, J., and Carlsson, C.G. 1998. Crossflow filtration: theory and pratice. John Wiley & Sons Ltd., New York.

Ripperger, S., and Altamnn, J. 2002. Crossflow microfiltration – State of the art. Separation and Purification Technology, **26**: 19-31.

Sanders, R.S., Schaan, J., Hughes, R., and Shook, C. 2004. Performance of sand slurry pipelines in the oil sands industry. The Canadian Journal of Chemical Engineering, **82**: 850-857.

Sethi, S., and Wiesner, M.R. 1997. Modeling of transient permeate flux in cross-flow membrane filtration incorporating multiple particle transport mechanisms. Journal of Membrane Science, **136**: 191-205.

Sobkowicz, J.C., and Morgenstern, N.R. 2009. A geotechnical perspective on oil sands tailings. *In* Proceedings of the 13th International Conference on Tailings and Mine Waste, Banff, AB, Canada., 1-4 November 2009. University of Alberta Geotechnical Center, Edmonton, AB, Canada, pp. xvii-xli.

Xu, Y., Dabros, T., and Kan, J. 2008. Filterability of oil sands tailings. Process Safety and Environment Protection, **86**: 268-276.

Yan, D., Parker, T., and Ryan, S. 2003. Dewatering of fine slurries by the Kalgoorlie Filter Pipe. Minerals Engineering, **16**: 283-289.

2.9 Figures and Tables

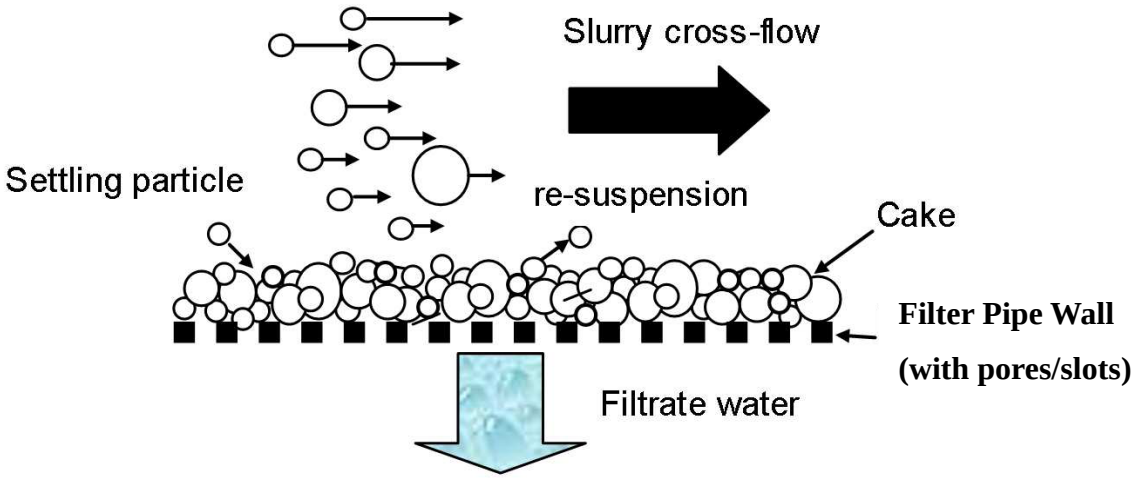

Figure 2.1 Working mechanism of cross flow filtration (Beier and Sego, 2008)

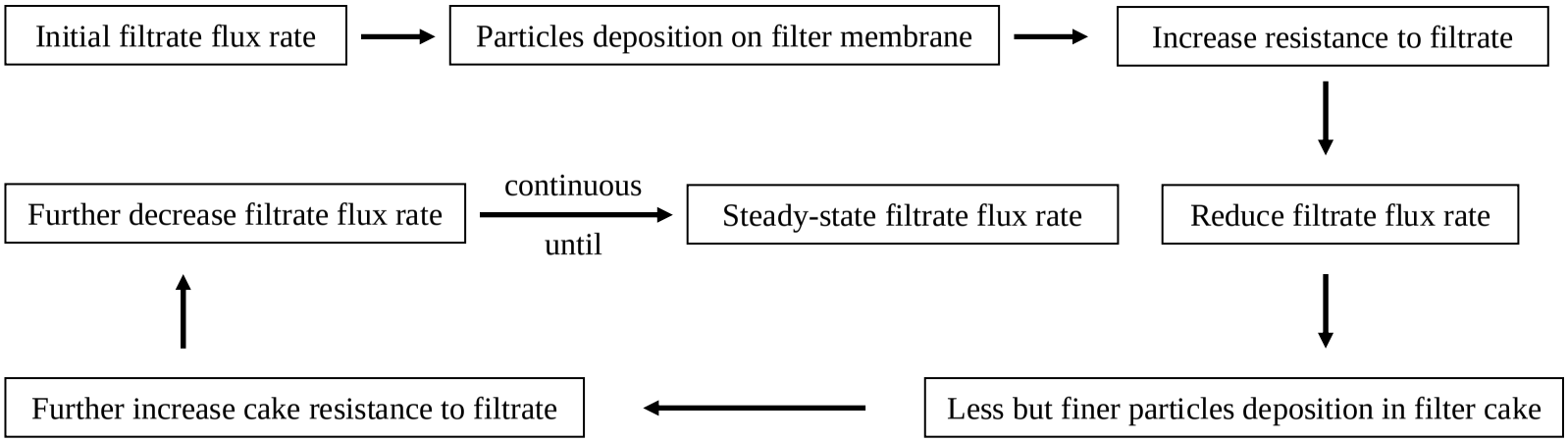

Figure 2.2 Process to achieve steady state filtrate flux rate in cross flow filtration

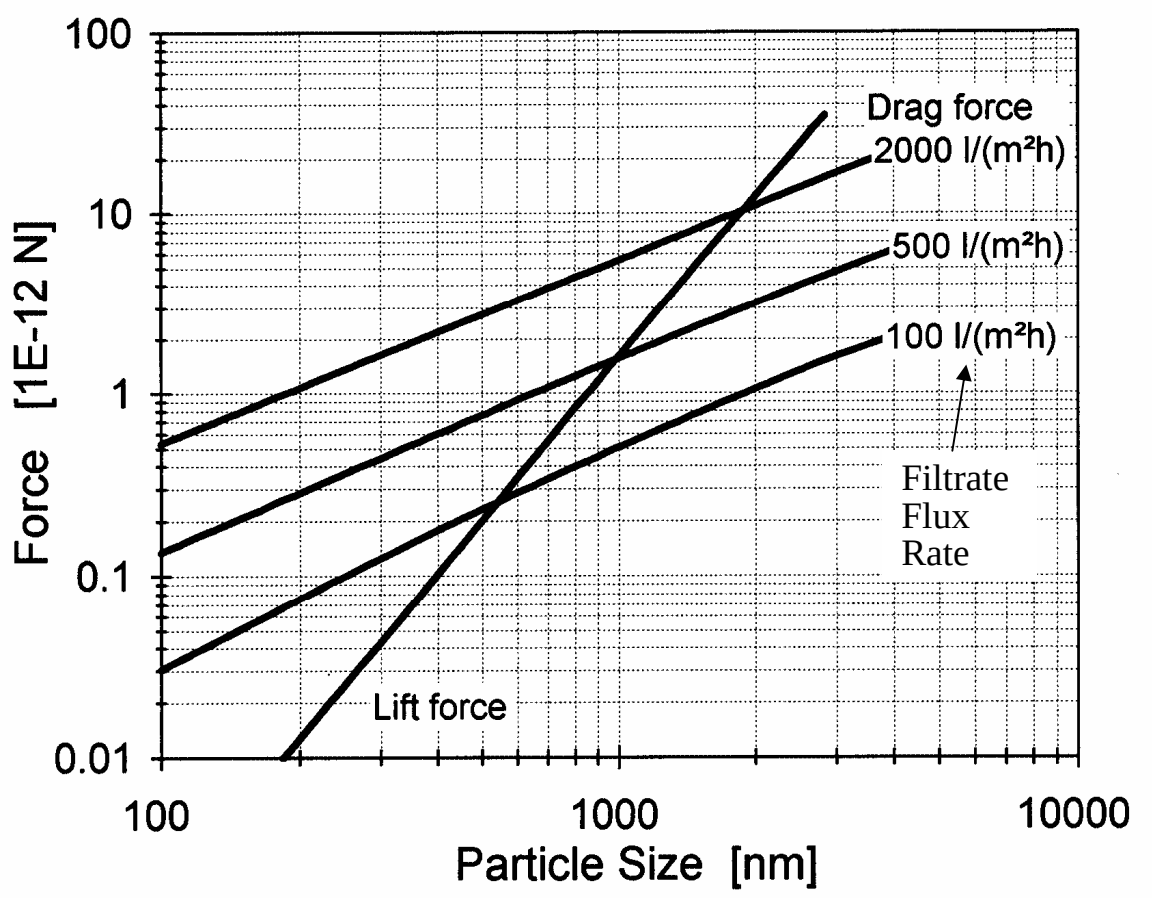

Figure 2.3 Estimation of the drag force and lift force versus particle size in cross flow filtration (from Ripperger and Altmann 2002)

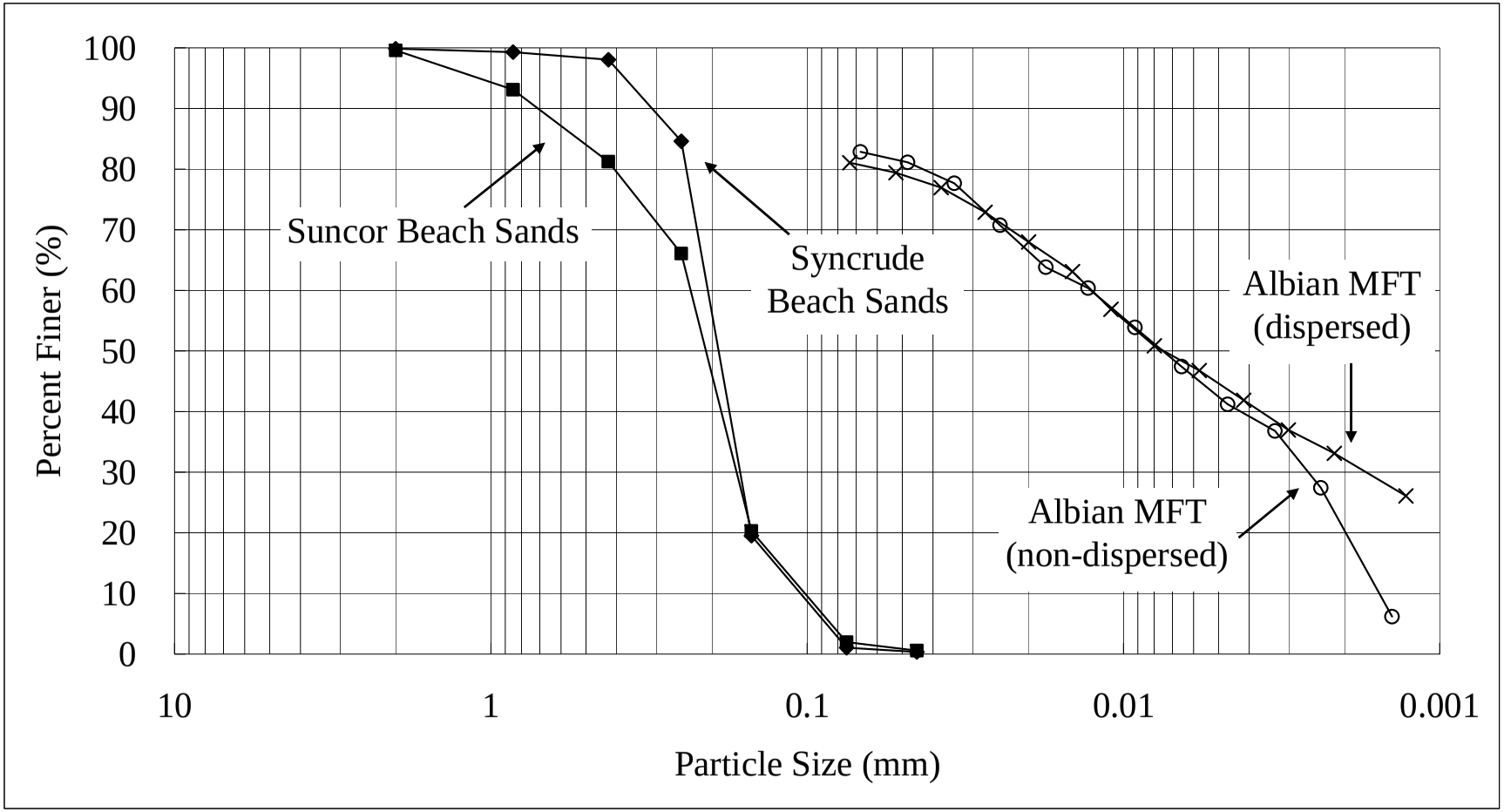

Figure 2.4 Particle size distribution of beach sand and MFT

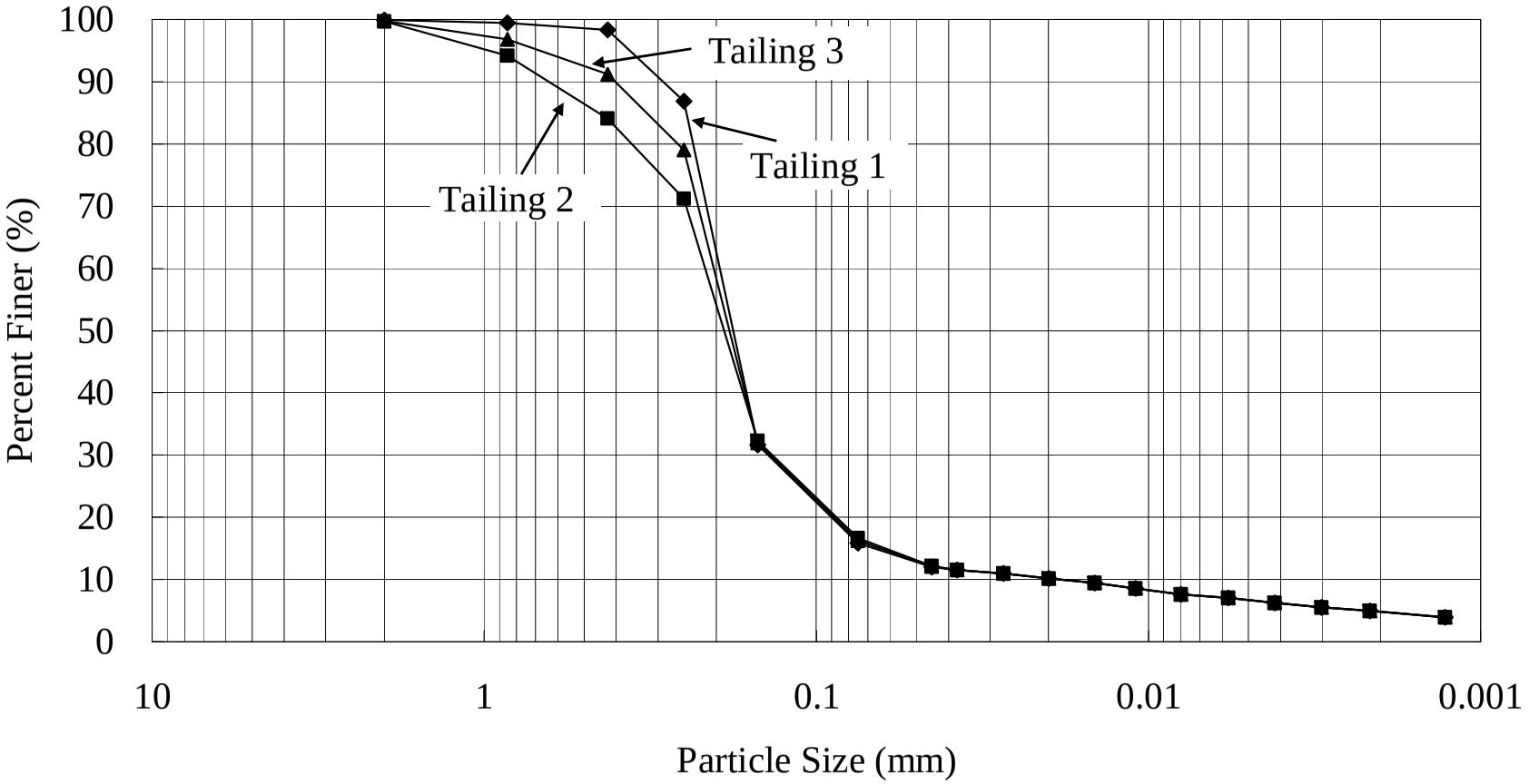

Figure 2.5 Particle size distribution of experimental tailings (based on dispersed MFT condition)

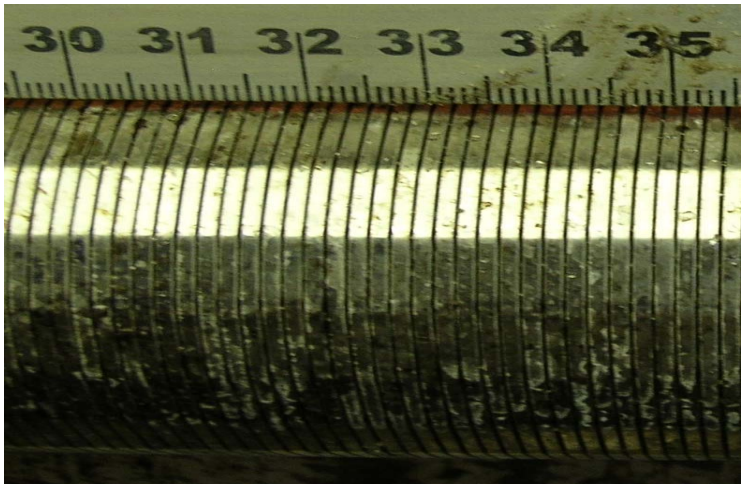

Stainless Steel Porous Pipe **Stainless Steel Slotted Pipe**

Figure 2.6 Photographs of two filter pipes

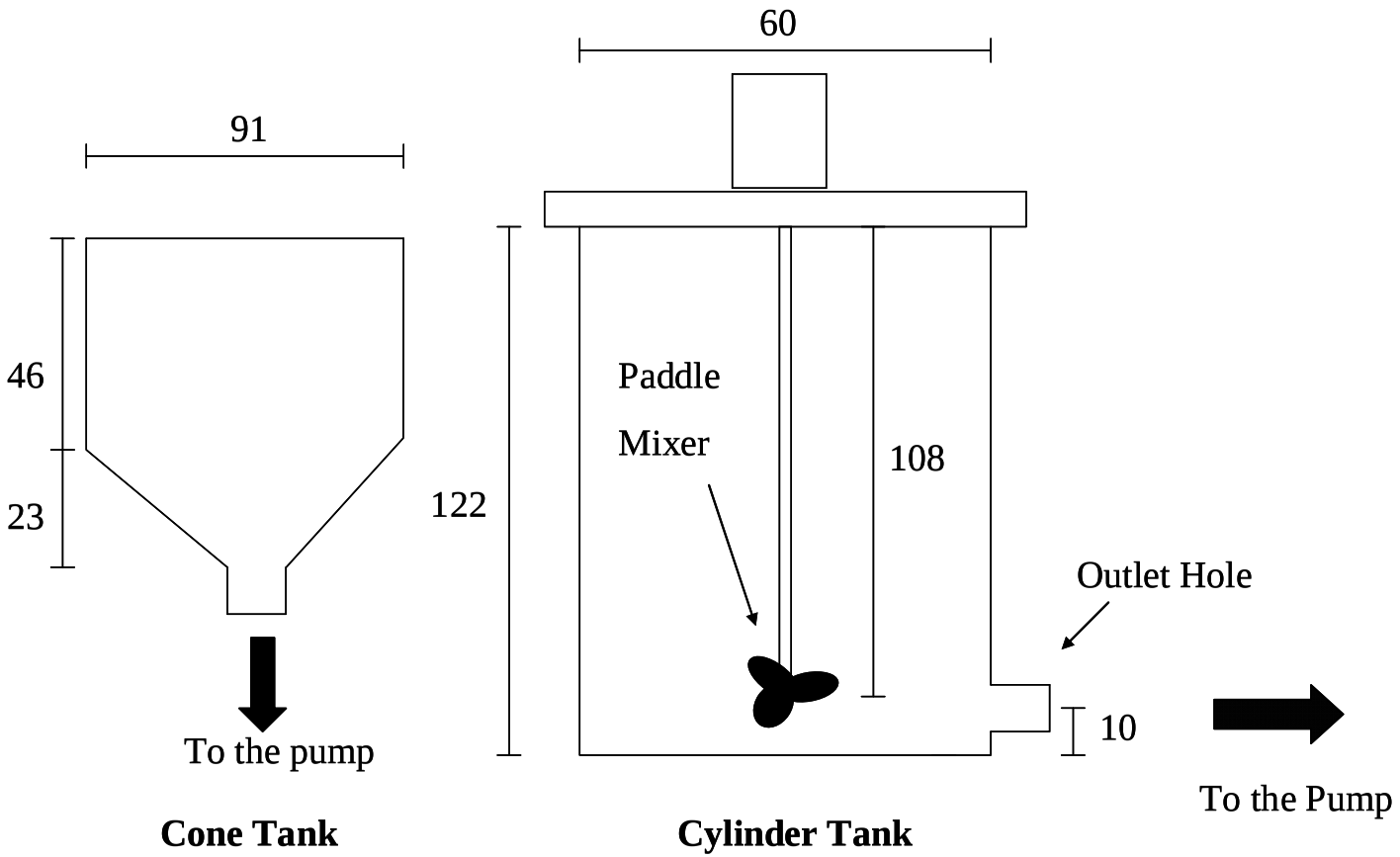

Figure 2.7 Sketch of two feed tanks

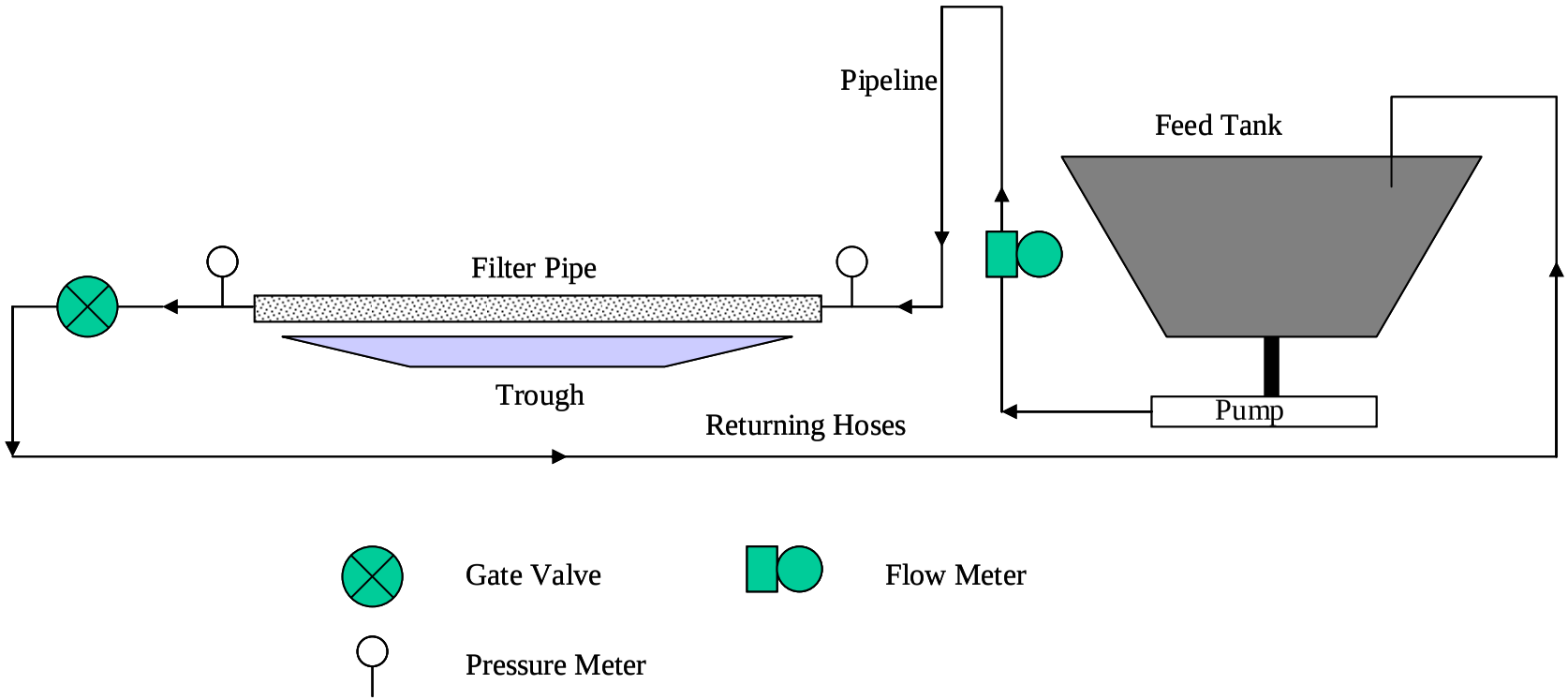

Figure 2.8 Cross flow filtration experiment setup

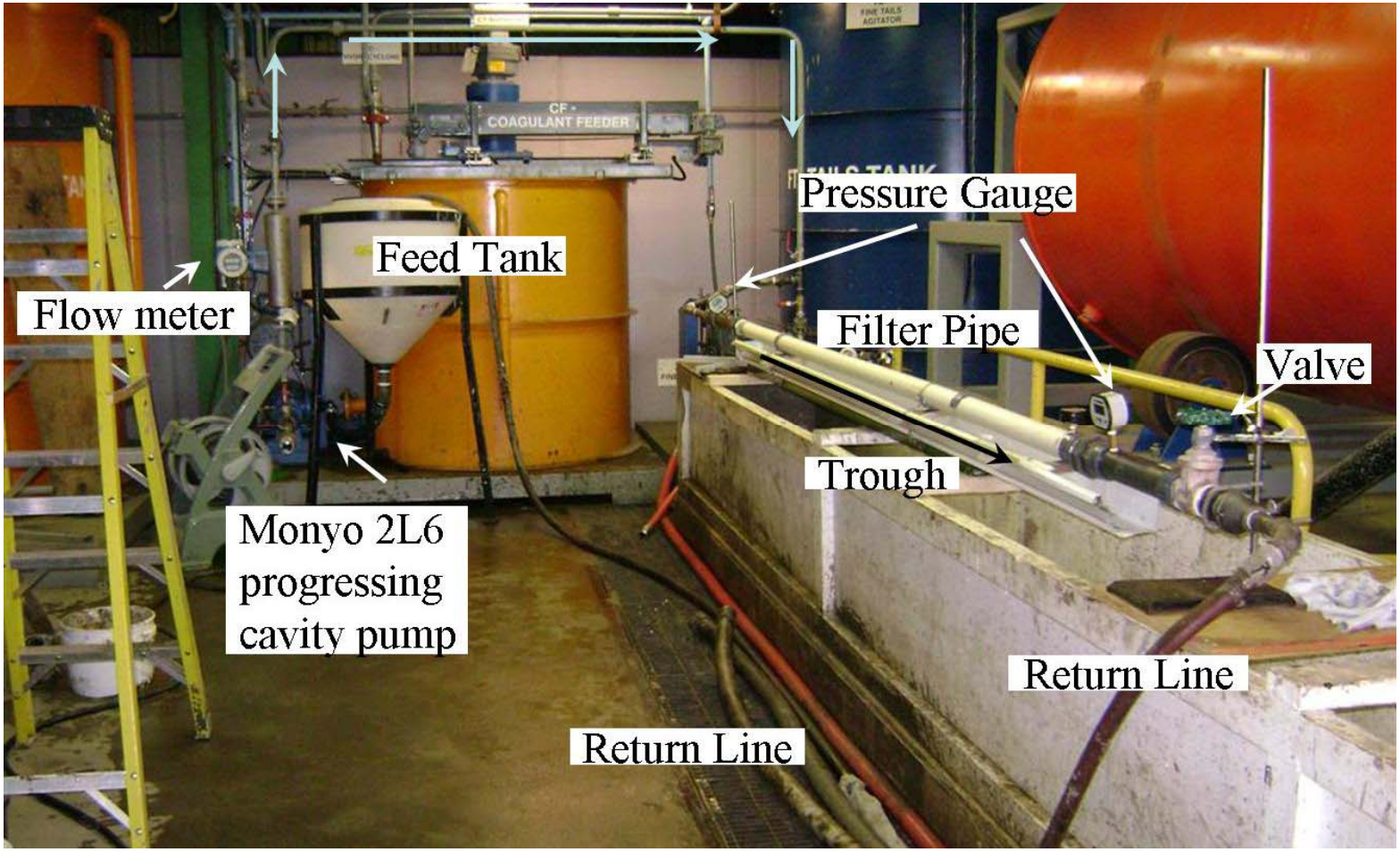

Figure 2.9 Photograph of cross flow filtration experiment setup

Figure 2.10 Photograph of twin Monyo® 500 36701 progressing cavity pump

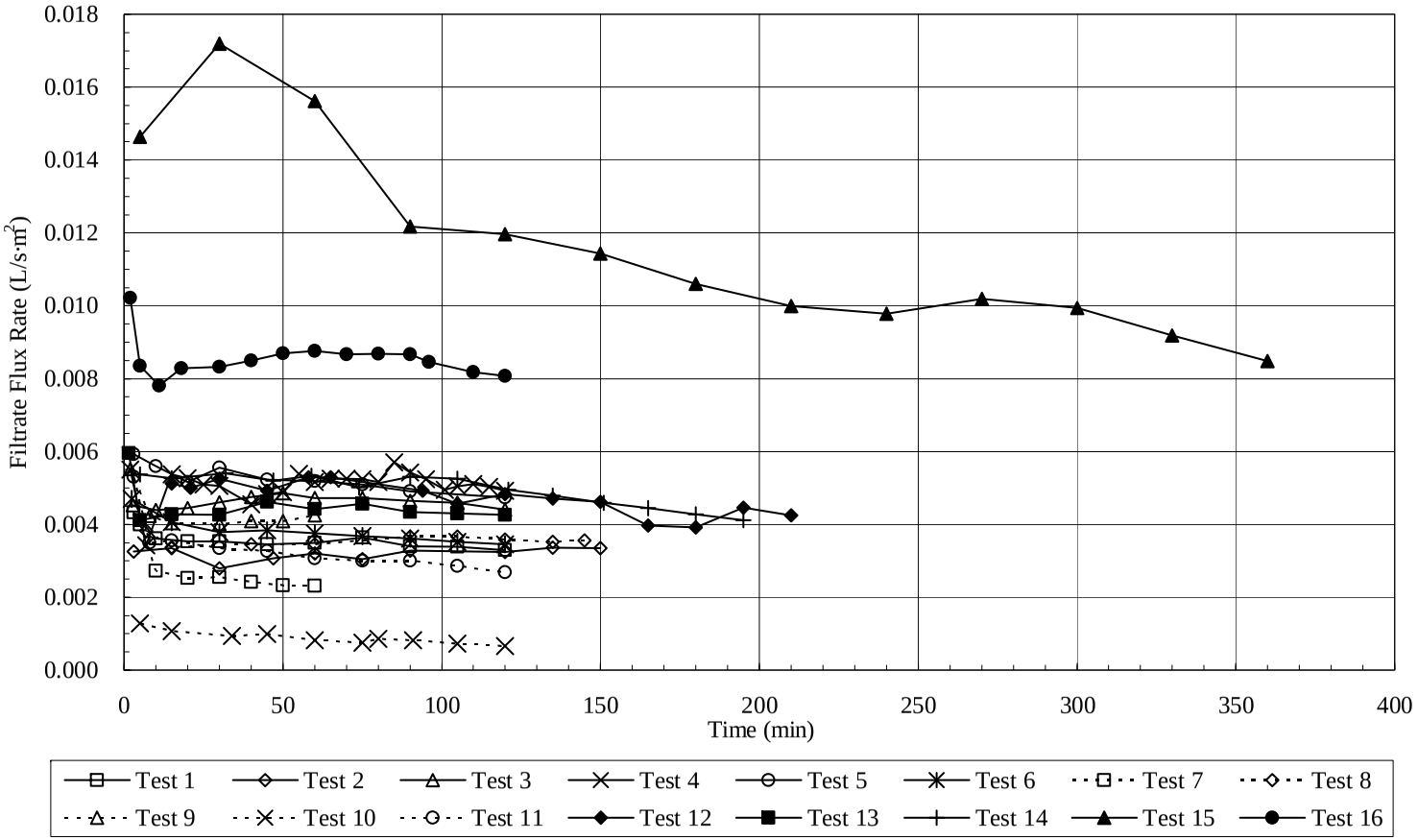

Figure 2.11 Filtrate flux rate data of all tests

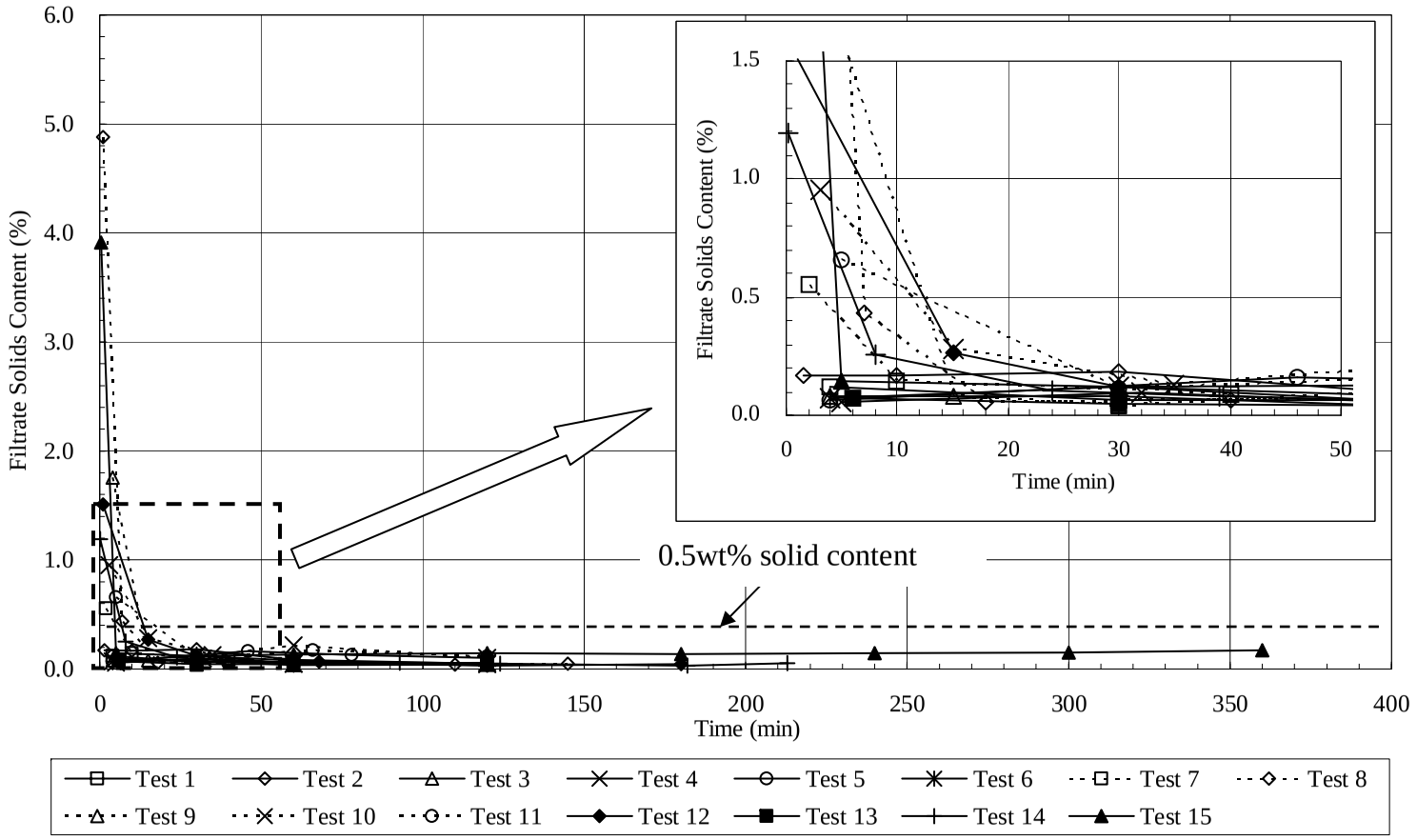

Figure 2.12 Filtrate solid content data of all tests (except Test 16)

Figure 2.13 Photograph of clean filtrate water drop during test operation

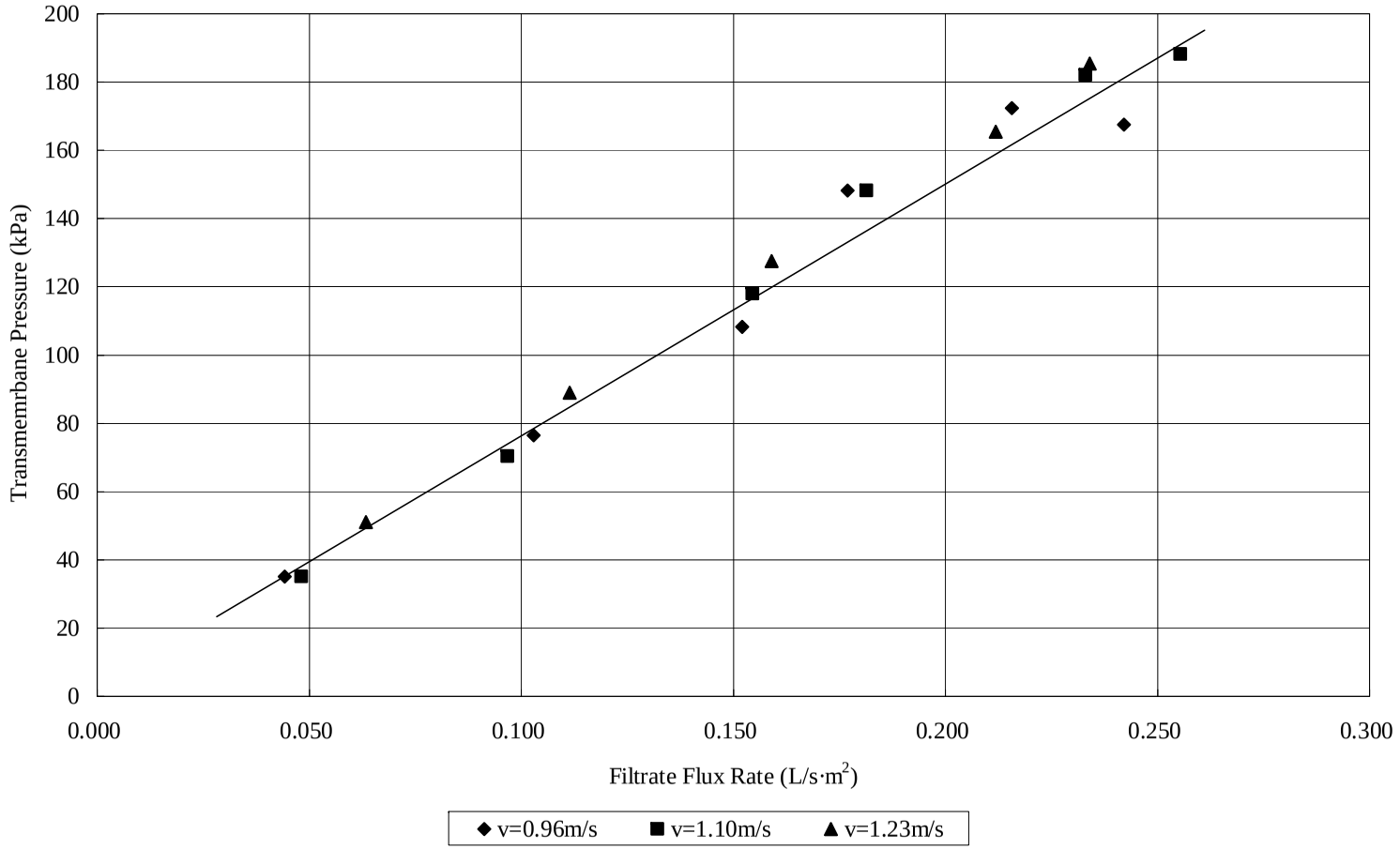

Figure 2.14 Filtrate flux rate data of pure water tests (porous pipe)

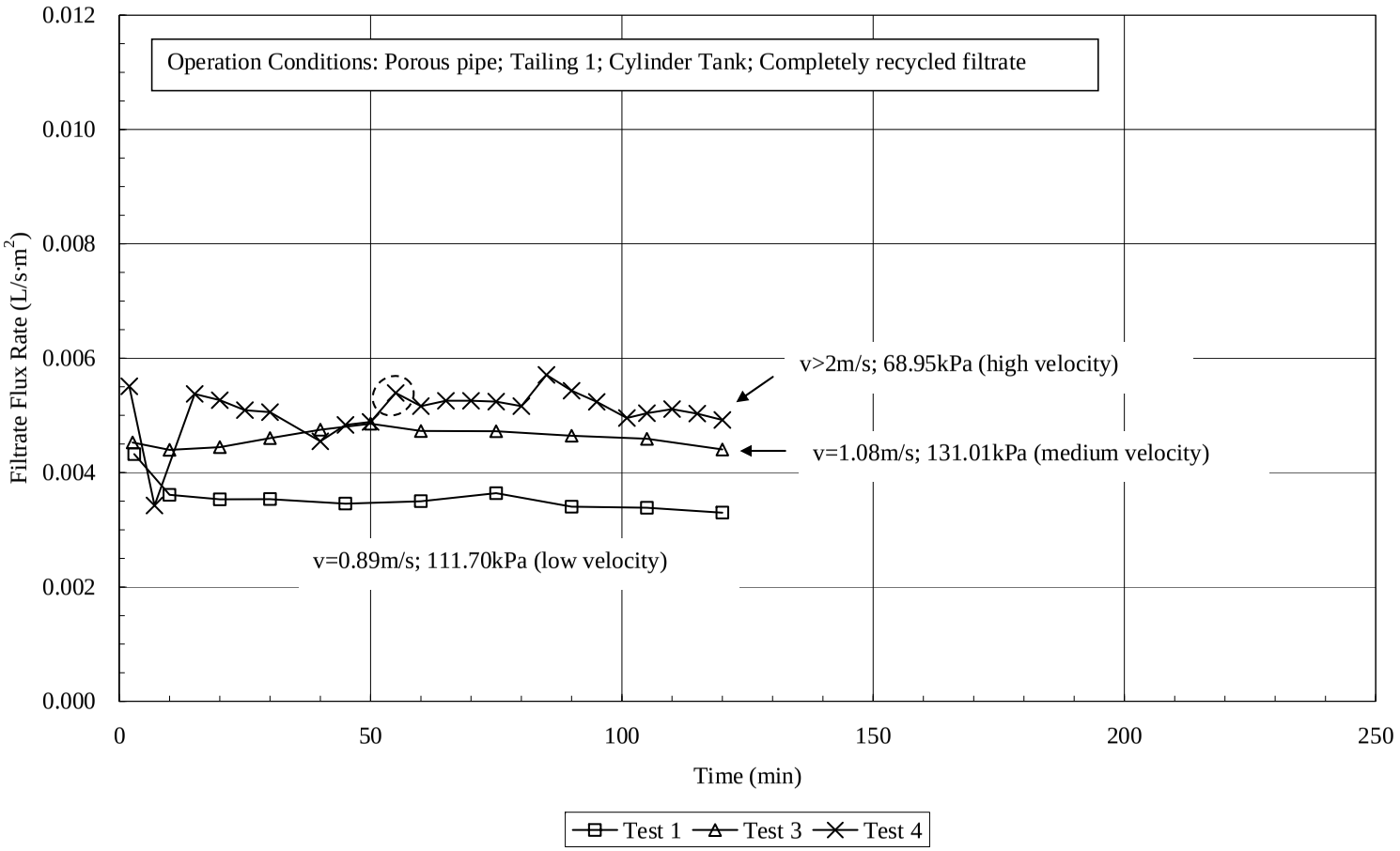

Figure 2.15 Effect of slurry velocity on filtrate flux rate (porous pipe)

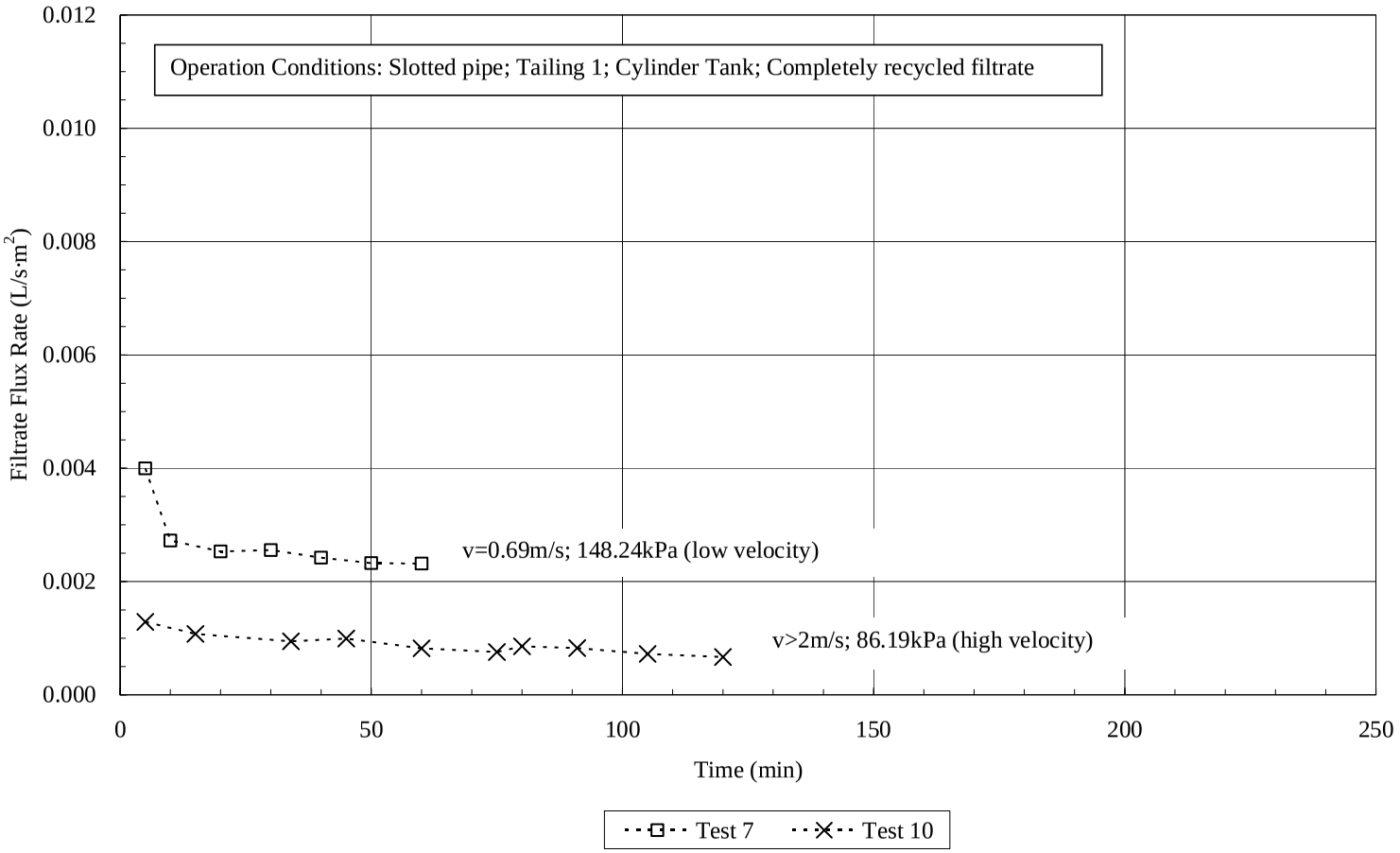

Figure 2.16 Effect of slurry velocity on filtrate flux rate (slotted pipe)

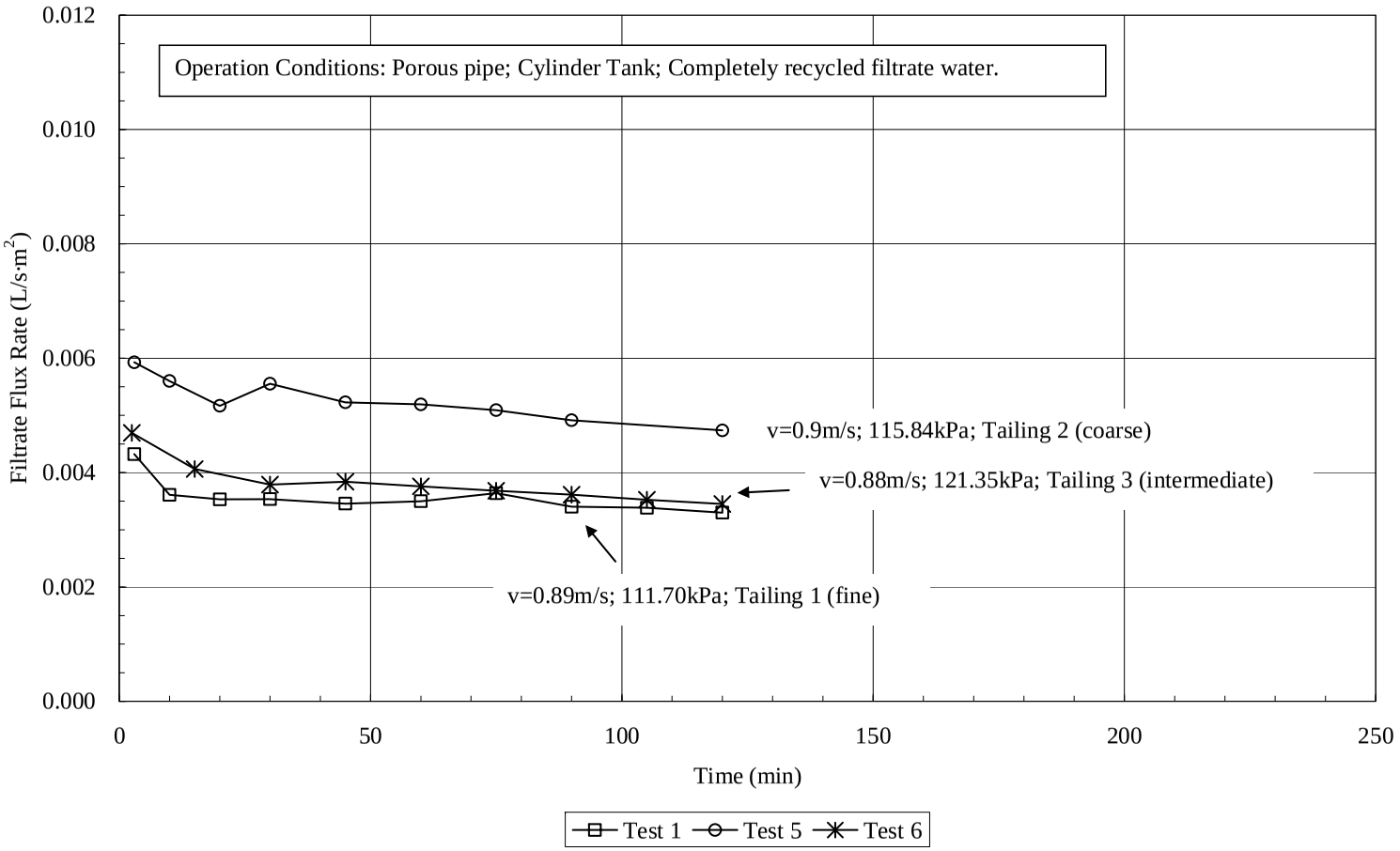

Figure 2.17 Effect of tailings particle size (sand fraction) on filtrate flux rate (porous pipe)

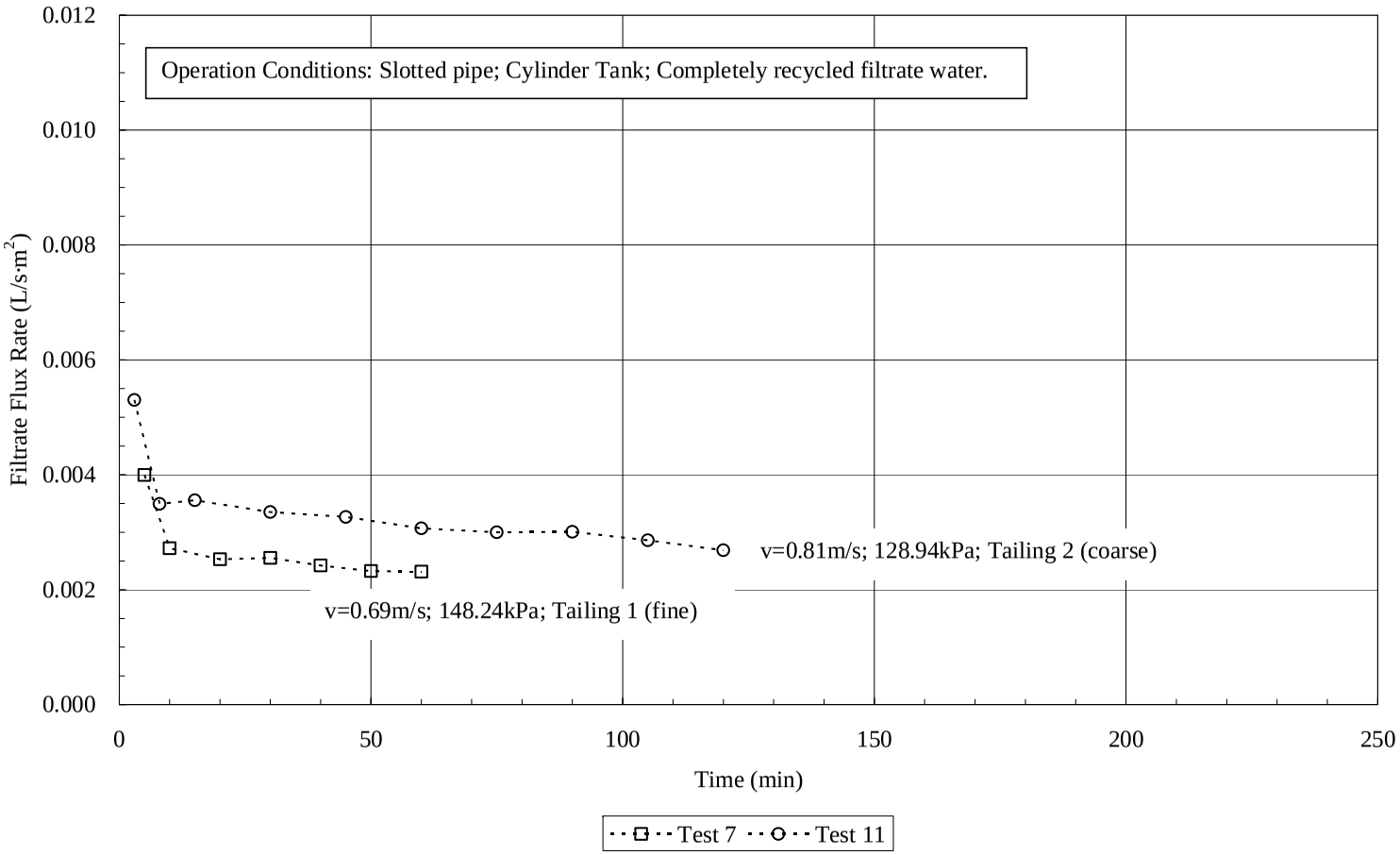

Figure 2.18 Effect of tailings particle size (sand fraction) on filtrate flux rate (slotted pipe)

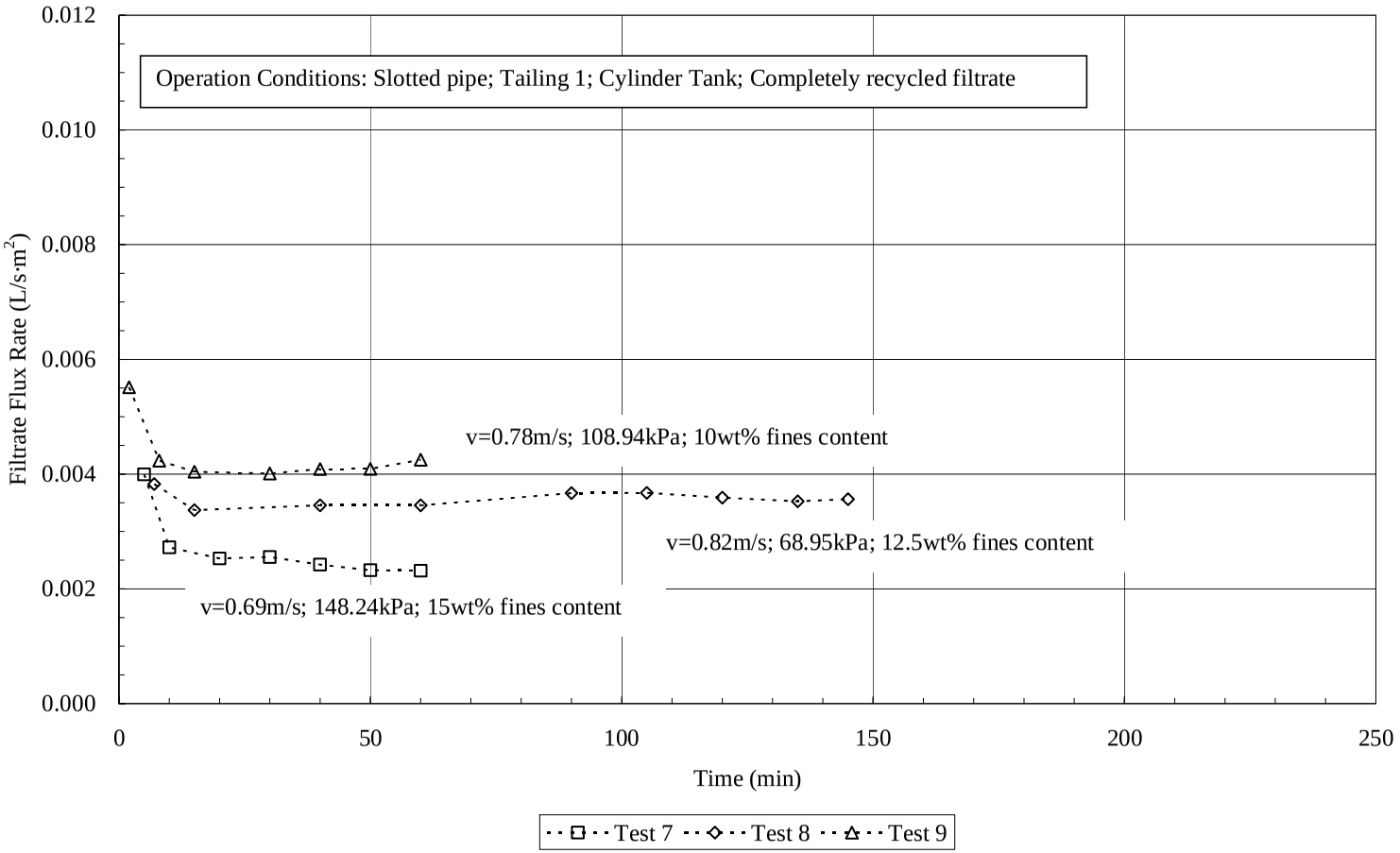

Figure 2.19 Effect of tailings particle size (fines content) on filtrate flux rate (slotted pipe)

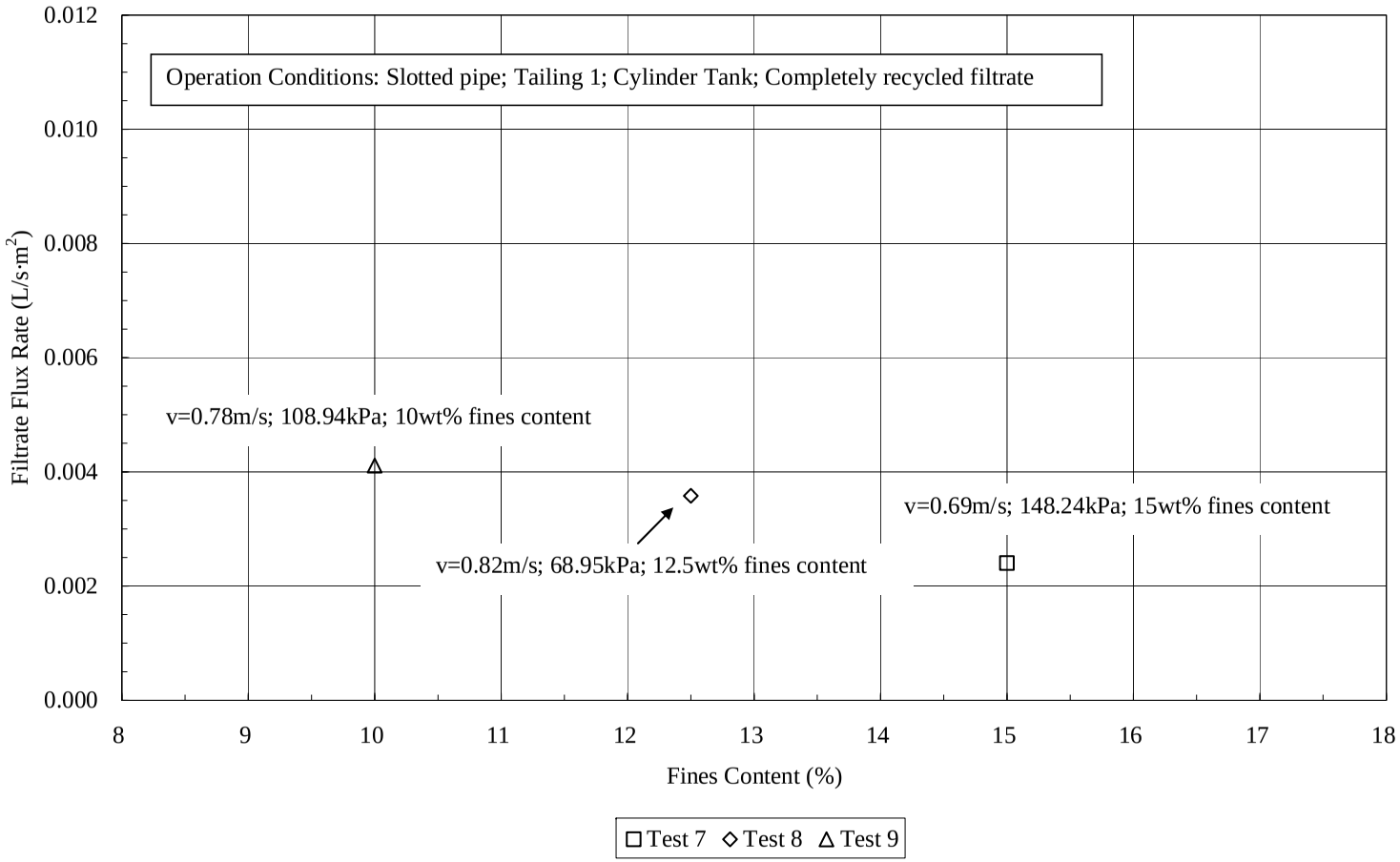

Figure 2.20 Effect of fines content on quasi-steady state filtrate flux rate (slotted pipe)

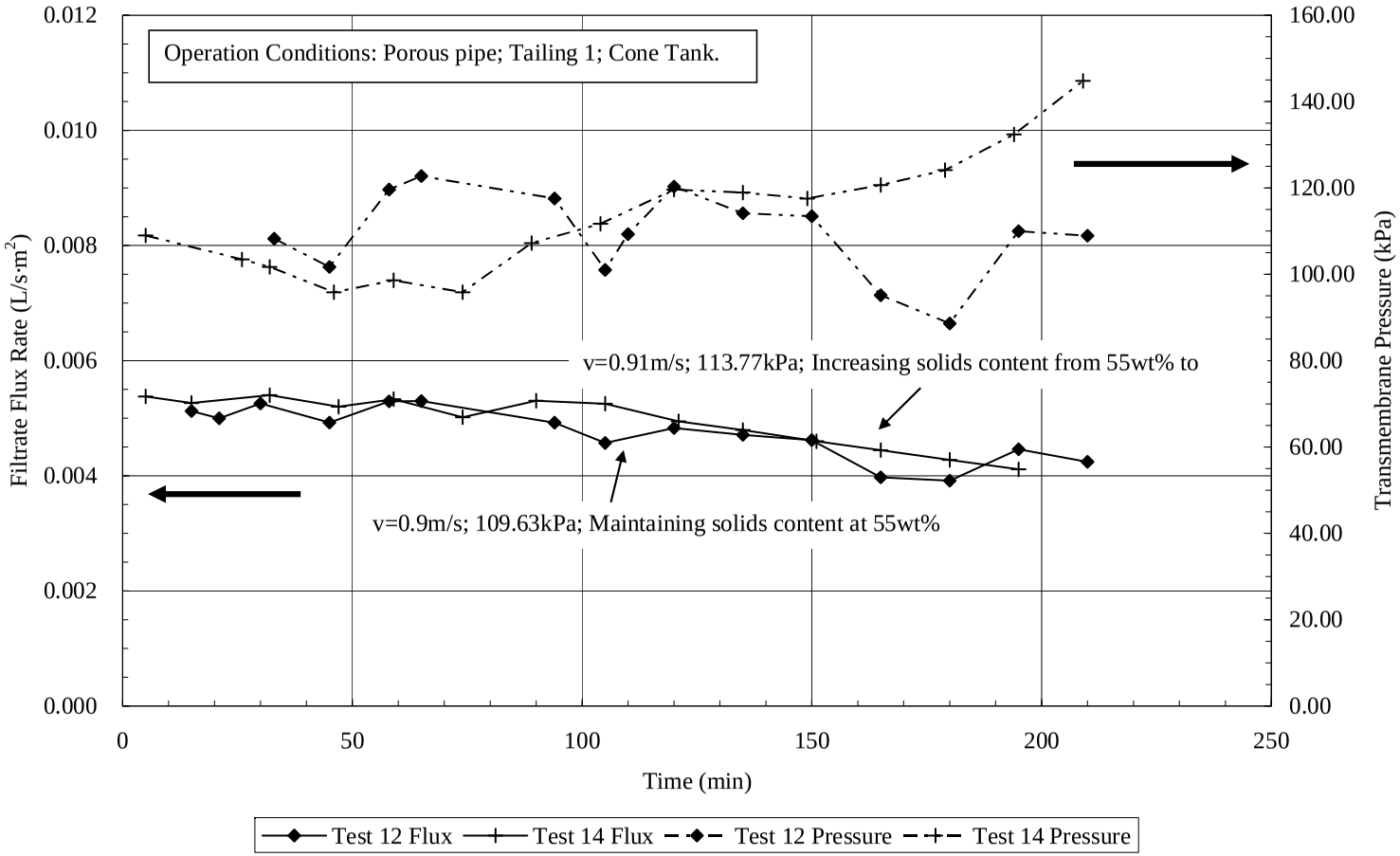

Figure 2.21 Effect of tailing slurry solid content on filtrate flux rate (porous pipe)

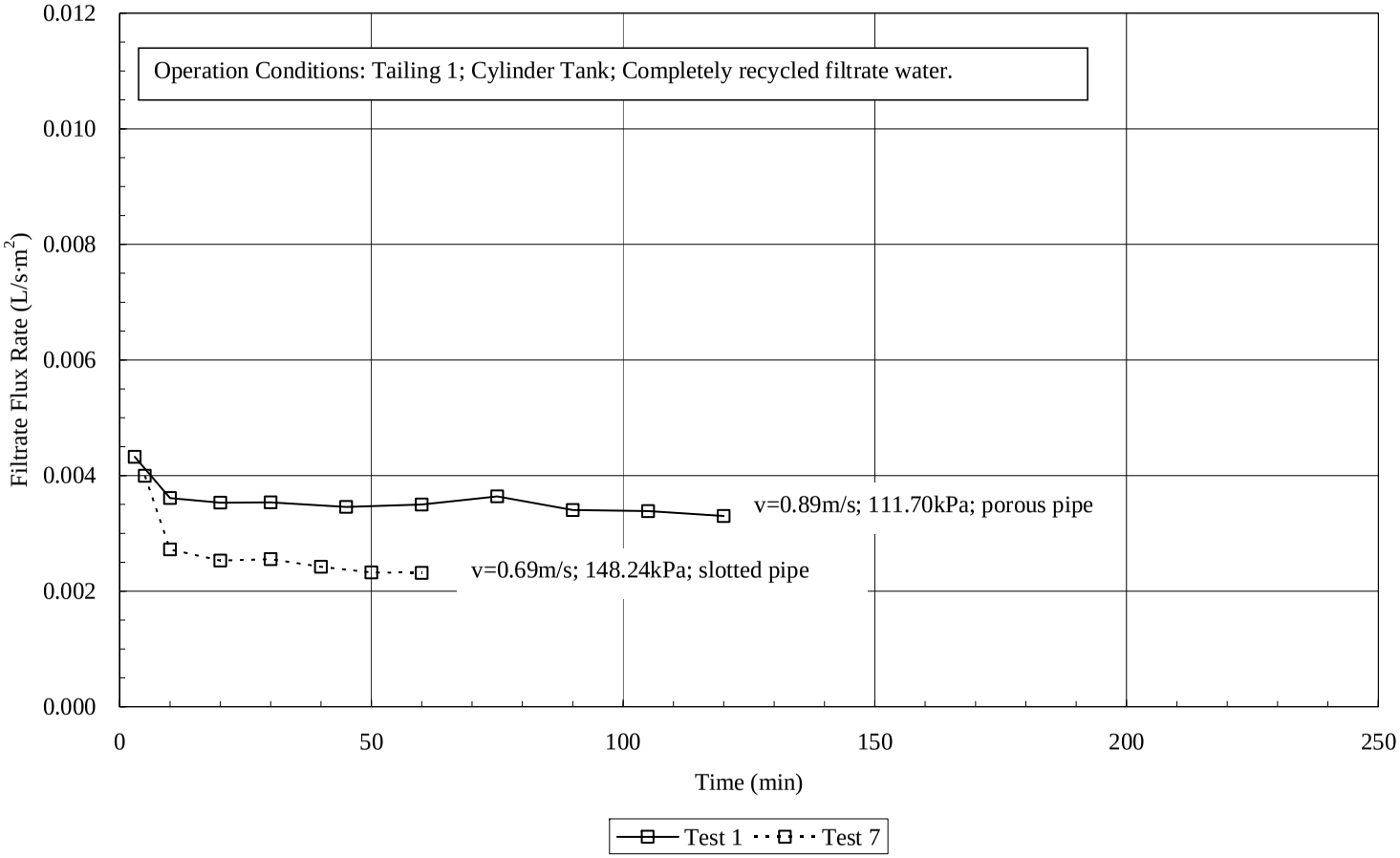

Figure 2.22 Effect of filter pipe on filtrate flux rate (Tailing 1)

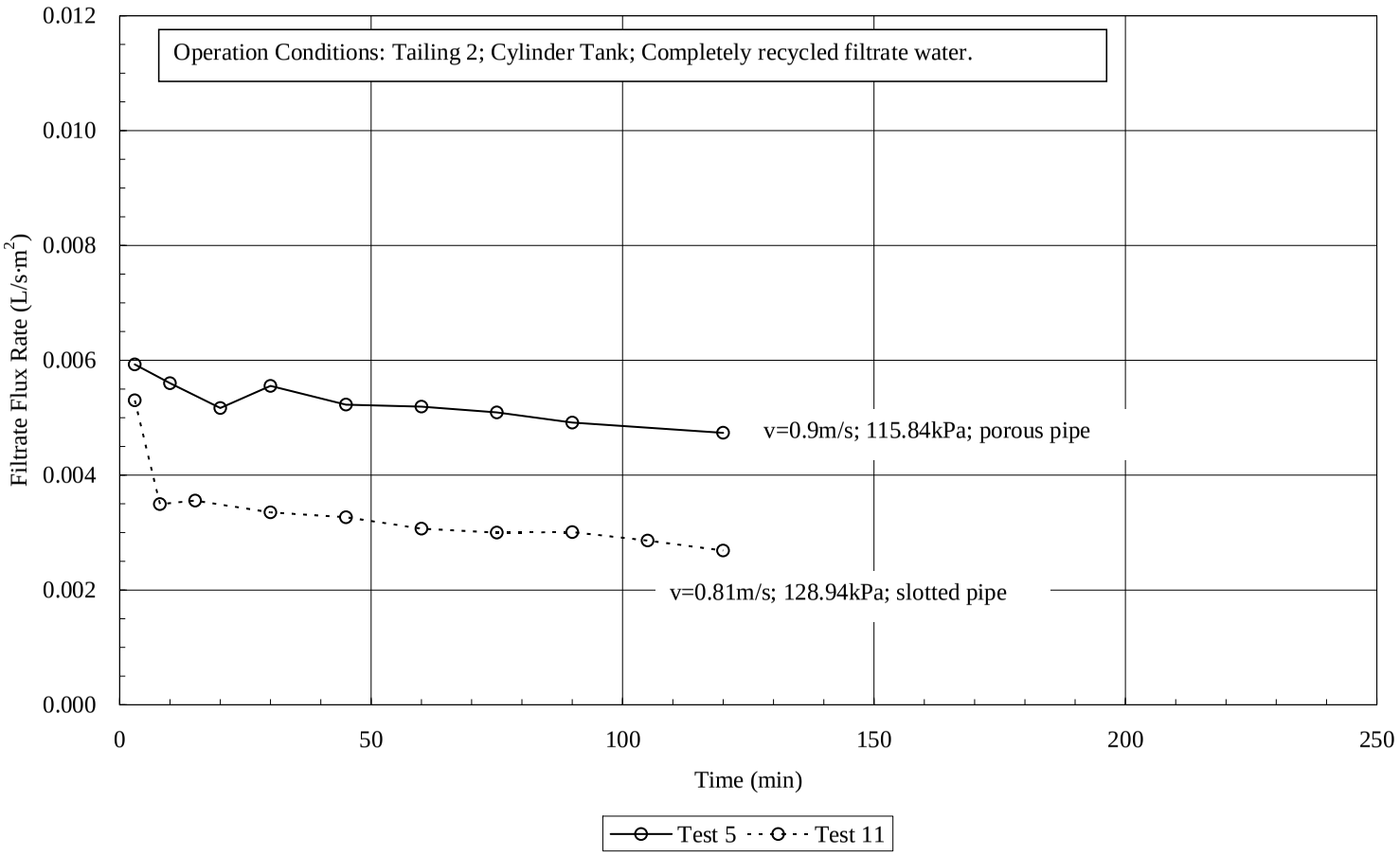

Figure 2.23 Effect of filter pipe on filtrate flux rate (Tailing 2)

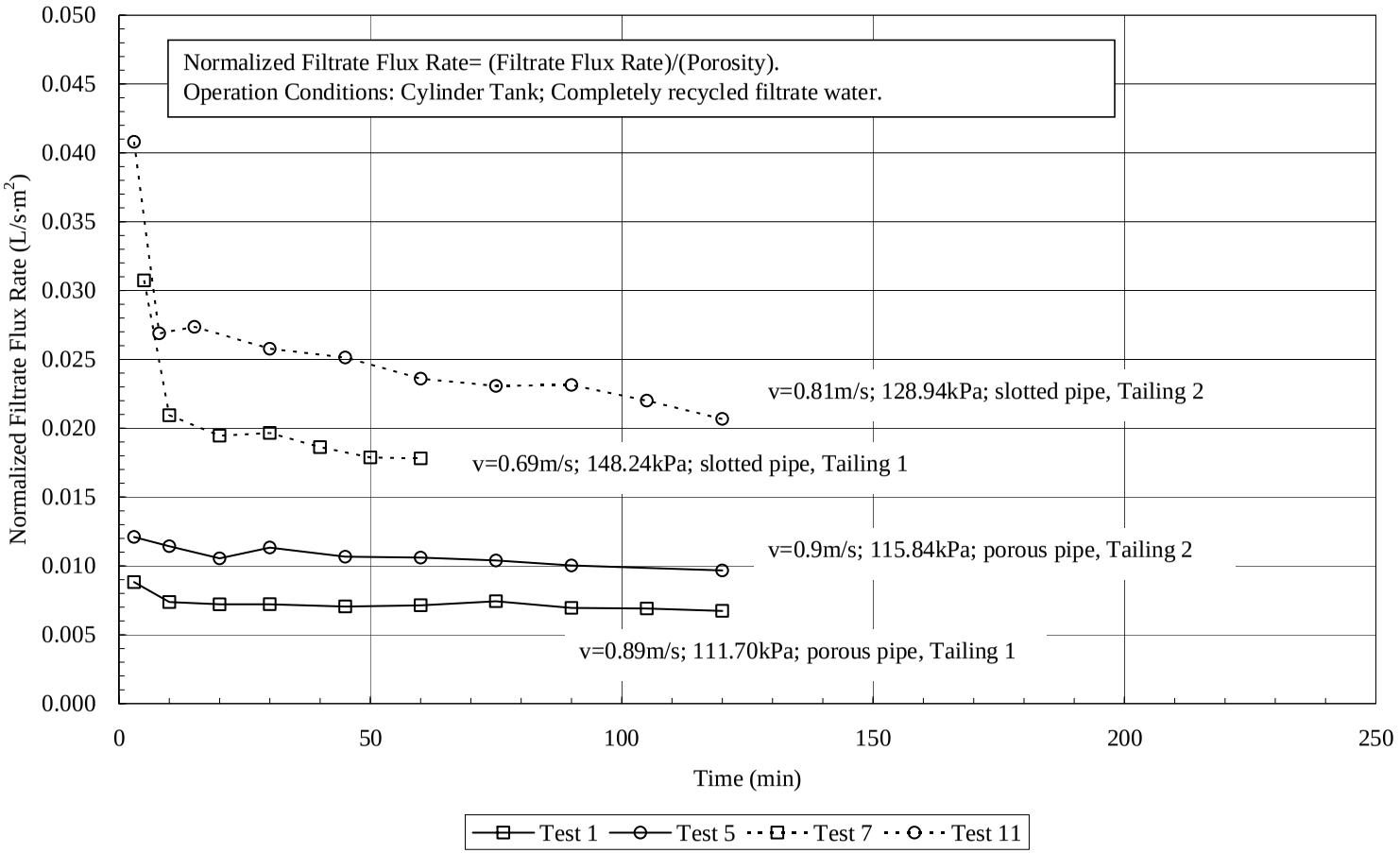

Figure 2.24 Effect of filter pipe on filtrate flux rate (normalized flux; (filtrate flux rate)/(porosity))

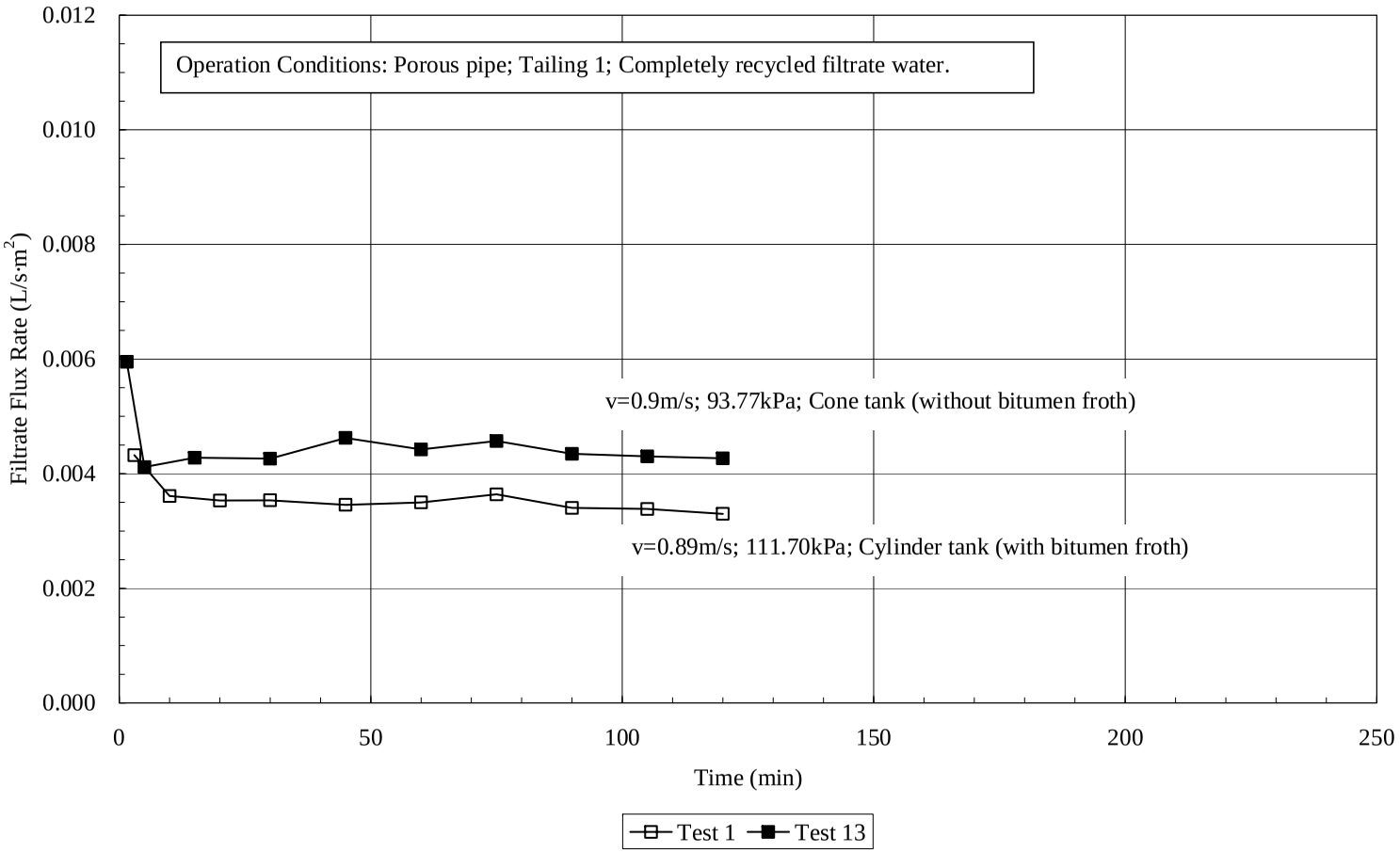

Figure 2.25 Effect of bitumen froth on filtrate flux rate (Tailing 1)

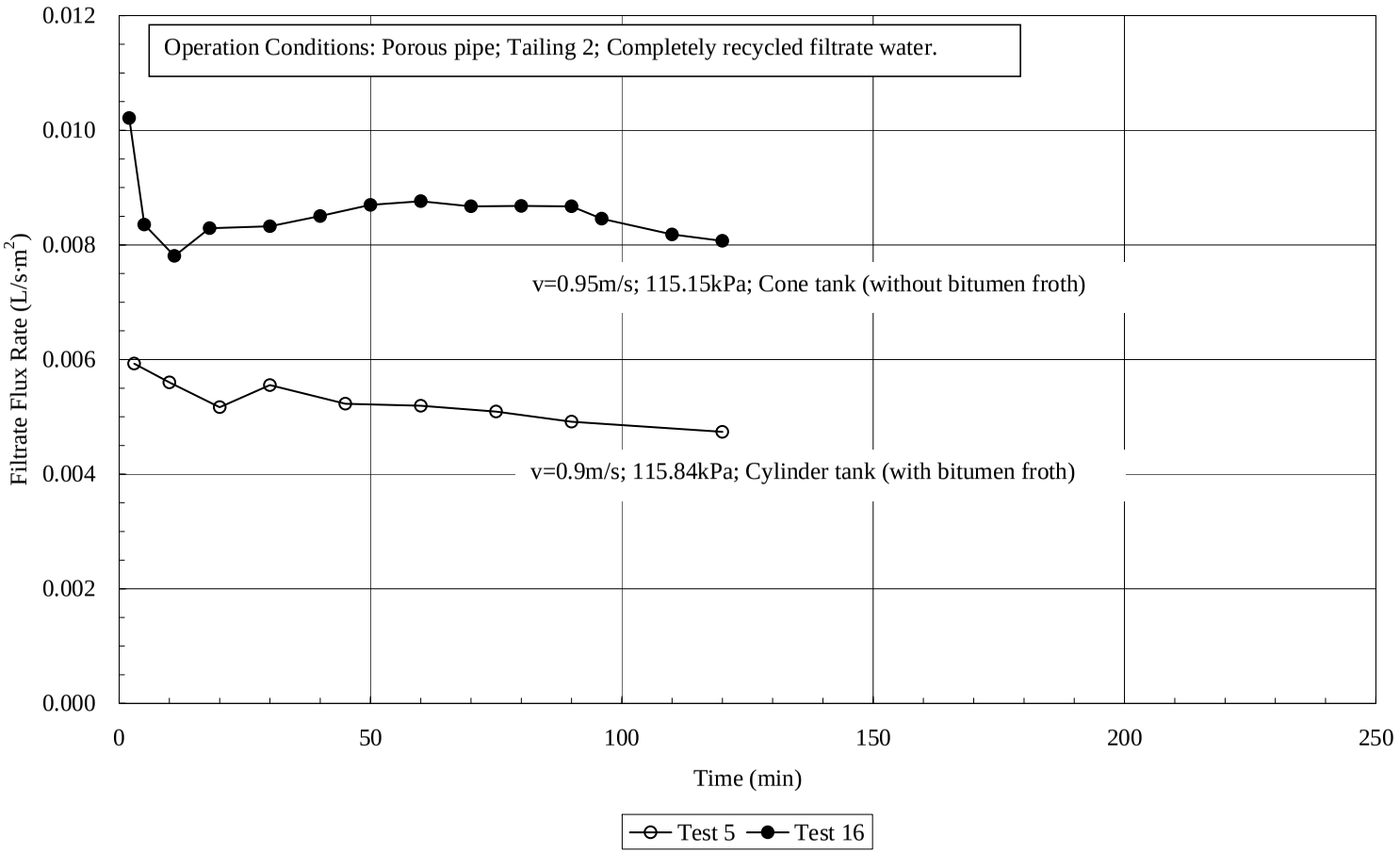

Figure 2.26 Effect of bitumen froth on filtrate flux rate (Tailing 2)

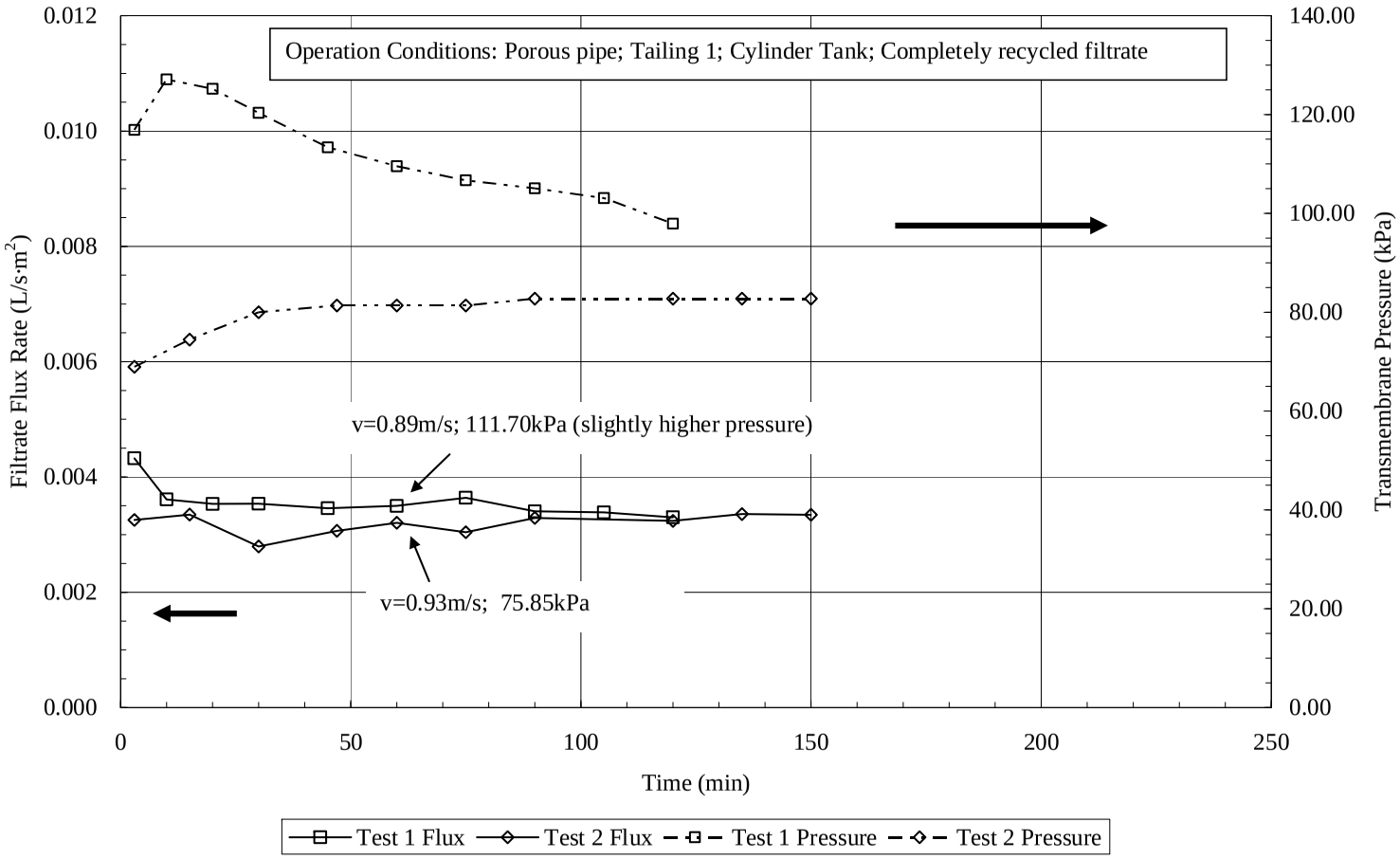

Figure 2.27 Effect of slightly transmembrane pressure increase on filtrate flux rate (porous pipe)

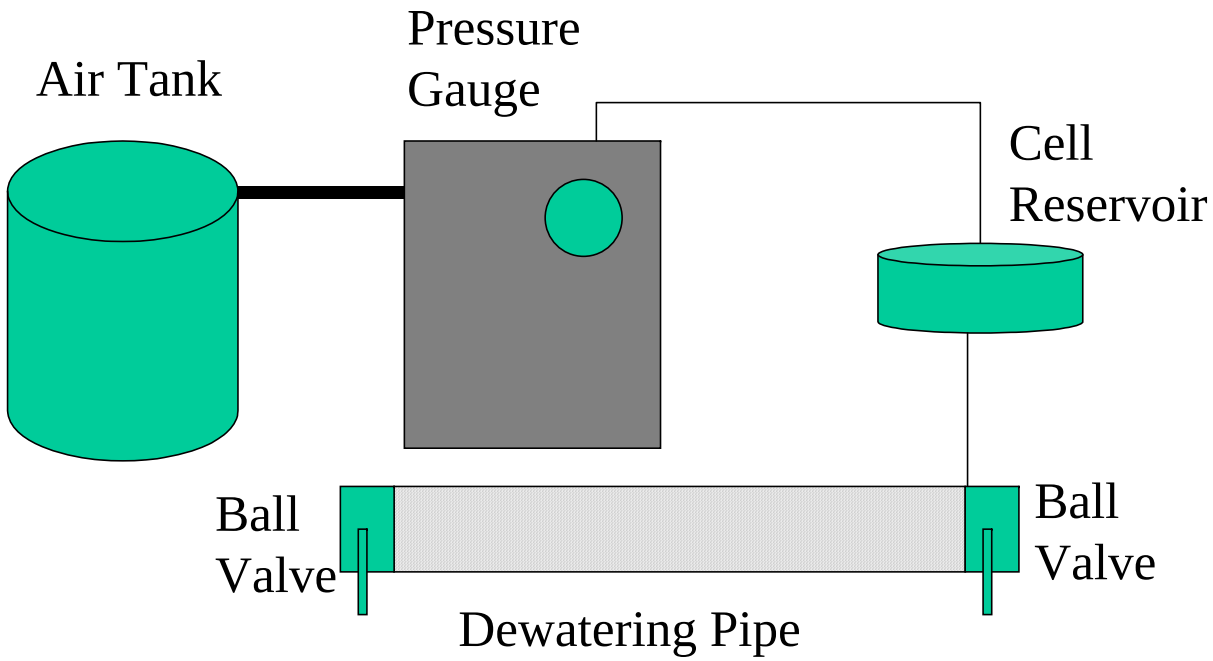

Figure 2.28 Sketch of high pressure test setup

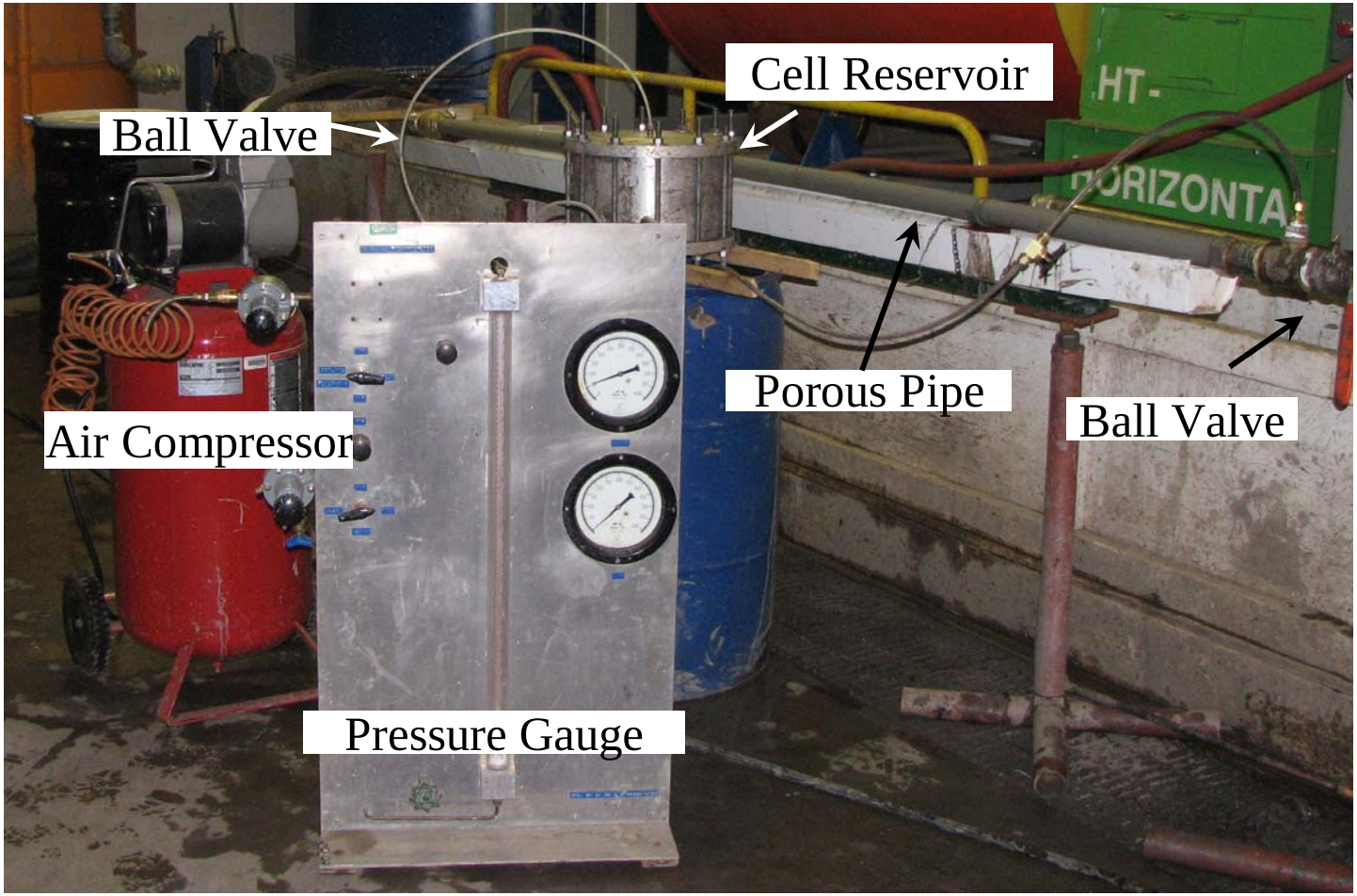

Figure 2.29 Photograph of high pressure test setup

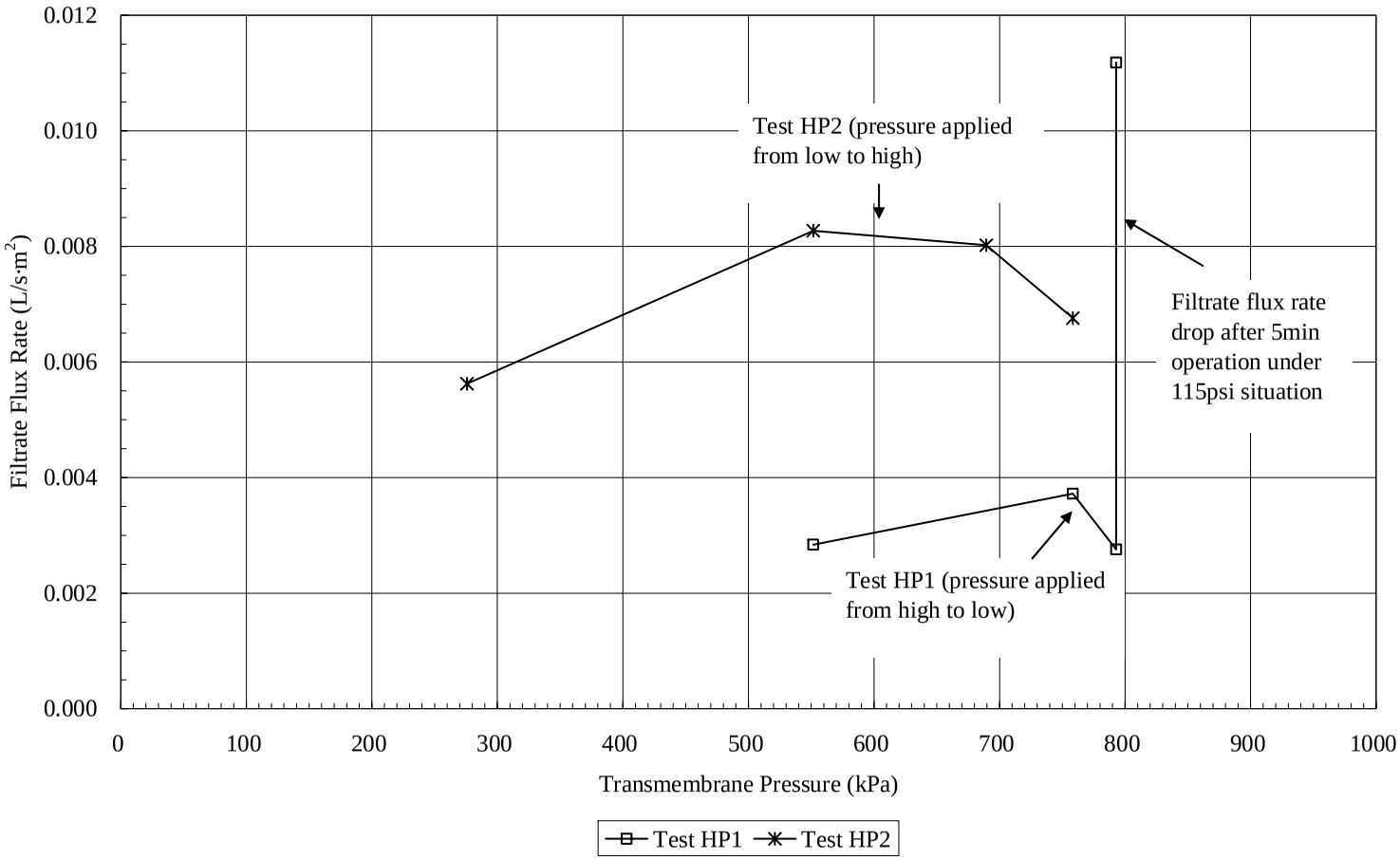

Figure 2.30 Relationship between filtrate flux rate and transmembrane pressure (High Pressure Test)

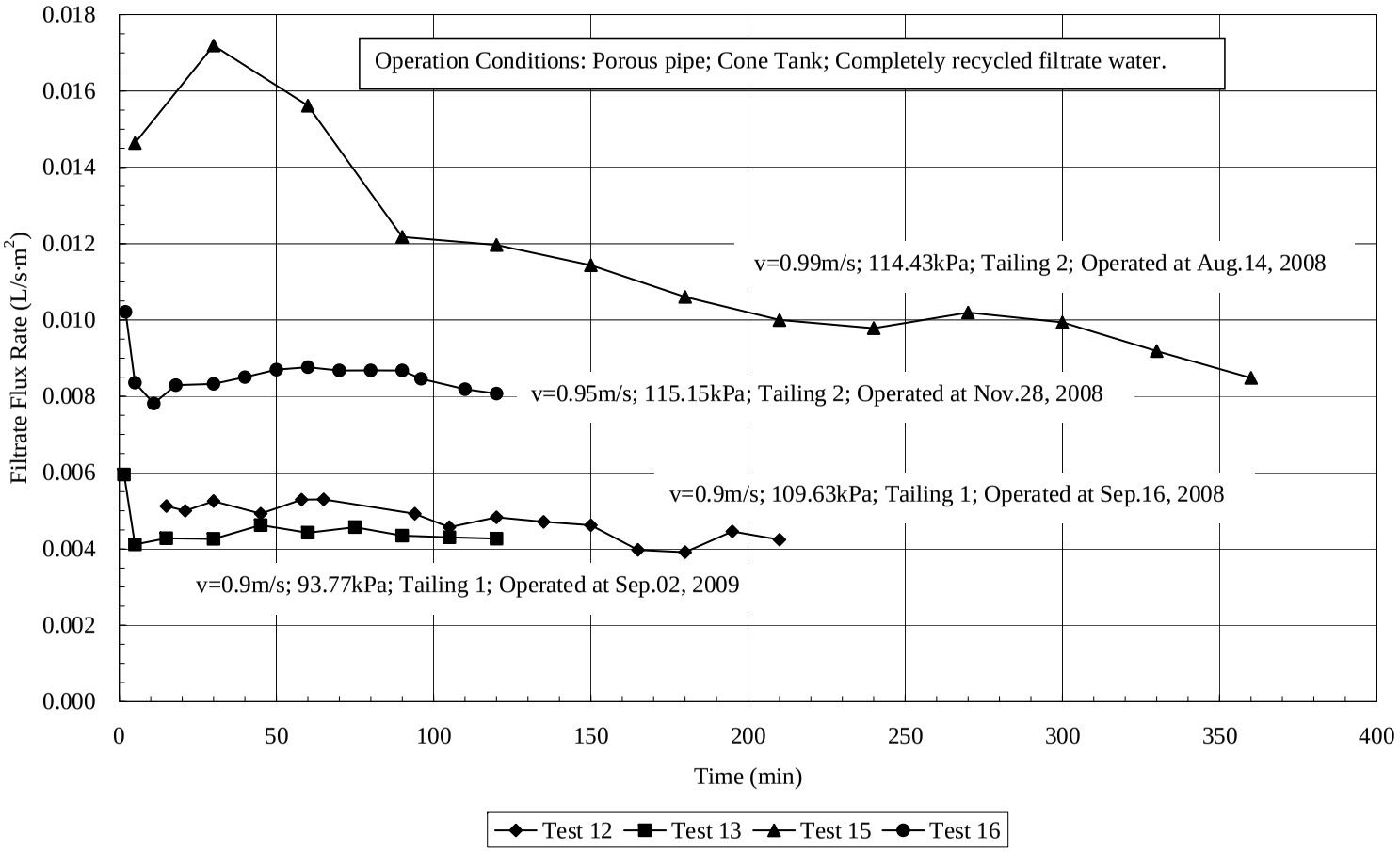

Figure 2.31 Effect of pores plug on filtrate flux rate after one-year operation (porous pipe)

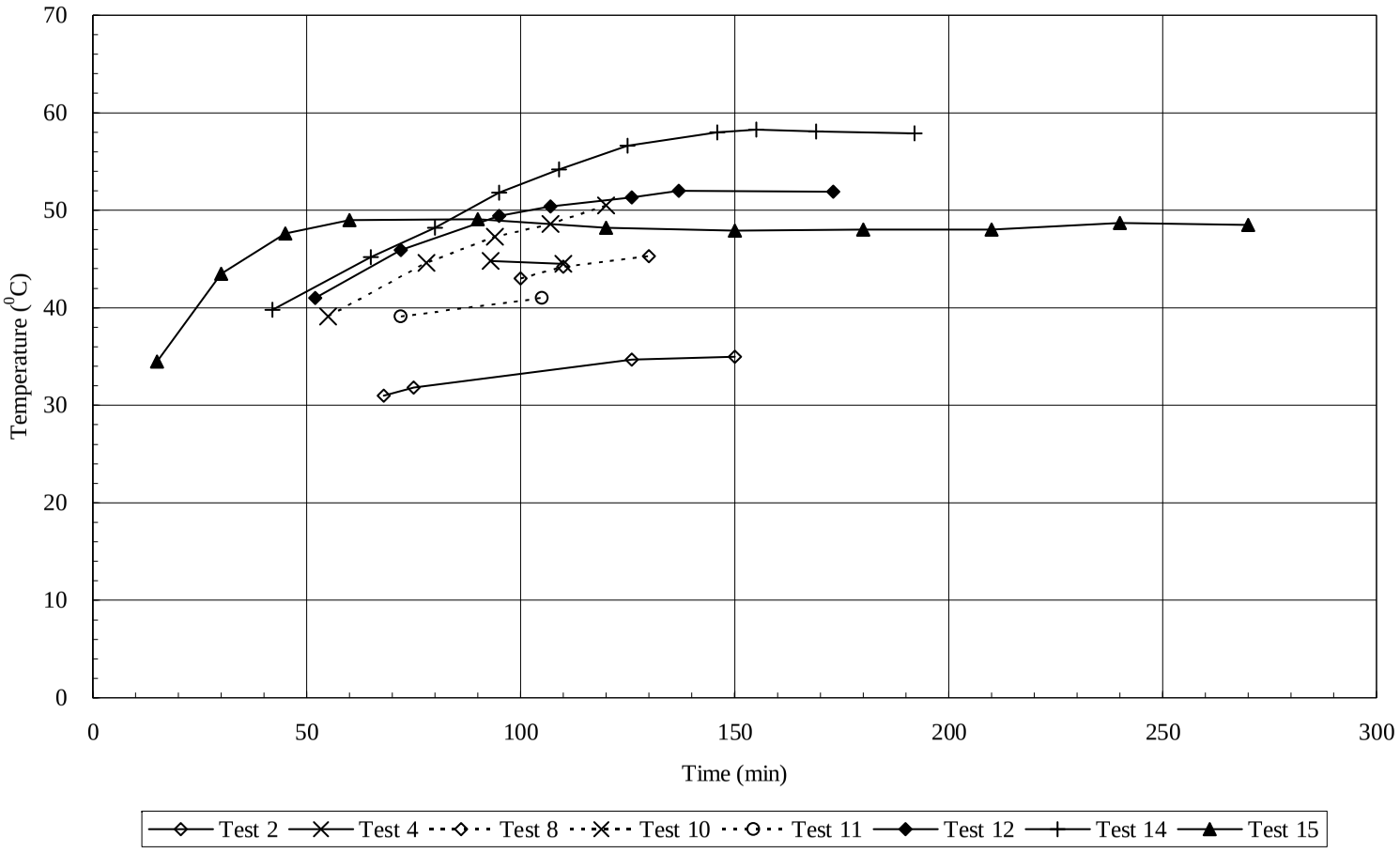

Figure 2.32 Heat generation during cross flow filtration test operation

Table 2.1 Information of two dewatering pipe

Pipe	Porous Pipe	Slotted Pipe
Length (m)	3.48	3.49
Pore Size/Slot Width (μm)	40	250
Inner Diameter (mm)	42	52
Porosity	49%	13%
Pipe Surface Area (m^2)	0.46	0.57

Note: Porosity is defined as (pores/slots open area)/(pipe surface area).

Table 2.2 Summary of all cross flow filtration tests operation condition

Test	Pipe	Tailings	Tank	Velocity (m/s)	Pressure (psi)	Pressure (kPa)	Other
Test 1	porous	Tailing 1	Cylinder	0.89	16.2	111.70	
Test 2	porous	Tailing 1	Cylinder	0.93	11	75.85	
Test 3	porous	Tailing 1	Cylinder	1.08	19	131.01	
Test 4	porous	Tailing 1	Cylinder	>2	10	68.95	pump capacity was at 60% at the beginning, up to 65% at 7min, 70% at 53min
Test 5	porous	Tailing 2	Cylinder	0.9	16.8	115.84	
Test 6	porous	Tailing 3	Cylinder	0.88	17.6	121.35	
Test 7	slotted	Tailing 1	Cylinder	0.69	21.5	148.24	15% fines content (original)
Test 8	slotted	Tailing 1	Cylinder	0.82	10	68.95	12.5% fines content

Table 2.2 Summary of all cross flow filtration tests operation condition (continuous)

Test	Pipe	Tailings	Tank	Velocity (m/s)	Pressure (psi)	Pressure (kPa)	Other
Test 9	slotted	Tailing 1	Cylinder	0.78	15.8	108.94	10% fines content
Test 10	slotted	Tailing 1	Cylinder	>2	12.5	86.19	pump capacity was at 80% at the beginning, up to 85% at 25min, 90% at 78min
Test 11	slotted	Tailing 2	Cylinder	0.81	18.7	128.94	
Test 12	porous	Tailing 1	Cone	0.9	15.9	109.63	
Test 13	porous	Tailing 1	Cone	0.9	13.6	93.77	operated after one year of Test 12
Test 14	porous	Tailing 1	Cone	0.91	16.5	113.77	increasing solid content during test
Test 15	porous	Tailing 2	Cone	0.99	16.6	114.43	first operation
Test 16	porous	Tailing 2	Cone	0.95	16.7	115.15	

Note (Table 2.2):

All tests (except Test 8&9) were started with 55wt% solids content and 15wt% fines content. All tests (except Test 14) were kept recycling filtrate water and maintained solids content during tests operation.

Velocity listed in Table 2.2 was calculated as (feed flow rate)/(pipe cross area). Feed flow rate used in the calculation was the average value during each test operation.

Transmembrane pressure value listed in Table 2.2 was the average pressure value of two digital pressure gauges at both ends of filter pipe and of the entire test operation.

Pump capacity listed in "Other" section of Test 4 and Test 10 was related to the feed flow rate. Generally, the increase in pump capacity enhances feed slurry flow rate (velocity). Since the flow meter used in these two tests did not work well (detailed described in section 2.5.1), an estimated value (>2m/s) was used to represent operation condition of Test 4 and Test 10.

Table 2.3 High pressure test filtrate flux rate and filtrate solid content

Test HP1				
Pressure (psi)	Pressure (kPa)	Flux (L/s·m^2)	Solid Content (%)	Flux (L/s·m^2) (cross flow filtration)
115 (0min)	792.93	0.01118	3.54	0.00330-0.00361
115 (5min)	792.93	0.00276	0.34	
110	758.45	0.00372		
80	551.60	0.00284	0.25	

Table 2.3 High pressure test filtrate flux rate and filtrate solid content (continuous)

Test HP2				
Pressure (psi)	Pressure (kPa)	Flux (L/s·m^2)	Solid Content (%)	Flux (L/s·m^2) (cross flow filtration)
40	275.80	0.00562		0.00345-0.00406
80	551.60	0.00827	0.08	
100	689.5	0.00802		
110	758.45	0.00676	0.1	

3 DIMENSIONAL ANALYSIS

3.1 Introduction

The cross flow filtration experiments presented in Chapter 2 were completed at laboratory scale. A dimensional analysis is presented in this chapter using this experiment data to establish the relationships between different variables in cross flow filtration. Dimensional analysis will provide insight to guide future experiments and to predict requirements and feasibility for large-scale testing of the technology.

3.2 Dimensional Analysis Procedure

The first step in dimensional analysis is to develop the equation, in which the dependent variable is expressed in terms of independent variables. In cross flow filtration, the objective of the dimensional analysis is to find the relationship between filtrate flux rate and the important parameters. Therefore the steady state filtrate flux rate (J; $m^3/m^2 \cdot s$) is selected as the dependent variable. The determination of independent variables in cross flow filtration dimensional analysis will be discussed in the following.

Equation 3.1 is a sample equation. Generally, the M-L-T (mass-length-time) system is chosen for dimensional analysis since this system eliminates the force dimension in fluid mechanics (Potter & Wiggert, 1997).

$$y = f(x_1, x_2, ..., x_{n-1}) \qquad 3.1$$

There are in total *n* variables in the original equation and one of them

is the dependent variable (y) and the others (x_1~x_{n-1}) are independent variables. Each dependent variable and independent variable should be represented using all 3 dimensions or at least 1, i.e. M, L and/or T. Then m of the $(n-1)$ independent variables (generally no more than three) are selected as repeating variables. The dependent variable (y) and remaining ($n-m-1$) independent variables will then be combined into m variables to form dimensionless parameters. Therefore the original equation will be written in dimensionless form. This procedure is known as the Buckingham Pi Theorem and the selected repeating variables should include all of the basic dimensions (Potter & Wiggert, 1997).

3.3 Dimensional Analysis of Cross Flow Filtration

In geotechnical engineering, water flows through a fully saturated soil can be represented using Darcy's Law (Craig, 1997). In cross flow filtration, filtrate flowing through the filter cake is similar to the water flow in soil. Therefore the filtrate flow rate in cross flow filtration can be represented using Darcy's law, which is a function of coefficient of hydraulic conductivity (k; m/s), hydraulic gradient (i; dimensionless) and filtrate area (A_f; m^2). The equation is shown as:

$$Q = kiA_f = k \cdot \frac{\Delta P / \gamma_w}{t_{cake}} \cdot (L \cdot C) \qquad 3.2$$

Q: filtrate flow rate; m^3/s

k: coefficient of hydraulic conductivity; m/s

i: hydraulic gradient; dimensionless

A_f: filtrate area; m^2

ΔP: transmembrane pressure; Pa (N/m^2)

γ_w: unit weight of water; kN/m^3

t_{cake}: thickness of cake; m

L: length of dewatering pipe; m

C: perimeter of cake; m

Filtrate flux rate (J; m^3/m^2·s) is calculated as (filtrate flow rate)/(total filtrate area) and is expressed as:

$$J = \frac{Q}{A_s} = k\frac{\Delta P/\gamma_w}{t_{cake}}\frac{(L\cdot C)}{(\frac{\pi L D_{pipe}^2}{4})} \text{ or } J = f(k, \Delta P, \gamma_w, t_{cake}, \pi, C, D_{pipe}) \quad 3.3$$

J: steady state filtrate flux rate; m^3/m^2·s

A_s: surface area of inside of filter pipe; m^2

D_{pipe}: filter pipe inner diameter; m

In equation 3.3, the coefficient of hydraulic conductivity (k), perimeter of cake (C) and cake thickness (t_{cake}) are not independent variables. The coefficient of permeability depends on the particle size distribution, particle shape, and soil structure that develops in the cake and viscosity of water (Craig, 1997). As discussed in Chapter 2, the slurry velocity can affect filter cake thickness and make up (particle size distribution). High slurry velocity causes more fine grained particles to enter cake structure and lower slurry velocity results in coarse particles being deposited to make up the cake. Therefore, the coefficient of hydraulic conductivity can be expressed as:

$$k = f(v_s, \mu_w, d_{cake}) \quad 3.4$$

k: coefficient of hydraulic conductivity; m/s

v_s: slurry velocity; m/s

μ_w: viscosity of filtrate water; N·s /m^2

d_{cake}: particle size within cake structure; m

The perimeter of filter cake is geometrically related to the thickness of filter cake and filter pipe diameter. The expression is shown below:

$$C = f(t_{cake}, D_{pipe}) \quad 3.5$$

C: perimeter of cake; m

t_{cake}: thickness of cake; m

D_{pipe}: filter pipe inner diameter; m

The feed slurry velocity is an important factor that affects filter cake thickness. Generally, higher feed velocity leads to higher shear forces at the slurry-cake boundary and reduces cake thickness (Hwang and Hong, 2006; Lu et al., 1993; Yan et al., 2003). Ripperger and Altmann's (2002) observed that an increase in transmembrane pressure results a linear increase in cake thickness. Other factors that affect cake thickness are particle size distribution in tailings and pipe diameter. Therefore, the expression for the filter cake thickness is given as:

$$t_{cake} = f(v_s, d_s, D_{pipe}, \Delta P) \quad 3.6$$

t_{cake}: thickness of cake; m

v_s: slurry velocity; m/s

d_s: Sauter mean diameter; m

D_{pipe}: filter pipe diameter; m

ΔP: transmembrane pressure; N/m^2

The Sauter mean diameter (d_s) is used to represent the particle size distribution in tailings slurry. According to Altmann and Ripperger (1997), the Sauter mean diameter of the particles deposited within the cake was used to calculate the filter cake resistance. The Sauter mean diameter is the particle diameter which has the same specific surface as all the particles in the original system (Richardson et al., 2002). The calculation of Sauter mean diameter is determined as:

$$d_s = \frac{\sum p_n}{\sum\left(\frac{p_n}{d_n}\right)} = \frac{p_1 + p_2 + \ldots + p_n}{\left(\frac{p_1}{d_1} + \frac{p_2}{d_2} + \ldots + \frac{p_n}{d_n}\right)} = \frac{1}{\sum\left(\frac{p_n}{d_n}\right)} \qquad 3.7$$

d_s: Sauter mean diameter; m

p_n: mass fraction of different particle size; %

d_n: particle size in tailings slurry; m

As described in equation 3.7, the Sauter mean diameter considers both particle size and the distribution of different particle size. Generally, the tailings slurry with more coarse particles and fewer fine particles has a larger Sauter mean diameter. Therefore, the Sauter mean diameter (d_s) is introduced to represent the particle size distribution in tailings slurry.

When equation 3.6 is substituted into equation 3.5, t_{cake} can be eliminated and after combining similar variables, equation 3.5 can be expressed as:

$$C = f(v_s, d_s, D_{pipe}, \Delta P) \qquad 3.8$$

Substitution of equation 3.4, 3.6 and 3.8 into equation 3.3 and rearranging the terms result in:

$$J = f(v_s, D_{pipe}, \mu_w, d_s, d_{cake}, \Delta P, \gamma_w, \pi) \quad 3.9$$

J: steady state filtrate flux rate; $m^3/m^2 \cdot s$

v_s: slurry velocity; m/s

D_{pipe}: filter pipe diameter; m

μ_w: viscosity of filtrate water; $N \cdot s/m^2$

d_s: Sauter mean diameter; m

d_{cake}: particle size within cake structure; m

ΔP: transmembrane pressure; Pa (N/m^2)

γ_w: unit weight of water; kN/m^3

As discussed in section 2.6.4, both filter pipe pore/slot size and porosity of filter pipe affect the measured filtrate flux rate. Therefore, a new parameter D_{pore} is introduced and a normalized filtrate flux rate (J/n_p) is used to replace the original filtrate flux rate in equation 3.9 to represent the effect of filter pipe pore/slot size and porosity of the filter pipe respectively.

The variable d_{cake} (particle size within cake structure) in equation 3.9 is related to the slurry velocity (v_s) and particle size distribution of feed tailings, which is the Sauter mean diameter (d_s), which have been discussed in section 2.6.1 and 2.6.2. Therefore, the variable d_{cake} can be replaced by v_s and d_s in equation 3.9.

As discussed in section 2.5.8, the porous pipe resistance to filtrate

water also affects filtrate flux rate. The presence of bitumen and fines in the slurry can increase pipe resistance significantly. Therefore, the filter pipe resistance is also introduced into equation 3.9. According to Ripperger and Altmann (2002), the total layer resistance can be calculated as:

$$R_c + R_p = \frac{\Delta P}{\mu_w \cdot J} \qquad 3.10$$

R_c: filter cake resistance to water, 1/m

R_p: filter pipe resistance to water, 1/m

ΔP: transmembrane pressure; Pa (N/m^2)

μ_w: viscosity of filtrate water; $N \cdot s/m^2$

J: steady state filtrate flux rate; $m^3/m^2 \cdot s$

Since no cake was formed during the pure water tests introduced in section 2.5.1 (Figure 3.1), R_c is assumed 0 and the pure water filtrate flux rate (J_w) is used to replace the steady state filtrate flux rate (J) in equation 3.11. R_p is then calculated as 1.38×10^{12} m^{-1} for porous pipe and 0 m^{-1} for slotted pipe.

The slurry solids content is not included in equation 3.9 since based on the discussion in section 2.6.3, the slurry solids content does not affect filtrate flux rate. It is therefore reasonable to leave it out of equation 3.9.

After these modifications, the revised equation is then written as:

$$\frac{J}{n_p} = f(v_s, D_{pore}, D_{pipe}, \mu_w, \Delta P, d_s, R_p, \pi, \gamma_w) \qquad 3.11$$

J: steady state filtrate flux rate; $m^3/m^2 \cdot s$

n_p: porosity of the porous pipe; dimensionless

v_s: slurry velocity; m/s

D_{pore}: pipe pore/slot size; m

D_{pipe}: filter pipe diameter; m

μ_w: viscosity of filtrate water; $N \cdot s/m^2$

ΔP: transmembrane pressure; Pa (N/m^2)

d_s: Sauter mean diameter; m

R_p: porous filter pipe resistance to water, 1/m

γ_w: unit weight of water; kN/m^3

This equation includes all parameters introduced in section 2.3, which are the important parameters controlling the performance of cross flow filtration in porous pipe. In equation 3.11, the effect of slurry velocity, transmembrane pressure and slurry particle size distribution are directly represented. Filter pipe properties are represented by the pipe diameter, pipe resistance, pore/slot size and porosity. Temperature is represented by the viscosity of filtrate water.

Slurry velocity (v_s), filter pipe diameter (D_{pipe}) and viscosity of filtrate water (μ_w) are chosen as repeating variables since these variables include all basic dimensions introduced in section 3.3. The equation is then written as:

$$\frac{J}{n_p \cdot v_s} = f\left(\frac{\Delta P \cdot D_{pipe}}{\mu_w \cdot v_s}, \frac{D_{pore}}{D_{pipe}}, \frac{d_s}{D_{pipe}}, R_p \cdot D_{pipe}, \pi, \frac{\gamma_w \cdot D_{pipe}^2}{\mu_w \cdot v_s}\right) \quad 3.12$$

Another option is to use filter pipe pore/slot size (D_{pore}) to replace filter pipe diameter (D_{pipe}) as the repeating variable. Therefore the equation can be written as:

$$\frac{J}{n_p \cdot v_s} = f\left(\frac{\Delta P \cdot D_{pore}}{\mu_w \cdot v_s}, \frac{D_{pipe}}{D_{pore}}, \frac{d_s}{D_{pore}}, R_p \cdot D_{pore}, \pi, \frac{\gamma_w \cdot D_{pore}^2}{\mu_w \cdot v_s}\right) \quad 3.13$$

Equation 3.12 and equation 3.13 provide information from two aspects. Equation 3.12 provides observation about the effect of the filter pipe pore/slot size (D_{pore}) on the relationship between filtrate flux rate and other parameters, while equation 3.13 provides the effect of filter pipe diameter (D_{pipe}) on the relationship between filtrate flux rate and other parameters.

3.4 Dimensional Analysis Results

Figure 3.2 shows the filtrate flux rate values of all cross flow filtration tests discussed in Chapter 2. Since the test operations did not fully achieve steady-state, the quasi-steady state filtrate flux rate approaches a constant value during each test and was used for analysis. The quasi-steady state of most tests was achieved after one hour of operation. For those tests with only one hour operation (Test 7 and Test 9), the quasi-steady state was achieved after half hour (Figure 3.2). Therefore an average value after half hour was used in these two tests. In Test 4 and Test 10, since the feed velocity was not available, an estimated value of 2m/s for both tests is used in this dimensional

analysis. All dimensional analysis parameters are shown in Table 3.1 and Table 3.2.

Figure 3.3 and Figure 3.4 show the dimensional analysis results based on equation 3.12 and 3.13 respectively. The name “cylinder porous T1 (15% FC)” shows the feed tank type (cylinder), filter pipe type (porous), tailings type (T1: Tailing 1) and fines content (15% FC: 15wt% fines content).

The boundary condition in determining the best fitted curve for the tests using Tailing 1 (“cylinder porous T1 (15% FC)”, “cone porous T1 (15% FC)” and “cylinder slotted T1 (15% FC)”) is that the curve goes through the origin. Based on the observation from each test, no filtrate flow was obtained after the feed pump was turned off and transmembrane pressure was released. In preparation for the high pressure tests discussed in Chapter 2, even when the porous pipe was full of tailings, no filtrate flow was obtained until pressure was applied. Therefore, the power function curve is selected as the best fitted curve for “cylinder porous T1 (15% FC)” and “cone porous T1 (15% FC)” tests and the equations and R^2 values are shown in the figures. Since there are only two data points for “cylinder slotted T1 (15% FC)”, a straight line going though the origin is selected and shown in each figure.

3.5 Dimensional Analysis Discussion

As shown in both figures, if all independent variables are fixed except the transmembrane pressure (ΔP), the filtrate flux rate increases with

pressure and the increasing rate decreases as the pressure increases. This observation is consistent with the discussion in section 2.6.6 that the presence of an optimal transmembrane pressure producing the highest filtrate flux rate is possible. With larger Sauter mean diameter, higher filtrate flux rate is obtained under the same operation conditions. It seems the filtrate flux rate using slotted pipe (larger pore/slot size) is more sensitive to the Sauter mean diameter, i.e. particle size distribution of tailings slurry.

The two solid lines, “cylinder porous T1 (15% FC)” and “cone porous T1 (15% FC)”, have similar trends (slope). This indicates the decrease in filtrate flux rate using the cylinder feed tank is mainly due to the presence of bitumen froth that enters the filter pipe since all other conditions between these two sets of tests remain the same.

In Figure 3.3, the slope of “cylinder slotted T1 (15% FC)” is steeper than the slope of “cylinder porous T1 (15% FC)”. This probably means that, if the filter pipe diameter and porosity are the same, the increase in filtrate flux rate with transmembrane pressure is faster with the larger pore/slot size (larger D_{pore}/D_{pipe} value). Since there are only two tests for the “cylinder slotted T1 (15% FC)” condition, it requires additional tests using the slotted pipe or porous pipe with larger pores to verify this observation.

The scale in Figure 3.4 is too large to clearly show the variation in the data for the “cylinder porous T1 (15% FC)” and “cone porous T1 (15% FC)” tests so an enlarged figure of the dashed area in Figure 3.4

is presented in Figure 3.5. As shown in Figure 3.5, for the same porosity and pore/slot size, a larger diameter filter pipe (larger D_{pipe}/D_{pore} value) generates greater filtrate flux rate for the same transmembrane pressures. According to Yan et al. (2003), a larger diameter filter pipe is expected to increase the available filtrate area under the same shear rate, resulting in higher filtrate flux rate for the same transmembrane pressure. Tests using larger diameter porous pipe (same pore size and porosity) to verify this observation are needed.

3.6 Conclusion and Future Work

A dimensional analysis is presented. The dimensionless equations were derived from the Darcy's law and then modified using cross flow filtration theory. The Sauter mean diameter is introduced in this dimensional analysis to represent the particle size distribution within the tailings. The ultimate equation (equation 3.11) includes the effect of the important parameters in cross flow filtration.

The filtrate flux rate data from tests using Tailing 1 are analyzed and power function equations proves the best fit to the tests data and boundary condition (no filtrate flow under zero pressure situation).

Based on the dimensional analysis, an increase in transmembrane pressure leads to higher filtrate flux rate but the increasing rate decreases at high pressures. This indicates the presence of an optimal pressure that provides the greatest filtrate flux rate. Tailings with larger Sauter mean diameter provides higher filtrate flux rate under the same operation conditions.

Another observation is that, the filter pipe with a larger pore/slot size has a faster filtrate flux increasing rate with pressure. Larger diameter filter pipe have higher filtrate flux rate even under the same pressure level.

From the above discussion, cross flow filtration tests with larger diameter and pore/slot size filter pipes are needed to demonstrate the effect of filter pipe properties to enhance the dimensional analysis and improve its application for different mine tailings.

3.7 References

Altamnn, J., and Ripperger, S.1997. Particle deposition and layer formation at the crossflow microfiltration. Journal of Membrane Science, **124**: 119-128.

Beier, N., and Sego, D. 2008. Dewatering of oil sands tailings using cross flow filtration. *In* Proceedings of the 61st Canadian Geotechnical Conference, Edmonton, AB., 21-24 September 2008. Canadian Geotechnical Society, Edmonton, pp. 761-768

Craig, R.F. 1997. Seepage. *In* Soil Mechanics, 6th edition. Spon Press, London and New York. pp. 38-80

Hwang, K.J., and Hong, M.T. 2006. Effect of slurry rheology on the performance of cross-flow filtration. Journal of Chemical Engineering of Japan, **39**(7): 693-702

Lu, Wei-ming., Hwang, Kuo-jen., and Ju, Shang-Chung. 1993. Studies on the mechanism of cross-flow filtration. Chemical Engineering Science, **48**(5): 863-872

Potter, M.C., and Wiggert, M.C. 1997. Dimensional analysis and similitude. *In* Mechanics of fluids, 2nd edition. Prentice-Hall, Inc., NJ, pp. 225-257

Richardson, J.F., Harker, J.H., and Backhurst, J.R. 2002. Particle characterization. *In* Coulson and Richardson's chemical engineering: Particle technology and separation processes, Vol 2, 5th edition. Butterworth Heinemann, Oxford. pp. 2-22.

Ripperger, S., and Altamnn, J. 2002. Crossflow microfiltration – State of the art. Separation and Purification Technology, **26**: 19-31.

Yan, D., Parker, T., and Ryan, S. 2003. Dewatering of fine slurries by the Kalgoorlie Filter Pipe. Minerals Engineering, **16**: 283-289.

3.8 Figures and Tables

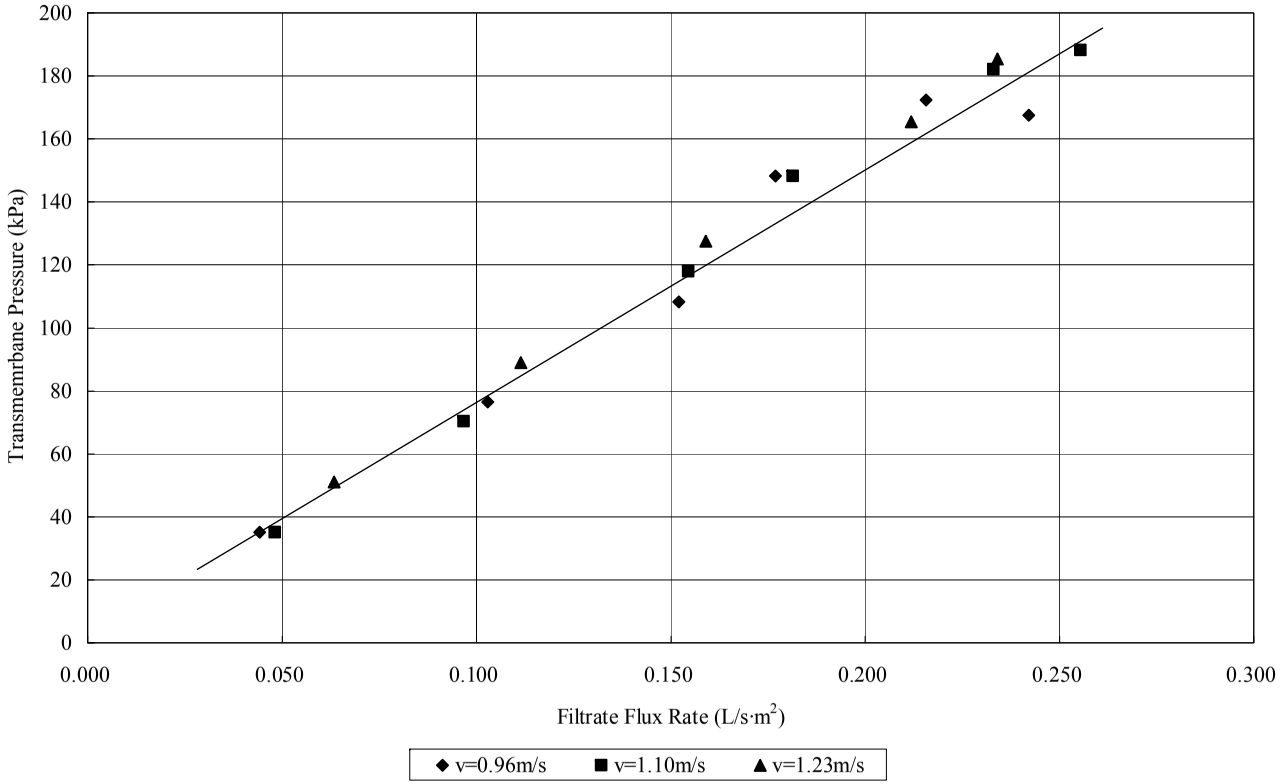

Figure 3.1 Filtrate flux rate data of pure water tests (porous pipe)

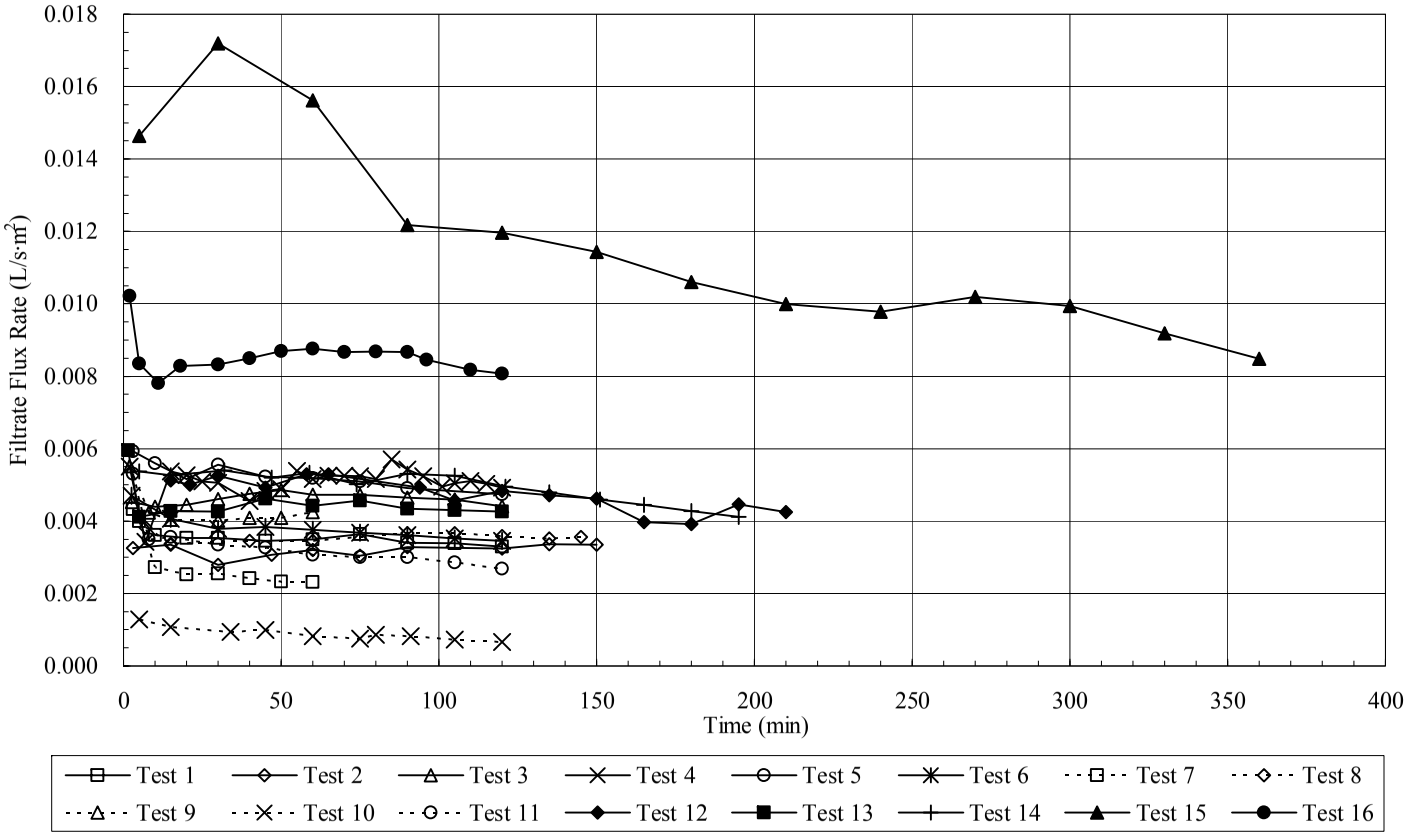

Figure 3.2 Filtrate flux rate data of all tests

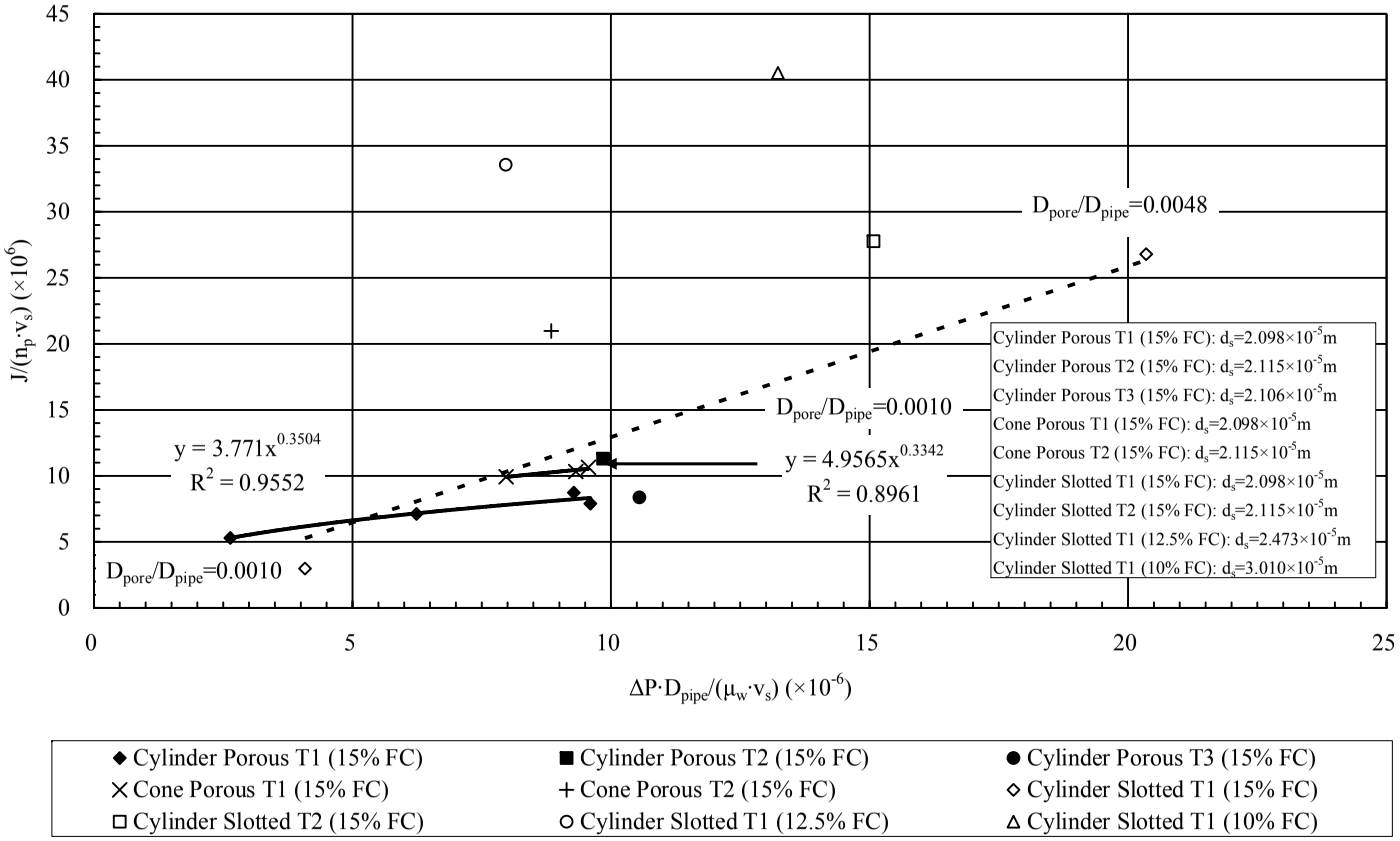

Figure 3.3 Dimensional analysis based on equation 3.12

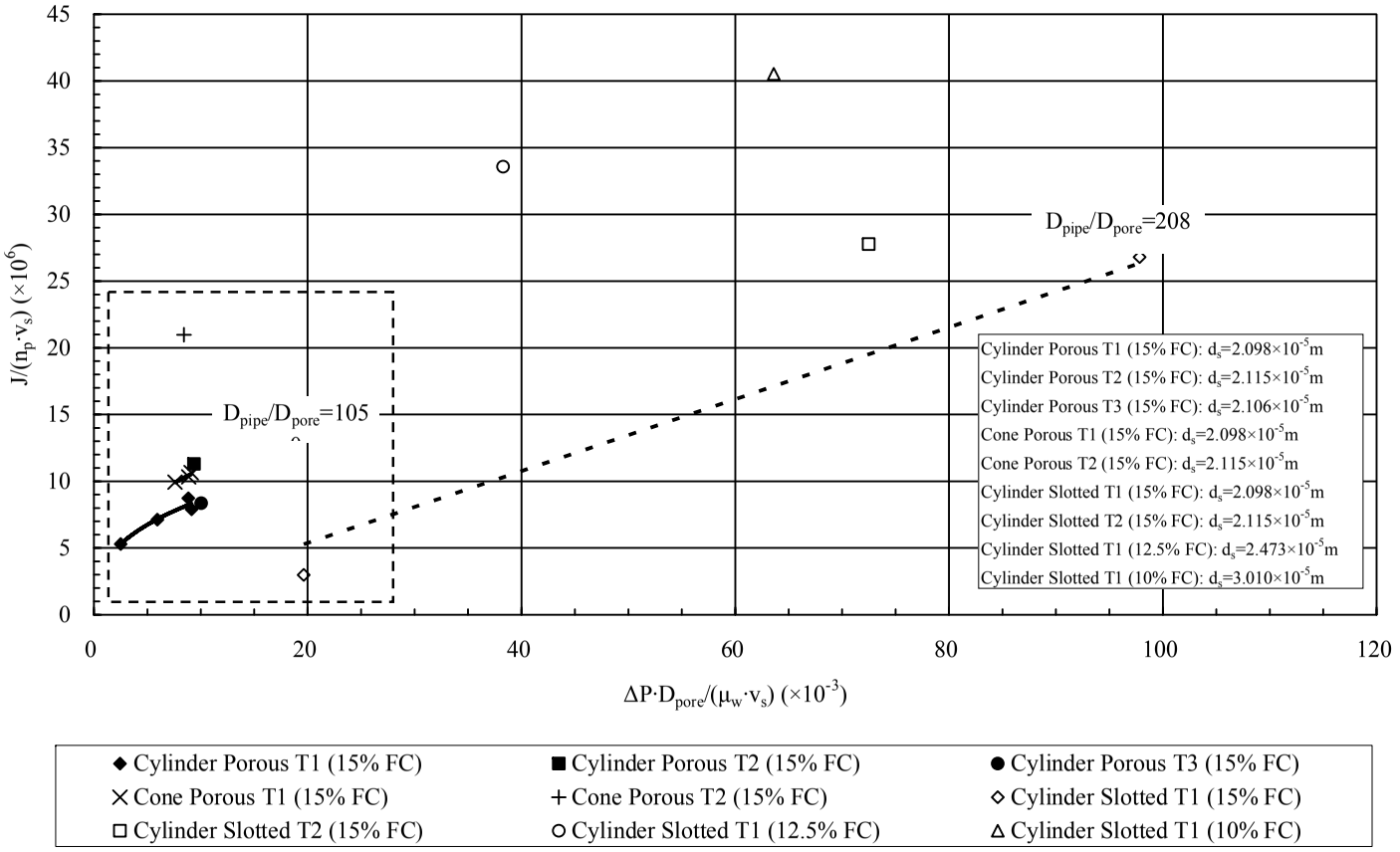

Figure 3.4 Dimensional analysis based on equation 3.13

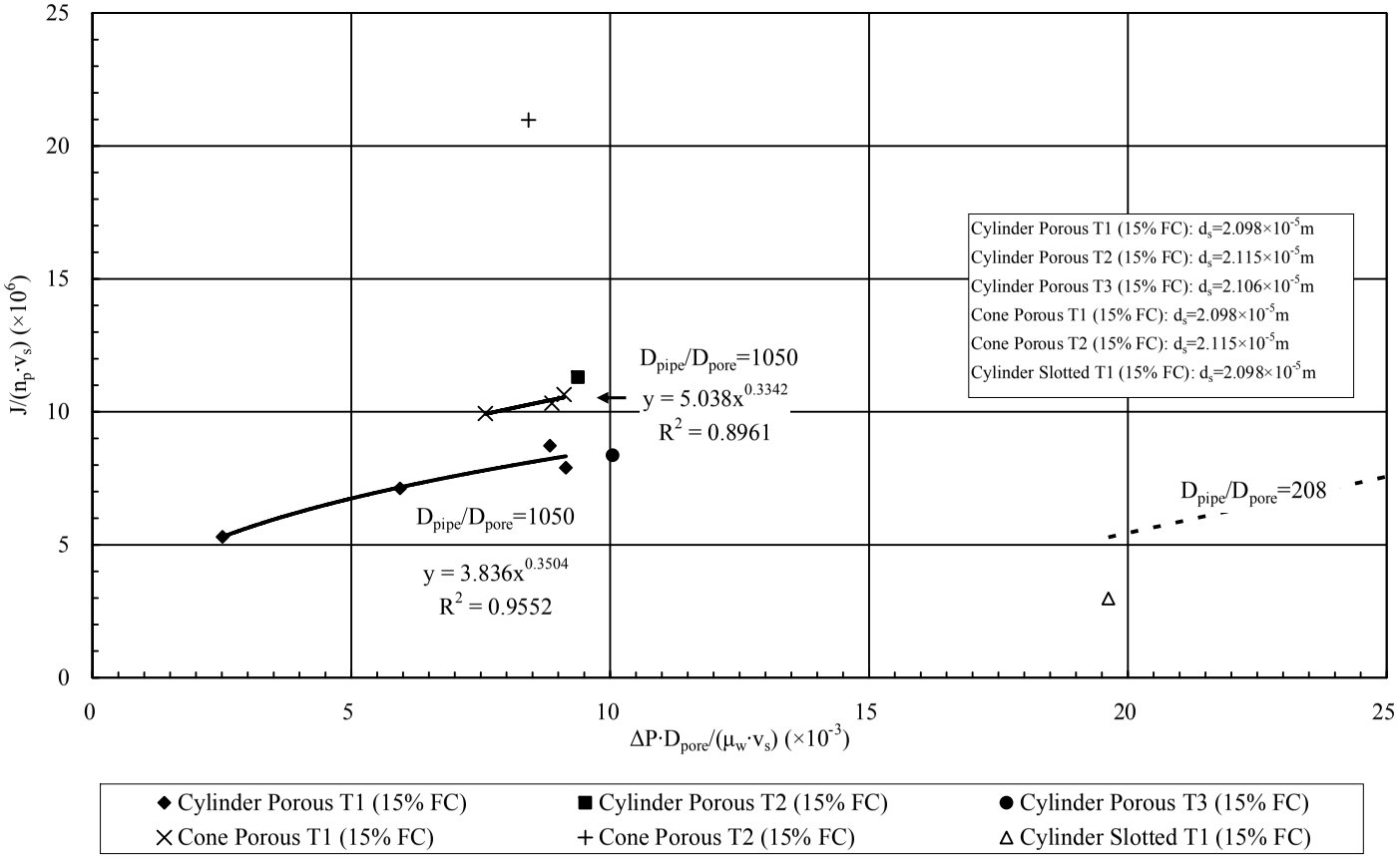

Figure 3.5 Enlarged figure for dashed area in Figure 3.4

Table 3.1 Dimensional analysis

Test	Pipe	Tailing	Tank	Velocity (m/s)	Pipe Diameter (m)	Porosity	Pore/Slot size (m)	Pressure (kPa / kN/m^2)	Filtrate Flux Rate ($L/s \cdot m^2$)	Sauter mean diameter (m)
Test 1	porous	Tailing 1	Cylinder	0.89	4.2×10^{-2}	49%	4.0×10^{-5}	111.70	0.00345	2.098×10^{-5}
Test 2	porous	Tailing 1	Cylinder	0.93	4.2×10^{-2}	49%	4.0×10^{-5}	75.85	0.00324	2.098×10^{-5}
Test 3	porous	Tailing 1	Cylinder	1.08	4.2×10^{-2}	49%	4.0×10^{-5}	131.01	0.00462	2.098×10^{-5}
Test 4	porous	Tailing 1	Cylinder	2	4.2×10^{-2}	49%	4.0×10^{-5}	68.95	0.00519	2.098×10^{-5}
Test 5	porous	Tailing 2	Cylinder	0.9	4.2×10^{-2}	49%	4.0×10^{-5}	115.84	0.00498	2.115×10^{-5}
Test 6	porous	Tailing 3	Cylinder	0.88	4.2×10^{-2}	49%	4.0×10^{-5}	121.35	0.00361	2.106×10^{-5}
Test 7	slotted	Tailing 1	Cylinder	0.69	5.2×10^{-2}	13%	2.50×10^{-4}	148.24	0.00240	2.098×10^{-5}
Test 8	slotted	Tailing 1	Cylinder	0.82	5.2×10^{-2}	13%	2.50×10^{-4}	68.95	0.00358	2.473×10^{-5}
Test 9	slotted	Tailing 1	Cylinder	0.78	5.2×10^{-2}	13%	2.50×10^{-4}	108.94	0.00411	3.010×10^{-5}
Test 10	slotted	Tailing 1	Cylinder	2	5.2×10^{-2}	13%	2.50×10^{-4}	86.19	0.00077	2.098×10^{-5}
Test 11	slotted	Tailing 2	Cylinder	0.81	5.2×10^{-2}	13%	2.50×10^{-4}	128.94	0.00292	2.115×10^{-5}
Test 12	porous	Tailing 1	Cone	0.9	4.2×10^{-2}	49%	4.0×10^{-5}	109.63	0.00455	2.098×10^{-5}
Test 13	porous	Tailing 1	Cone	0.9	4.2×10^{-2}	49%	4.0×10^{-5}	93.77	0.00438	2.098×10^{-5}
Test 14	porous	Tailing 1	Cone	0.91	4.2×10^{-2}	49%	4.0×10^{-5}	113.77	0.00475	2.098×10^{-5}
Test 15	porous	Tailing 2	Cone	0.99	4.2×10^{-2}	49%	4.0×10^{-5}	114.46	0.01018	2.115×10^{-5}
Test 16	porous	Tailing 2	Cone	0.95	4.2×10^{-2}	49%	4.0×10^{-5}	115.15	0.00850	2.115×10^{-5}

Note: The filtrate water viscosity (μ_w) and unit weight (γ_w) are $5.49\cdot10^{-4}$ Pa·s (50^0C) and $9.8kN/m^3$ for all tests.

π is 3.14 for all tests; R_p is then calculated as 1.38×10^{12} m^{-1} for porous pipe and 0 m^{-1} for slotted pipe.

Table 3.2 Dimensional analysis calculation results

Test	Pipe	Tailing	Tank	$\frac{J}{(n_p \cdot v_s)}$	$\frac{\Delta P \cdot D_{pipe}}{(\mu_w \cdot v_s)}$	$\frac{\Delta P \cdot D_{pore}}{(\mu_w \cdot v_s)}$	$\frac{D_{pore}}{D_{pipe}}$	$\frac{D_{pipe}}{D_{pore}}$	$\frac{d_s}{D_{pipe}}$	$\frac{d_s}{D_{pore}}$	$\frac{\gamma_w \cdot D^2_{pipe}}{(\mu_w \cdot v_s)}$	$\frac{\gamma_w \cdot D^2_{pore}}{(\mu_w \cdot v_s)}$
Test 1	porous	Tailing 1	Cylinder	7.90E-06	9.60E+06	9.14E+03	0.0010	1050	5.00E-04	0.525	3.54E+04	0.032
Test 2	porous	Tailing 1	Cylinder	7.12E-06	6.24E+06	5.94E+03	0.0010	1050	5.00E-04	0.525	3.39E+04	0.031
Test 3	porous	Tailing 1	Cylinder	8.73E-06	9.28E+06	8.84E+03	0.0010	1050	5.00E-04	0.525	2.92E+04	0.026
Test 4	porous	Tailing 1	Cylinder	5.30E-06	2.64E+06	2.51E+03	0.0010	1050	5.00E-04	0.525	1.57E+04	0.014
Test 5	porous	Tailing 2	Cylinder	1.13E-05	9.85E+06	9.38E+03	0.0010	1050	5.04E-04	0.529	3.50E+04	0.032
Test 6	porous	Tailing 3	Cylinder	8.36E-06	1.05E+07	1.00E+04	0.0010	1050	5.02E-04	0.527	3.58E+04	0.032
Test 7	slotted	Tailing 1	Cylinder	2.68E-05	2.03E+07	9.78E+04	0.0048	208	4.03E-04	0.0839	7.00E+04	1.617
Test 8	slotted	Tailing 1	Cylinder	3.36E-05	7.96E+06	3.83E+04	0.0048	208	4.76E-04	0.0989	5.89E+04	1.361
Test 9	slotted	Tailing 1	Cylinder	4.05E-05	1.32E+07	6.36E+04	0.0048	208	5.79E-04	0.120	6.19E+04	1.430
Test 10	slotted	Tailing 1	Cylinder	2.98E-06	4.08E+06	1.96E+04	0.0048	208	4.03E-04	0.0839	2.41E+04	0.558
Test 11	slotted	Tailing 2	Cylinder	2.78E-05	1.51E+07	7.25E+04	0.0048	208	4.07E-04	0.0846	5.96E+04	1.377
Test 12	porous	Tailing 1	Cone	1.03E-05	9.32E+06	8.88E+03	0.0010	1050	5.00E-04	0.525	3.50E+04	0.032
Test 13	porous	Tailing 1	Cone	9.94E-06	7.97E+06	7.59E+03	0.0010	1050	5.00E-04	0.525	3.50E+04	0.032
Test 14	porous	Tailing 1	Cone	1.07E-05	9.56E+06	9.11E+03	0.0010	1050	5.00E-04	0.525	3.46E+04	0.031
Test 15	porous	Tailing 2	Cone	2.10E-05	8.84E+06	8.42E+03	0.0010	1050	5.04E-04	0.529	3.18E+04	0.029
Test 16	porous	Tailing 2	Cone	1.83E-05	9.27E+06	8.83E+03	0.0010	1050	5.04E-04	0.529	3.31E+04	0.030

Note: The porous pipe resistance (R_p) is determined based on the tests operated after Test 15 and is not available for Test 15.

$R_p \cdot D_{pipe}$ is 5.88×10^{10} (porous pipe) and 0 (slotted pipe); $R_p \cdot D_{pore}$ is 5.60×10^{7} (porous pipe) and 0 (slotted pipe)

4 CONCLUSION

The purpose of this research was to investigate the application of cross flow filtration for dewatering oil sands total tailings. Cross flow filtration may provide an alternative method to prevent segregation and the filtrate water released can be reused directly thus returning heated water to the extraction circuit and reducing energy usage. Laboratory tests were conducted to investigate the dewatering capacity of cross flow filtration of total tailings. Results from the laboratory experiments were then used in a dimensional analysis to establish the relationships between measured parameters and to assist and guide future experiments. The following sections summarized the conclusions and recommendations for future research based on this program.

4.1 Laboratory Experiment Results

The purpose of laboratory experiments was to investigate the feasibility of cross flow filtration to dewater oil sands total tailings and to evaluate the influence of different parameters on filtrate quality and quantity. A brief conclusion of laboratory tests is given in this section and the detail conclusion is referred to section 2.7.

High quality filtrate water (<0.5wt% solids content) can be generated from all tests carried out under different operating conditions.

Higher slurry velocity and coarser tailings slurry result in greater filtrate flux rate. Increasing velocity from 0.89m/s to 1.08m/s and from 1.08m/s to over 2m/s result in improvements of 0.0012L/s·m^2

and 0.0006L/s·m^2 respectively. Tailings with coarse particle size distribution generate higher filtrate flux rate (0.003-0.005L/s·m^2) than tailings with fine particle size distribution (0.0024-0.0035L/s·m^2).

It is expected that a better filtrate flux rate can be obtained using the following procedure. At the beginning of cross flow filtration operation a low velocity is applied to allow a coarse cake structure to develop. After the stable cake has formed, the slurry velocity is increased to reduce cake thickness and improve filtrate flux rate. This procedure would minimize the fines formation in cake structure allowing an optimal filtrate flux rate from the pipe.

The presence of bitumen in filter pipe reduces filtrate area and filtrate flux rate (ΔJ=0.001-0.0035L/s·m^2). A pre-treatment to prevent the bitumen froth entering the filter pipe is required to achieve better filtrate flux rate.

Filter pipes with higher porosity give higher filtrate flux rate. Although larger filter pipe pore/slot size requires longer time to initially generate clean filtrate water, it is expected that with the same porosity, larger pore/slot size can provide higher filtrate flux rate (0.018-0.023L/s·m^2 for slotted pipe; (0.007-0.01L/s·m^2 for porous pipe). Another advantage of larger pore/slot size is the low pipe resistance associated with the clogging of bitumen and fines during cross flow filtration operation.

The performance of cross flow filtration is less sensitive to the tailings slurry solids concentration. A higher transmembrane pressure may be required under high solids content situation.

There is an optimal transmembrane pressure providing the highest filtrate flux rate. The coarser cake structure undergoes less compaction under higher pressure.

4.2 Dimensional Analysis Results

A dimensional analysis utilizing experiment results was conducted in this research. The dimensionless equations are derived from Darcy's law and include all important parameters in cross flow filtration. The dimensional analysis shows that the increase of filtrate flux rate becomes smaller under high transmembrane pressure situation and this observation indicates the presence of optimal pressure value in cross flow filtration. The dimensional analysis also shows that the increase of filter pipe size may lead to higher filtrate flux rate even under the same transmembrane pressure situation. With the increase of filter pipe pore/slot size, the increasing rate of filtrate flux rate with transmembrane pressure becomes faster.

4.3 Recommendations for Future Work

4.3.1 Future Work on Cross Flow Filtration

Cross flow filtration tests using slotted filter pipe need to be carried out to improve the dimensional analysis. Tests using different pore/slot size with similar porosity, e.g. the same porous pipe with larger pore size, are needed to observe the effect of filter pipe pore/slot

size on filtrate flux rate. Larger filter pipe size tests are needed to observe the size effect on filtrate flux rate. Tests using longer filter pipes are also needed to further confirm that increasing slurry solids content has little effect on filtrate flux rate.

4.3.2 Future Work on Membrane Cleaning

Although slurry velocity could limit the cake thickness in cross flow filtration, the internal clogging of fines within cake structure and filter membrane is a problem. Eventually the filtrate flux rate may become uneconomically low and membrane cleaning needs to be performed (Murkes and Carlsson, 1988). The objective of membrane cleaning is trying to obtain the maximum restored filtrate flux rate with the minimum consumption of wash liquid and chemicals. Moreover, the washing frequency, duration and sequence need to be taken into concern (Murkes and Carlsson, 1988).

One effective cleaning method is backflushing with pure water or filtrate liquid. Backflushing involves reversal of the filtrate flow by applying pressure on the filter membrane from the permeate side. The applied pressure should be higher than the feed pressure in order to lift the cake off the membrane and then cross flow slurry could sweep the deposition away. Internal clogging within membrane pores may also be partially or completely removed during backflushing (Kuberkar and Davis, 2001). Therefore, a cross flow filtration system including the application of backflushing or other cleaning methods is required for future work, especially for long time operation.

4.4 References

Kuberkar, V.T., and Davis, D.H. 2001. Microfiltration of protein-cell mixtures with crossflushing or backflushing. Journal of Membrane Science, **183**: 1-14

Murkes, J., and Carlsson, C.G. 1998. Crossflow filtration: theory and pratice. John Wiley & Sons Ltd., New York.

APPENDIX A: DEWATER VOLUME CALCULATION

A.1 Dewater Volume Calculation

As introduced in Chapter 1, to achieve a nonsegregating tailings using a dewatering method and without changing fines content, a solids content about 70wt% needs to be obtained. This is illustrated in Figure A.1 by plotting a straight line (dotted line) from total tailings stream region down to the nonsegregating region.

The calculation for the water volume that needs to be removed from the total tailings stream is shown below:

mass of solid: $M_s = s_w \times M_t$ A.1

mass of water: $M_w = M_t - M_s = \frac{M_s}{s} - M_s$ A.2

M_s: mass of solids; kg

M_t: total mass of tailings; kg

M_w: mass of water; kg

s_w: solid content of total tailings slurry by weight; %

Since no solids loss during the dewatering process, the assumption that M_s will not change during dewatering is acceptable. Using solids specific gravity G_s=2.65 and initial tailing solid content s_w=55wt%, the water mass before and after dewatering are shown below represented by M_s:

Water mass before dewatering: $M_{w(before)} = 0.82 M_s$ A.3

Water mass after dewatering: $M_{w(after)} = 0.43 M_s$ A.4

The calculation illustrates that the dewatering work needs to remove about 50wt% of water from total tailings stream, 33% of the original tailings volume, to make nonsegregrating tailings, which is consistent with Beier and Sego's (2008) assumption.

A.2 References:

Beier, N., Sego, D. 2008. Dewatering of oil sands tailings using cross flow filtration. Proceedings of the 61st Canadian Geotechnical Conference, Edmonton AB.

A.3 Figures and Tables

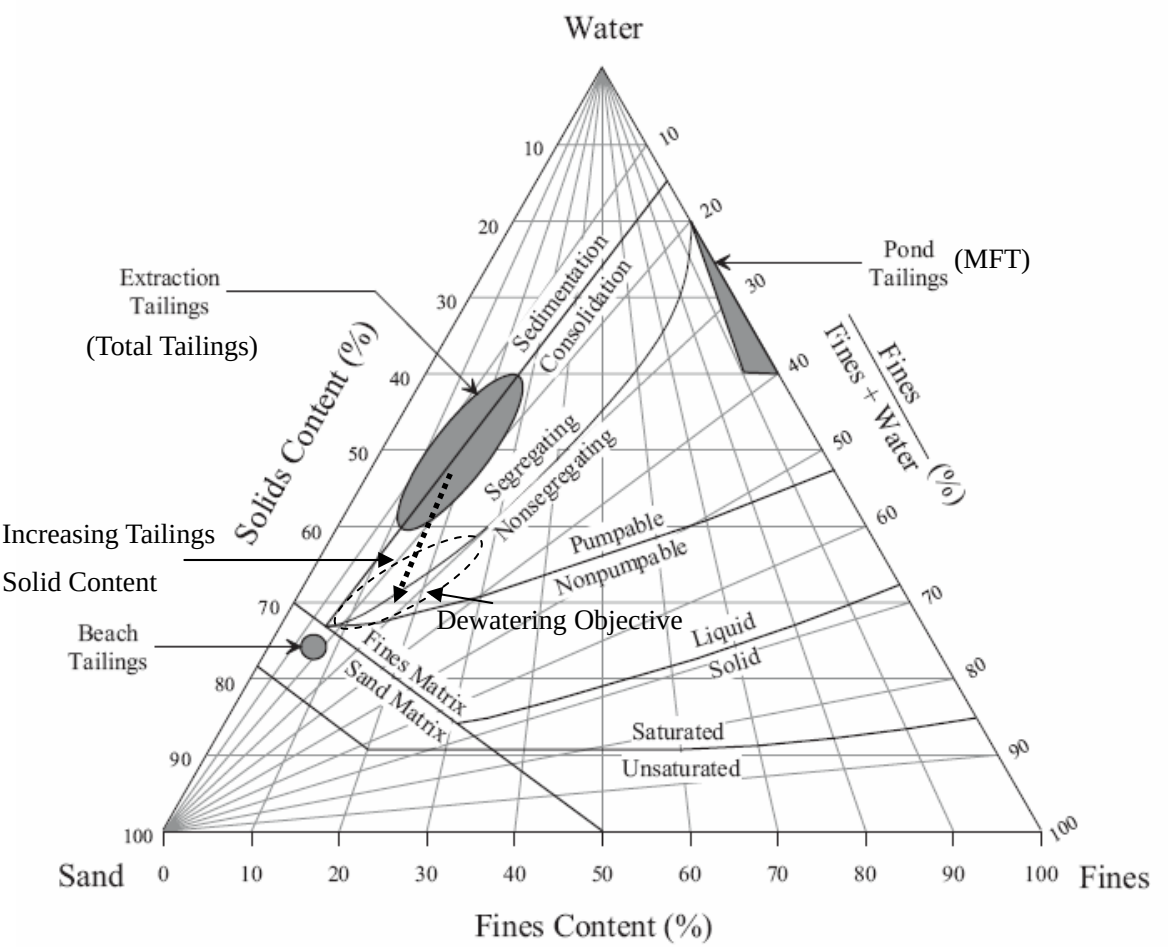

Figure A.1 Dewatering purpose to achieve nonsegregating condition (modified after Azam and Scott, 2005 and Beier and Sego, 2008)

APPENDIX B: CROSS FLOW FILTRATION TEST IMFORMATION

B.0 Introduction

1. The detail information of each test is listed below.
2. The feed tailings solids content were measured with operation time in Test 4, Test 10, Test 12, Test 14 and Test 15. It was observed that the solids content of the feed tailings was maintained similar during the test if the filtrate water was recycled.
3. The measured fines content with time showed large variation. A control on the feed tailings fines content was then used t in each test.
4. The transmembrane pressure with time is the average value of the measured feed and discharge pressure. Generally, no more than 1 psi pressure drop along the filter pipe length (about 3.5m), even with increasing solids content condition (Test 14), was observed.

B.1 Test 1 records

Operation date	Oct.21, 2009		
Tailings type	Tailing 1	**Feed tank type**	Cylinder
Filter pipe	porous	**Filtrate area (m^2)**	0.46
Solids content	55wt%	**Fines content**	15wt%
Velocity (m/s)	0.89	**Pressure (psi/kPa)**	16.2/111.70

Test 1 results

Time (min)	Feed flow rate (m^3/hour)	Feed velocity (m/s)	Transmembrane pressure (psi)	Transmembrane pressure (kPa)
3	4.57	76.17	17.0	116.89
10	4.49	74.83	18.4	127.11
20	4.52	75.33	18.2	125.22
30	4.51	75.17	17.5	120.36
45	4.5	75.00	16.4	113.36
60	4.47	74.50	15.9	109.54
75	4.44	74.00	15.5	106.71
90	4.42	73.67	15.2	105.07
105	4.35	72.50	15.0	103.09
120	4.21	70.17	14.2	97.94

Test 1 results (continuous)

Time (min)	Filtrate flow rate (L/s)	Filtrate flux rate (L/s·m^2)	Filtrate solids content (wt%)
3	0.00199	0.00432	0.12
10	0.00166	0.00361	
20	0.00162	0.00353	
30	0.00163	0.00354	0.06
45	0.00159	0.00346	
60	0.00161	0.00350	0.07
75	0.00167	0.00364	
90	0.00157	0.00340	
105	0.00156	0.00338	
120	0.00152	0.00330	0.05

B.2 Test 2 records

Operation date	Aug.31, 2009		
Tailings type	Tailing 1	**Feed tank type**	Cylinder
Filter pipe	porous	**Filtrate area (m^2)**	0.46
Solids content	55wt%	**Fines content**	15wt%
Velocity (m/s)	0.93	**Pressure (psi/kPa)**	11/75.85

Test 2 results

Time (min)	Feed flow rate (m^3/hour)	Feed velocity (m/s)	Transmembrane pressure (psi)	Transmembrane pressure (kPa)
3	4.67	0.94	10	68.95
15	4.83	0.97	10.8	74.47
30	4.83	0.97	11.6	79.98
47	4.66	0.93	11.8	81.36
60	4.62	0.93	11.8	81.36
75	4.6	0.92	11.8	81.36
90	4.57	0.92	12	82.74
120	4.4	0.88	12	82.74
135			12	82.74
150			12	82.74

Test 2 results (continuous)

Time (min)	Filtrate flow rate (L/s)	Filtrate flux rate (L/s·m^2)	Filtrate solids content (wt%)
1.5			0.17
3	0.00150	0.00325	
10			0.17
15	0.00154	0.00335	
30	0.00129	0.00279	0.18
47	0.00141	0.00307	
60	0.00147	0.00321	0.08
75	0.00140	0.00304	
90	0.00151	0.00329	
120	0.00149	0.00324	0.05
135	0.00154	0.00336	
150	0.00154	0.00334	

Note:

The feed flow meter went wrong and did not show flow rate data after 2 hour operation.

B.3 Test 3 records

Operation date	Sep.28, 2009		
Tailings type	Tailing 1	**Feed tank type**	Cylinder
Filter pipe	porous	**Filtrate area (m^2)**	0.46
Solids content	55wt%	**Fines content**	15wt%
Velocity (m/s)	1.08	**Pressure (psi/kPa)**	19/131.01

Test 3 results

Time (min)	Feed flow rate (m^3/hour)	Feed velocity (m/s)	Transmembrane pressure (psi)	Transmembrane pressure (kPa)
2.66	5.43	1.09	18	124.11
10	5.43	1.09	18	124.11
20	5.41	1.08	18.8	129.63
30	5.36	1.07	19	131.01
40	5.33	1.07	19.5	134.45
50	5.45	1.09	20	137.90
60	5.4	1.08	20	137.90
75	5.41	1.08	20	137.90
90	5.4	1.08	20	137.90
105	5.37	1.08	20	137.90
120	5.32	1.07	20	137.90

Test 3 results (continuous)

Time (min)	Filtrate flow rate (L/s)	Filtrate flux rate (L/s·m^2)	Filtrate solids content (wt%)
2.66	0.00208	0.00453	
4			0.08
10	0.00202	0.00440	
20	0.00204	0.00445	
30	0.00212	0.00460	0.08
40	0.00218	0.00475	
50	0.00223	0.00486	
60	0.00217	0.00473	0.04
75	0.00217	0.00472	
90	0.00214	0.00464	
105	0.00211	0.00459	
120	0.00203	0.00440	0.04

B.4 Test 4 records

Operation date	Oct.01, 2009		
Tailings type	Tailing 1	**Feed tank type**	Cylinder
Filter pipe	porous	**Filtrate area (m^2)**	0.46
Solids content	55wt%	**Fines content**	15wt%
Velocity (m/s)	>2	**Pressure (psi/kPa)**	10/68.95

Test 4 results

Time (min)	Transmembrane pressure (psi)	Transmembrane pressure (kPa)	Temperature (^{0}C)
2	10	68.95	
7	10	68.95	
15	10	68.95	
30	10	68.95	
60	10	68.95	
90	10	68.95	44.8
110	10	68.95	44.5
120	10	68.95	

Test 4 results (continuous)

Time (min)	Filtrate flow rate (L/s)	Filtrate flux rate (L/s·m^2)	Filtrate solids content (wt%)	Feed solids content (wt%)
2	0.00253	0.00551		
5			0.06	
7	0.00157	0.00342		
15	0.00247	0.00538		
20	0.00242	0.00527		
25	0.00234	0.00509		
30	0.00233	0.00506	0.10	55.03
40	0.00209	0.00455		
45	0.00222	0.00483		
50	0.00225	0.00489		
55	0.00248	0.00539		
60	0.00237	0.00516	0.05	55.29
65	0.00242	0.00526		
70	0.00242	0.00526		
75	0.00241	0.00524		
80	0.00237	0.00516		
85	0.00263	0.00571		
90	0.00250	0.00543		54.65
95	0.00241	0.00524		

Test 4 results (continuous)

Time (min)	Filtrate flow rate (L/s)	Filtrate flux rate ($L/s \cdot m^2$)	Filtrate solids content (wt%)	Feed solids content (wt%)
101	0.00228	0.00496		
105	0.00232	0.00504		
110	0.00235	0.00511		
115	0.00231	0.00503		
120	0.00226	0.00492	0.04	55.15

Note:

The feed flow meter did not work well and an estimated velocity (>2m/s) was used to represent test operation condition.

B.5 Test 5 records

Operation date	Sep.14, 2009		
Tailings type	Tailing 2	**Feed tank type**	Cylinder
Filter pipe	porous	**Filtrate area (m^2)**	0.46
Solids content	55wt%	**Fines content**	15wt%
Velocity (m/s)	0.9	**Pressure (psi/kPa)**	16.8/115.84

Test 5 results

Time (min)	Feed flow rate (m^3/hour)	Feed velocity (m/s)	Transmembrane pressure (psi)	Transmembrane pressure (kPa)
3	4.51	0.90	16.4	113.08
10	4.43	0.89	16.6	114.11
20	4.47	0.90	17.2	118.59
30	4.66	0.93	18.3	126.18
45	4.57	0.92	17.1	117.90
60	4.51	0.90	16.7	114.80
75	4.57	0.92	16.8	115.49
90	4.5	0.90	16.2	111.35
120	4.4	0.88	15.7	107.91

Test 5 results (continuous)

Time (min)	Filtrate flow rate (L/s)	Filtrate flux rate (L/s·m^2)	Filtrate solids content (wt%)
3	0.00273	0.00593	0.07
10	0.00258	0.00560	
20	0.00238	0.00517	
30	0.00255	0.00555	
45	0.00241	0.00523	0.16
60	0.00239	0.00519	
75	0.00234	0.00509	
78			0.13
90	0.00226	0.00492	
120	0.00218	0.00474	0.10

B.6 Test 6 records

Operation date	Oct.16, 2009		
Tailings type	Tailing 3	**Feed tank type**	Cylinder
Filter pipe	porous	**Filtrate area (m^2)**	0.46
Solids content	55wt%	**Fines content**	15wt%
Velocity (m/s)	0.88	**Pressure (psi/kPa)**	18.7/128.94

Test 6 results

Time (min)	Feed flow rate (m^3/hour)	Feed velocity (m/s)	Transmembrane pressure (psi)	Transmembrane pressure (kPa)
2.5	4.46	0.89	16.1	110.66
15	4.43	0.89	17.8	122.73
30	4.41	0.88	17.8	122.73
45	4.43	0.89	18.1	124.80
60	4.39	0.88	18.0	124.11
75	4.38	0.88	18.2	125.14
90	4.39	0.88	18.0	123.77
105	4.38	0.88	17.6	121.01
120	4.34	0.87	17.1	117.56

Test 6 results (continuous)

Time (min)	Filtrate flow rate (L/s)	Filtrate flux rate (L/s·m^2)	Filtrate solids content (wt%)
2.5	0.00216	0.00469	
4			0.07
15	0.00187	0.00406	
30	0.00174	0.00379	0.12
45	0.00177	0.00384	
60	0.00173	0.00376	0.05
75	0.00169	0.00368	
90	0.00166	0.00361	
105	0.00162	0.00353	
120	0.00159	0.00345	0.06

B.7 Test 7 records

Operation date	Oct.21, 2009		
Tailings type	Tailing 1	**Feed tank type**	Cylinder
Filter pipe	slotted	**Filtrate area (m^2)**	0.57
Solids content	55wt%	**Fines content**	15wt%
Velocity (m/s)	0.69	**Pressure (psi/kPa)**	21.5/148.24

Test 7 results

Time (min)	Feed flow rate (m^3/hour)	Feed velocity (m/s)	Transmembrane pressure (psi)	Transmembrane pressure (kPa)
5	5.34	0.70	22.7	156.52
10	5.34	0.70	21.4	147.21
20	5.3	0.69	20.8	143.07
30	5.24	0.69	22.3	153.41
40	5.17	0.68	21.5	148.24
50	5.1	0.67	21.1	145.48
60	6.07	0.79	21.1	145.14

Test 7 results (continuous)

Time (min)	Filtrate flow rate (L/s)	Filtrate flux rate (L/s·m^2)	Filtrate solids content (wt%)
2			0.56
5	0.00228	0.00400	
10	0.00155	0.00272	0.14
20	0.00144	0.00253	
30	0.00146	0.00255	
40	0.00138	0.00242	0.09
50	0.00132	0.00232	
60	0.00132	0.00232	

B.8 Test 8 records

Operation date	Aug.25, 2009		
Tailings type	Tailing 1	**Feed tank type**	Cylinder
Filter pipe	slotted	**Filtrate area (m^2)**	0.57
Solids content	55wt%	**Fines content**	12.5wt%
Velocity (m/s)	0.82	**Pressure (psi/kPa)**	10/68.95

Test 8 results

Time (min)	Feed flow rate (m^3/hour)	Feed velocity (m/s)	Transmembrane pressure (psi)	Transmembrane pressure (kPa)	Temperature (^{0}C)
7	6.62	0.87	7.2	49.64	
15	6.63	0.87	7.7	53.09	
40	6.61	0.86	8	55.16	
60	6.4	0.84	8.8	60.68	
90	6.4	0.84	9.8	67.57	
100					43
105	6.15	0.80	10	68.95	
110					44.2
120	5.66	0.74	10	68.95	
130					45.3
135	5	0.65	10	68.95	
145	4	0.52	10	68.95	

Test 8 results (continuous)

Time (min)	Filtrate flow rate (L/s)	Filtrate flux rate (L/s·m^2)	Filtrate solids content (wt%)
1			4.88
7	0.00218	0.00382	0.44
15	0.00192	0.00337	
18			0.06
40	0.00197	0.00346	0.06
60	0.00197	0.00346	
90	0.00209	0.00367	
100			
105	0.00209	0.00367	
110			0.04
120	0.00205	0.00359	
130			
135	0.00201	0.00352	
145	0.00203	0.00356	0.05

B.9 Test 9 records

Operation date	Sep.24, 2009		
Tailings type	Tailing 1	**Feed tank type**	Cylinder
Filter pipe	slotted	**Filtrate area (m^2)**	0.57
Solids content	55wt%	**Fines content**	10wt%
Velocity (m/s)	0.78	**Pressure (psi/kPa)**	15.8/108.94

Test 9 results

Time (min)	Feed flow rate (m^3/hour)	Feed velocity (m/s)	Transmembrane pressure (psi)	Transmembrane pressure (kPa)
2	5.94	0.78	15.8	108.94
8	5.94	0.78	16.3	112.39
15	5.94	0.78	16.2	111.70
30	6	0.78	15.1	104.11
40	5.83	0.76	16	110.32
50	5.97	0.78	15.4	106.18
60	5.81	0.76	15.9	109.63

Test 9 results (continuous)

Time (min)	Filtrate flow rate (L/s)	Filtrate flux rate (L/s·m^2)	Filtrate solids content (wt%)
2	0.00314	0.00551	
4			1.76
8	0.00241	0.00423	
15	0.00230	0.00404	0.08
30	0.00229	0.00401	0.04
40	0.00233	0.00409	
50	0.00233	0.00409	
60	0.00242	0.00425	0.11

B.10 Test 10 records

Operation date	Oct.02, 2009		
Tailings type	Tailing 1	**Feed tank type**	Cylinder
Filter pipe	slotted	**Filtrate area (m^2)**	0.57
Solids content	55wt%	**Fines content**	15wt%
Velocity (m/s)	>2	**Pressure (psi/kPa)**	14/96.53

Test 10 results

Time (min)	Transmembrane pressure (psi)	Transmembrane pressure (kPa)	Temperature (^{0}C)
5	10.7	73.78	
15	11.6	79.98	
34	12.3	84.81	
55			39.1
60	12.0	82.74	
75	12.5	86.19	
78			44.6
91	13.5	93.08	
94			47.3
105	12.6	86.88	
107			48.6
120	12.8	87.91	50.5

Test 10 results (continuous)

Time (min)	Filtrate flow rate (L/s)	Filtrate flux rate ($L/s \cdot m^2$)	Filtrate solids content (wt%)	Feed solids content (wt%)
3			0.95	
5	0.00073	0.00129		
15	0.00061	0.00108	0.28	
30				54.13
34	0.00054	0.00094	0.13	
45	0.00057	0.00099		
60	0.00047	0.00082	0.22	56.08
75	0.00043	0.00076		
80	0.00049	0.00086		
91	0.00047	0.00082		57.65
105	0.00041	0.00072		
120	0.00038	0.00067	0.10	59.99

Note:

The feed flow meter did not work well and an estimated velocity (>2m/s) was used to represent test operation condition.

B.11 Test 11 records

Operation date	Sep.10, 2009		
Tailings type	Tailing 2	**Feed tank type**	Cylinder
Filter pipe	slotted	**Filtrate area (m^2)**	0.57
Solids content	55wt%	**Fines content**	15wt%
Velocity (m/s)	0.81	**Pressure (psi/kPa)**	18.7/128.94

Test 11 results

Time (min)	Feed flow rate (m^3/hour)	Feed velocity (m/s)	Transmembrane pressure (psi)	Transmembrane pressure (kPa)	Temperature (^{0}C)
3	6.36	0.83	19	131.01	
8	6.33	0.83	18	124.11	
15	6.23	0.81	19.3	133.07	
30	6.22	0.81	19.3	133.07	
45	6.21	0.81	18.8	129.63	
60	6.2	0.81	18.7	128.94	
72					39.1
75	6.07	0.79	18.9	130.32	
90	6.13	0.80	18.6	128.25	
105	6.07	0.79	18.3	126.18	41
120	6	0.78	18	124.11	

Test 11 results (continuous)

Time (min)	Filtrate flow rate (L/s)	Filtrate flux rate (L/s·m^2)	Filtrate solids content (wt%)
3	0.00302	0.00530	
5			0.66
8	0.00199	0.00349	
15	0.00203	0.00356	
30	0.00191	0.00335	0.11
45	0.00186	0.00327	
60	0.00175	0.00307	
66			0.17
75	0.00171	0.00300	
90	0.00171	0.00301	
105	0.00163	0.00286	
120	0.00153	0.00269	0.12

B.12 Test 12 records

Operation date	Sep.16, 2008		
Tailings type	Tailing 1	**Feed tank type**	Cone
Filter pipe	porous	**Filtrate area (m^2)**	0.46
Solids content	55wt%	**Fines content**	15wt%
Velocity (m/s)	0.9	**Pressure (psi/kPa)**	15.9/109.63

Test 12 results

Time (min)	Feed flow rate (m^3/hour)	Feed velocity (m/s)	Transmembrane pressure (psi)	Transmembrane pressure (kPa)	Temperature (^{0}C)
15	4.55	0.91			
21	4.54	0.91			
30	4.53	0.91			
33			15.7	108.25	
45	4.49	0.90	14.8	101.70	
52					41
58	4.5	0.90	17.4	119.63	
65	4.485	0.90	17.8	122.73	
72					45.9
94	4.435	0.89	17.1	117.56	49.4
105	4.41	0.88	14.7	101.01	50.4

Test 12 results (continuous)

Time (min)	Feed flow rate (m^3/hour)	Feed velocity (m/s)	Transmembrane pressure (psi)	Transmembrane pressure (kPa)	Temperature (^{0}C)
110			15.9	109.29	
120	4.41	0.88	17.5	120.32	
126					51.3
135	4.38	0.88	16.6	114.11	52
150	4.37	0.88	16.5	113.42	
165	4.38	0.88	13.8	95.15	
173					51.9
180	4.44	0.89	12.9	88.60	
195	4.335	0.87	16.0	109.98	
210	4.31	0.86	15.8	108.94	

Test 12 results (continuous)

Time (min)	Filtrate flow rate (L/s)	Filtrate flux rate (L/s·m^2)	Filtrate solids content (wt%)	Feed solids content (wt%)
1			1.51	56.53
15	0.00235	0.00513	0.27	58.52
21	0.00229	0.00500		
30	0.00241	0.00526	0.12	55.95

Test 12 results (continuous)

Time (min)	Filtrate flow rate (L/s)	Filtrate flux rate (L/s·m^2)	Filtrate solids content (wt%)	Feed solids content (wt%)
45	0.00226	0.00492		
58	0.00243	0.00529		
65	0.00243	0.00530		
68			0.07	56.35
94	0.00226	0.00492		
105	0.00210	0.00457		
120	0.00222	0.00483	0.08	54.16
135	0.00216	0.00471		
150	0.00212	0.00462		
165	0.00182	0.00397		
180	0.00180	0.00392	0.04	55.68
195	0.00205	0.00446		
210	0.00195	0.00424	0.06	

B.13 Test 13 records

Operation date	Sep.02, 2009		
Tailings type	Tailing 1	**Feed tank type**	Cone
Filter pipe	porous	**Filtrate area (m^2)**	0.46
Solids content	55wt%	**Fines content**	15wt%
Velocity (m/s)	0.9	**Pressure (psi/kPa)**	13.6/93.77

Test 13 results

Time (min)	Feed flow rate (m^3/hour)	Feed velocity (m/s)	Transmembrane pressure (psi)	Transmembrane pressure (kPa)
1.5	4.22	0.85	13.4	92.39
5	4.46	0.89	13	89.64
15	4.59	0.92	14	96.53
30	4.52	0.91	14.4	99.29
45	4.65	0.93	14.4	99.29
60	4.52	0.91	13.7	94.46
75	4.59	0.92	13.7	94.46
90	4.54	0.91	13.3	91.70
105	4.57	0.92	13.3	91.70
120	4.6	0.92	13.3	91.70

Test 13 results (continuous)

Time (min)	Filtrate flow rate (L/s)	Filtrate flux rate (L/s·m^2)	Filtrate solids content (wt%)
1.5	0.00274	0.00595	
5	0.00189	0.00412	
6			0.07
15	0.00197	0.00428	
30	0.00196	0.00426	0.05
45	0.00213	0.00462	
60	0.00203	0.00442	0.04
75	0.00210	0.00457	
90	0.00200	0.00435	
105	0.00198	0.00430	
120	0.00196	0.00427	0.03

B.14 Test 14 records

Operation date	Aug.28, 2008		
Tailings type	Tailing 1	**Feed tank type**	Cone
Filter pipe	porous	**Filtrate area (m^2)**	0.46
Solids content	55wt%	**Fines content**	15wt%
Velocity (m/s)	0.91	**Pressure (psi/kPa)**	16.5/113.77

Test 14 results

Time (min)	Feed flow rate (m^3/hour)	Feed velocity (m/s)	Transmembrane pressure (psi)	Transmembrane pressure (kPa)	Temperature (^{0}C)
5	4.75	0.95	15.8	108.94	
26	4.69	0.94	15.0	103.43	
32	4.67	0.94	14.8	101.70	
42					29.8
46	4.7	0.94	13.9	95.84	
59	4.65	0.93	14.3	98.60	
65					45.2
74	4.6	0.92	13.9	95.84	
80					48.2
89	4.55	0.91	15.6	107.22	
95					51.8

Test 14 results (continuous)

Time (min)	Feed flow rate (m^3/hour)	Feed velocity (m/s)	Transmembrane pressure (psi)	Transmembrane pressure (kPa)	Temperature (^{0}C)
104	4.54	0.91	16.2	111.70	
109					54.2
120	4.48	0.90	17.4	119.63	
125					56.6
135	4.491	0.90	17.3	118.94	
146					58.0
149	4.48	0.90	17.1	117.56	
155					58.3
165	4.47	0.90	17.5	120.66	
169					58.1
179	4.5	0.90	18.0	124.11	
194			19.2	132.38	57.9
195	4.5	0.90			
210	4.53	0.91	21.0	144.80	

Test 14 results (continuous)

Time (min)	Filtrate flow rate (L/s)	Filtrate flux rate (L/s·m^2)	Filtrate solids content (wt%)	Feed solids content (wt%)
0.17			1.19	
5	0.00247	0.00538		
8			0.25	
15	0.00242	0.00526		55.90
24			0.11	
31	0.00248	0.00540		55.83
39			0.08	
46	0.00239	0.00520		56.19
59	0.00245	0.00533	0.06	57.14
75	0.00230	0.00502		58.43
90	0.00244	0.00530		60.02
93			0.06	
105	0.00241	0.00525		60.68
120	0.00227	0.00495		61.12
124			0.05	
135	0.00220	0.00479		62.57
150	0.00211	0.00460		62.95
165	0.00204	0.00444		64.25
181	0.00196	0.00428	0.03	64.68

Test 14 results (continuous)

Time (min)	Filtrate flow rate (L/s)	Filtrate flux rate ($L/s \cdot m^2$)	Filtrate solids content (wt%)	Feed solids content (wt%)
195	0.00189	0.00411		67.21
213			0.05	69.53

Note:

Filtrate water was removed 4L/hour during test operation.

B.15 Test 15 records

Operation date	Aug.14, 2008		
Tailings type	Tailing 2	**Feed tank type**	Cone
Filter pipe	porous	**Filtrate area (m^2)**	0.46
Solids content	55wt%	**Fines content**	15wt%
Velocity (m/s)	0.99	**Pressure (psi/kPa)**	16.6/114.43

Test 15 results

Time (min)	Feed flow rate (m^3/hour)	Feed velocity (m/s)	Transmembrane pressure (psi)	Transmembrane pressure (kPa)	Temperature (^{0}C)
1.5			17.5	120.66	
2	4.85	0.97			
5	4.93	0.99	19.0	130.66	
15					34.5
30	4.8	0.96	19.7	135.83	43.5
45					47.6
60	4.8	0.96	18.0	124.11	49.0
90	4.94	0.99	16.1	111.01	49.1
120	4.98	1.00	15.6	107.22	48.2
150	5.01	1.00	15.3	105.49	47.9
180	5.01	1.00	15.4	106.18	48.0

Test 15 results (continuous)

Time (min)	Feed flow rate (m^3/hour)	Feed velocity (m/s)	Transmembrane pressure (psi)	Transmembrane pressure (kPa)	Temperature (^{0}C)
210	5	1.00	15.6	107.56	48.0
240	4.95	0.99	16.2	111.35	48.7
270	4.95	0.99	15.7	107.91	48.5
300	4.92	0.99	15.8	108.94	
330	4.88	0.98	16.2	111.35	
360	4.89	0.98	16.5	113.77	

Test 15 results (continuous)

Time (min)	Filtrate flow rate (L/s)	Filtrate flux rate (L/s·m^2)	Filtrate solids content (wt%)	Feed solids content (wt%)
0.5			3.91	
5	0.0067	0.0146	0.14	54.00
15				
30	0.0079	0.0172	0.12	55.50
45				
60	0.0072	0.0156	0.13	55.00
90	0.0056	0.0122		
120	0.0055	0.0120	0.14	55.67

Test 15 results (continuous)

Time (min)	Filtrate flow rate (L/s)	Filtrate flux rate ($L/s \cdot m^2$)	Filtrate solids content (wt%)	Feed solids content (wt%)
150	0.0053	0.0114		
180	0.0049	0.0106	0.14	57.13
210	0.0046	0.0100		
240	0.0045	0.0098	0.14	58.75
270	0.0047	0.0102		
300	0.0046	0.0099	0.15	
330	0.0042	0.0092		
360	0.0039	0.0085	0.17	58.12

Note:

The first test operated using the stainless steel porous pipe.

B.16 Test 16 records

Operation date	Nov.28, 2008		
Tailings type	Tailing 2	**Feed tank type**	Cone
Filter pipe	porous	**Filtrate area (m^2)**	0.46
Solids content	55wt%	**Fines content**	15wt%
Velocity (m/s)	0.95	**Pressure (psi/kPa)**	16.7/115.15

Test 16 results

Time (min)	Feed flow rate (m^3/hour)	Feed velocity (m/s)	Transmembrane pressure (psi)	Transmembrane pressure (kPa)
2	4.78	0.96	15.4	106.18
5	4.78	0.96	15.5	106.87
11	4.75	0.95	16.0	109.98
30	4.75	0.95	17.0	116.87
40	4.73	0.95	17.3	119.28
50	4.735	0.95	17.8	122.39
60	4.7	0.94	17.7	122.04
70	4.68	0.94	17.3	118.94
80	4.73	0.95	17.1	117.90
90			16.8	115.84
96	4.73	0.95	16.5	113.42
110	4.75	0.95	16.1	111.01

Test 16 results (continuous)

Time (min)	Filtrate flow rate (L/s)	Filtrate flux rate (L/s·m^2)
2	0.00469	0.01021
5	0.00384	0.00835
11	0.00359	0.00781
18	0.00381	0.00829
30	0.00382	0.00832
40	0.00390	0.00850
50	0.00399	0.00870
60	0.00402	0.00876
70	0.00398	0.00867
80	0.00399	0.00868
90	0.00398	0.00867
96	0.00388	0.00846
110	0.00376	0.00818
120	0.00371	0.00807

Note:

Filtrate solids content did not measure in this test.

Clean filtrate water was observed within 5 minutes after test beginning.

APPENDIX C: DEPOSITION VELOCITY

C.1 Introduction

The prediction model of deposition velocity, which was established by Durand and Condolios and described in the Colorado School of Mines book in 1963, was introduced by Shook et al. (2002). This prediction method considers the tailings slurry with broad size distributions as a bimodal mixture, in which fine particles are part of the carrier fluid and coarse particles are settling particles. The deposition velocity (v_c) is predicted using the equation below:

$$v_c = F\sqrt{gD_{pipe}(S_s - 1)} \qquad \text{C.1}$$

v_c: deposition velocity; m/s

D_{pipe}: pipe diameter; m

S_s: density ratio (solid/fluid); dimensionless

F: Froude number; dimensionless

g: gravitational acceleration; m/s^2

The Froude number (F) introduced in this equation is given from the Archimedes number (Ar), which is a function of the particle and carrier fluid properties. The equation of Archimedes number (Ar) is:

$$Ar = \frac{(4/3)gd_p^3\rho_{cf}(\rho_{solid} - \rho_{cf})}{\mu_{cf}^2} \qquad \text{C.2}$$

A_r: Archimedes number; dimensionless

d_p: particle diameter; m

ρ_{cf}: density of carrier fluid (including fines); kg/m^3

ρ_{solid}: density of solid particles; kg/m^3

μ_{cf}: viscosity of carrier fluid (including fines); $N \cdot s/m^2$

The piecewise correlation between the Archimedes number (Ar) and the Froude number (F) is shown below:

$$\begin{aligned} 540 < Ar \qquad & F = 1.78 Ar^{-0.019} \\ 160 < Ar < 540 \quad & F = 1.19 Ar^{0.045} \\ 80 < Ar < 160 \quad & F = 0.197 Ar^{0.4} \end{aligned} \tag{C.3}$$

F: Froude number; dimensionless

A_r: Archimedes number; dimensionless

For particles with Archimedes number (Ar) less than 80, the correlation of Wilson and Judge is used. The approximate upper limit and lower limit of Δ for use of this correlation is from $1 \cdot 10^{-5}$~0.001.

$$\begin{aligned} F &= \sqrt{2}[2.0 + 0.3 \log_{10} \Delta] \\ \Delta &= d_p / D_p C_D \end{aligned} \tag{C.4}$$

F: Froude number; dimensionless

C_D: the drag coefficient; dimensionless

D_{pipe}: pipe diameter; m

d_p: particle diameter; m

The correlation between drag coefficient (C_D) and Archimedes number (Ar) is shown below:

$$\begin{aligned} 24 < Ar \le 80 \qquad & C_D = 80.9 Ar^{-0.475} \\ Ar \le 24 \qquad & C_D = 576 Ar^{-1} \end{aligned} \tag{C.5}$$

For broad size distributions slurry, a correlation between deposition velocity with density and viscosity of the complete slurry is needed. Unfortunately, no investigation of those relationships was reported

and for oil sand total tailings, experimental tests were required for pipeline design (Shook et al., 2002).

C.2 Sample Calculation

A detailed deposition velocity sample calculation procedure is in this section based on Shook et al. (2002). In this calculation, tailings slurry solids content is 55wt% and 15wt% of solids are fines (<45μm). The particle size used in this calculation is d_{90} of Tailing 1, which is 280μm. The deposition velocity calculation results for other particle size and solid content are shown in Table C.1 and Table C.2.

C.2.1 Conversion between Solids Content by Weight to Solid Content by Volume

First, tailings slurry solids content by weight has to be converted to solids content by volume and the conversion equation is shown below:

$$s_v = \frac{s_w}{s_w + G_s(1 - s_w)} \qquad \text{C.6}$$

s_w: solid content of total tailings slurry by weight; %

s_v: solid content of total tailings slurry by volume; %

G_s: specific gravity of solids (both sands and fines); dimensionless

The tailings stream solids content by volume is then calculated as:

$$s_v = \frac{55\%}{55\% + 2.65(1 - 55\%)} = 31.56\% \qquad \text{C.7}$$

C.2.2 Calculation of Carrier Fluid Viscosity

The fines content of total tailings slurry by volume is calculated as:

$$f_v = s_v \times f_w = 4.734\% \qquad \text{C.8}$$

f_v: fines content of total tailings slurry by volume; %

f_w: fines content of total solids by weight; %

s_v: solid content of total tailings slurry by volume; %

Since the specific gravity (G_s) of sands and fines used in this calculation are both 2.65, the fines content of total solids by weight (f_w) is equal to the fines content of total solids by volume (f_v). Therefore the fines concentration in the carried fluid, which is (fines + water) mixture, is:

$$f_{v(\,fines+water\,)} = \frac{f_v}{f_v + (1 - s_v)} = 6.47\% \qquad \text{C.9}$$

$f_{v(fines+water)}$: fines content of carried fluid by volume; %

f_v: fines content of total tailings slurry by volume; %

s_v: solid content of total tailings slurry by volume; %

According to Shook et al. (2002), the intrinsic viscosity of the fines in water is 30. Then the relative viscosity of the (fines + water) mixture is:

$$\mu_r = 1 + 30 \times 6.47\% = 2.94 \qquad \text{C.10}$$

μ_r: relative viscosity; dimensionless

Since the operation temperature for oil sands total tailings pipeline transportation is always high, the viscosity of water used in this calculation is chosen as the viscosity at 50^0C, which is 0.000549 N·s/m^2. Then the carried fluid viscosity is calculated as:

$$\mu_{cf} = \mu_r \times \mu_w = 2.94 \times 0.000549 = 0.00162 N \cdot s / m^2 \quad \text{C.11}$$

μ_{cf}: viscosity of carried fluid; N·s/m^2

μ_r: relative viscosity; dimensionless

μ_w: viscosity of water at 50^{0}C; N·s/m^2

C.2.3 Calculation of Deposition Velocity

The first step is to calculate Archimedes number (A_r) using equation C.2. The density of carried fluid, which is the (fines + water) mixture, is calculated using:

$$\begin{aligned} \rho_{cf} &= \frac{[(f_{v(fines+water)} \times \rho_{solid}) + ((1 - s_v) \times \rho_{water})]}{(f_{v(fines+water)} + (1 - s_v))} \\ &= \frac{[(6.46\% \times 2650) + ((1 - 31.56\%) \times 1000)]}{(6.46\% + (1 - 31.56\%))} \\ &= 1142.53 kg / m^3 \end{aligned} \quad \text{C.12}$$

ρ_{cf}: density of carried fluid; kg/m^3

ρ_{solid}: density of solids (including sand and fines); kg/m^3

ρ_{water}: density of water; kg/m^3

$f_{v(fines+water)}$: fines content of carried fluid by volume; %

s_v: solid content by volume; %

Therefore, the Archimedes number (A_r) is calculated as:

$$\begin{aligned} Ar &= \frac{(4/3) g d_p^3 \rho_{cf} (\rho_{solid} - \rho_{cf})}{\mu_{cf}^2} \\ &= \frac{(4/3) \times 9.81 \times (0.28 \times 10^{-3})^3 \times 1142.3 \times (2650 - 1142.3)}{0.00162^2} \\ &= 189.67 \end{aligned} \quad \text{C.13}$$

A_r: Archimedes number; dimensionless

d_p: particle diameter; m

ρ_{cf}: density of carrier fluid (including fines); kg/m^3

ρ_{solid}: density of solid particles; kg/m^3

μ_{cf}: viscosity of carrier fluid (including fines); N·s/m^2

g: gravitational acceleration; m/s^2

From equation C.3, when 160<Ar<540, the Froude number (F) is calculated as:

$$F = 1.19 Ar^{0.045} = 1.19 \times 189.67^{\ 0.045} = 1.507 \qquad \text{C.14}$$

F: Froude number; dimensionless

A_r: Archimedes number; dimensionless

Then the deposition velocity is obtained from equation C.1 as:

$$\begin{aligned} v_c &= F\sqrt{gD_{pipe}(S_s - 1)} = F\sqrt{gD_{pipe}((\rho_{solid}/\rho_{cf}) - 1)} \\ &= 1.507 \times \sqrt{9.81 \times 42 \times 10^{-3} \times ((2650/1142.53) - 1)} \\ &= 1.11\ m/s \end{aligned} \qquad \text{C.15}$$

v_c: deposition velocity; m/s

D_{pipe}: pipe diameter; m

S_s: density ratio (solid/fluid); dimensionless

ρ_{solid}: density of solid particles; kg/m^3

ρ_{cf}: density of carrier fluid (including fines); kg/m^3

F: Froude number; dimensionless

g: gravitational acceleration; m/s^2

C.3 References:

Shook, C.A., Gillies, R.G., and Sanders, R.S. 2002. Pipeline hydrotransport with applications in the oil sand industry. SRC Pipe Flow Technology Center, Saskatoon, SK.

C.4 Figures and Tables

Table C.1 Deposition velocity (55wt% solid content, 15wt% fines content) of different particles size

	Tailing 1		Tailing 2	
	Particle Size (m)	Deposition Velocity (m/s)	Particle Size (mm)	Deposition Velocity (m/s)
d_{90}	2.8×10^{-4}m	1.11		
d_{80}	2.4×10^{-4}m	0.98	3.6×10^{-4}m	1.15
d_{70}	2.2×10^{-4}m	0.88	2.4×10^{-4}m	0.98

Table C.2 Deposition velocity (d_{90}) of Tailing 1 (15wt% fines content) with different pipe size and solids content

Tailing 1	Pipe Diameter (m)				
$d_{90}=2.8\times10^{-4}$m	0.042 (porous)	0.051 (2 inch)	0.102 (4 inch)	0.203 (8 inch)	0.305 (12 inch)
Solids Content (wt%)	Deposition Velocity (m/s)				
55	1.11	1.22	1.73	2.44	2.99
60	1.04	1.14	1.62	2.29	2.80
65	0.90	0.99	1.40	1.97	2.42
70	0.75	0.83	1.17	1.66	2.03

Table C.3 Deposition velocity (d_{80}) of Tailing 2 (15wt% fines content) with different pipe size and solids content

Tailing 2	Pipe Diameter (m)				
$d_{80}=3.6\times10^{-4}$m	0.042 (porous)	0.051 (2 inch)	0.102 (4 inch)	0.203 (8 inch)	0.305 (12 inch)
Solids Content (wt%)	Deposition Velocity (m/s)				
55	1.15	1.26	1.79	2.53	3.10
60	1.10	1.21	1.72	2.43	2.97
65	1.05	1.15	1.63	2.31	2.83
70	0.98	1.08	1.53	2.17	2.65

APPENDIX D: REYNOLDS NUMBER CALCULATION

D.1 Introduction

According to Shook et al., (2002) the Reynolds number is defined as:

$$\mathrm{Re} = \frac{D_{pipe} v_s \rho_s}{\mu_s} \qquad \text{D.1}$$

Re: Reynolds number; dimensionless

D_{pipe}: pipe diameter; m

v_s: slurry velocity; m/s

ρ_s: slurry density; kg/m^3

μ_s: slurry viscosity; N·s/m^2

D.2 Sample Calculation

A sample Reynolds number calculation is shown this section. A typical cross flow filtration operation with porous pipe is used in this calculation (tailings slurry solid content is 55wt%; v_s=1m/s; D_{pipe}=42mm). The Reynolds number calculation results for other operation conditions are shown in Table D.1 and D.2.

D.2.1 Slurry Density Calculation

The conversion equation from tailings slurry solids content by weight to solids content by volume is shown below:

$$s_v = \frac{s_w}{s_w + G_s(1 - s_w)} = \frac{55\%}{55\% + 2.65(1 - 55\%)} = 31.56\% \qquad \text{D.2}$$

s_w: solid content of total tailings slurry by weight; %

s_v: solid content of total tailings slurry by volume; %

G_s: specific gravity of solids (both sands and fines); dimensionless

The tailings slurry density is then calculated as:

$$\begin{aligned}\rho_s &= [(s_v \times G_s) + ((1 - s_v))] \times \rho_{water} \\ &= [(31.56\% \times 2.65) + (1 - 31.56\%)] \times 1000 \\ &= 1520.80 kg/m^3\end{aligned} \qquad \text{D.3}$$

ρ_s: density of tailings slurry; kg/m^3

ρ_{water}: density of water; kg/m^3

s_v: solid content of total tailings slurry by volume; %

G_s: specific gravity of solids (both sands and fines); dimensionless

D.2.2 Slurry Viscosity Calculation

The relative viscosity of slurry based on solids volume fraction can then be found from Figure D.1 and for the slurry in this calculation the relative viscosity is 3.2. Since the operation temperature in oil sands total tailings pipeline transportation is always high, the viscosity of water used in this calculation is chosen as the viscosity at 50^{0}C, which is 0.000549 N·s/m^2. Then the tailings slurry viscosity is calculated as:

$$\mu_s = \mu_r \times \mu_w = 3.2 \times 0.000549 = 0.00176 N \cdot s/m^2 \qquad \text{D.4}$$

μ_s: viscosity of tailings slurry; N·s/m^2

μ_r: relative viscosity; dimensionless

μ_w: viscosity of water at 50^{0}C; N·s/m^2

D.2.3 Calculation of Reynolds Number

Reynolds number is calculated using equation D.1:

$$\text{Re} = \frac{D_{pipe} v_s \rho_s}{\mu_s} = \frac{0.042 \times 1 \times 1520.80}{0.00176} = 36358 \qquad \text{D.5}$$

According to Wasp et al. (1997), the critical value of Re for pipes is usually taken as 2300 to 2800. As shown in Table D.1 and Table D.2, the values of Reynolds number are always larger than 2800 and it seems the tailings slurry remains turbulent even under high solids content situation (70wt%).

D.3 References:

Wasp, E.J., Kenny, J.P., and Gandhi, R.L. 1977. Solid-liquid flow slurry pipeline transportation. Trans Tech Publications, Clausthal, Germany.

Shook, C.A., Gillies, R.G., and Sanders, R.S. 2002. Pipeline hydrotransport with applications in the oil sand industry. SRC Pipe Flow Technology Center, Saskatoon, SK.

D.4 Figures and Tables

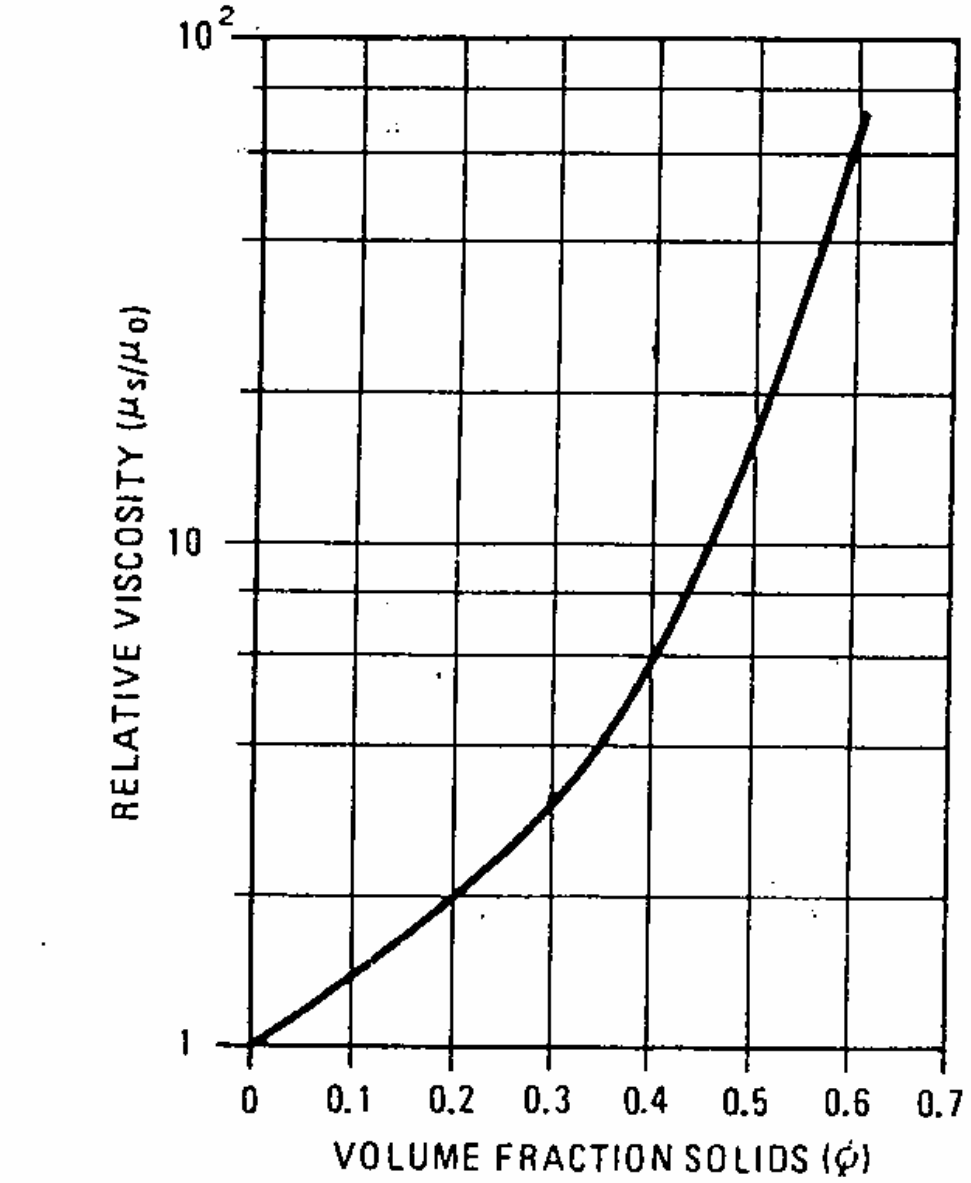

Figure D.1 Reduced relative viscosity versus volume fraction solids (Wasp et al., 1977)

Table D.1 Re for different pipe size and solids content (v=1m/s)

v=1m/s	Solids Content (wt%)			
	55	60	65	70
Pipe Diameter (m)	Re			
0.042	36358	31315	21068	15067
0.051 (2 inch)	43976	37876	25482	18224
0.102 (4 inch)	87952	75752	50965	36449
0.203 (8 inch)	175903	151504	101929	72898
0.305 (12 inch)	263855	227256	152894	109346

Table D.2 Re for different pipe size and solids content (v=3m/s)

v=3m/s	Solids Content (wt%)			
	55	60	65	70
Pipe Diameter (m)	Re			
0.042	109074	93945	63204	45202
0.051 (2 inch)	131928	113628	76447	54673
0.102 (4 inch)	263855	227256	152894	109346
0.203 (8 inch)	527710	454512	305787	218693
0.305 (12 inch)	791566	681769	458681	328039